IMPROVING THE JOINING PERFORMANCE OF CARBON FIBER/PEEK BASED THERMOPLASTIC COMPOSITES WITH LASER SURFACE TREATMENT

A Thesis Submitted to
the Graduate School of Engineering and Science of
İzmir Institute of Technology
in Partial Fulfillment of the Requirements for the Degree of

DOCTOR OF PHILOSOPHY

in Mechanical Engineering

by
Ceren TÜRKDOĞAN DAMAR

May 2024
İZMİR

We approve the thesis of **Ceren TÜRKDOĞAN DAMAR**

Examining Committee Members:

Prof. Dr. Metin TANOĞLU
Department of Mechanical Engineering, İzmir Institute of Technology

Prof. Dr. H. Seçil ARTEM
Department of Mechanical Engineering, İzmir Institute of Technology

Prof. Dr. Engin AKTAŞ
Department of Civil Engineering, İzmir Institute of Technology

Assoc. Prof. Dr. Aylin ZİYLAN
Department of Metallurgical and Materials Engineering, Dokuz Eylul University

Assoc. Prof. Dr. Seçkin ERDEN
Department of Mechanical Engineering, Ege University

21 May 2024

Prof. Dr. Metin TANOĞLU
Supervisor, Department of Mechanical
Engineering, İzmir Institute of Technology

Prof. Dr. M. İ. Can DEDE
Head of the Department of Mechanical Engineering

Prof. Dr. Mehtap EANES
Dean of the Graduate School

ACKNOWLEDGMENTS

I would like to express my sincere gratitude and appreciation to my advisor Professor Dr. Metin TANOĞLU, for his contributions and guidance in my studies during my Ph.D.

I would also like to appreciate my thesis committee members, Prof. H. Seçil ARTEM and Prof. Engin AKTAŞ for their valuable comments, encouragement, and support.

I would like to thank The Scientific and Technological Research Council of Türkiye (TÜBİTAK) 2244-Industrial PhD Fellowship Program (Project number:118C086), which provided financial support for the study, and the project coordinator, Dr. Sinan YILMAZ, for his support and all his valuable contributions.

I would like to thank the industrial advisor of the project, Serkan DEHNELİLER and the Turkish Aerospace Inc. (TAI) for their support and guidance.

Thanks to all members of Composite Materials Laboratory-Mechanical Engineering Department-IZTECH for their endless supports, expertise, and contributions.

I would also like to thank Dr. Aref CEVAHİR for valuable contributions, and support during my thesis.

I would also like to thank IZTECH Center for Materials Research for their contribution to the analysis in this thesis.

I dedicate my dissertation to my beloved family who has given me their love, patience, and support throughout my life. I would like to thank my mother Ayten TÜRKDOĞAN, my father Cemal TÜRKDOĞAN, my brother Görkem TÜRKDOĞAN, my sister Esra TÜRKDOĞAN and my little niece Doğa TÜRKDOĞAN for always supporting and encouraging me. I would never be where I am today without your endless love and support.

Finally, I would like to acknowledge the DAMAR family and especially my husband, Volkan Deniz DAMAR, for their everlasting support, motivation, always being there for me, help and understanding throughout my thesis.

ABSTRACT

IMPROVING THE JOINING PERFORMANCE OF CARBON FIBER/PEEK BASED THERMOPLASTIC COMPOSITES WITH LASER SURFACE TREATMENT

The objective of this Ph.D. thesis is to improve the bonding region performance of carbon fiber/polyether ether ketone (CF/PEEK) composites using nanosecond pulsed IR-Yb (infrared ytterbium) fiber laser surface treatment. The effects of varying the laser process parameters on the surface, microstructural and mechanical properties of the CF/PEEK composite structure in the joint area are revealed and discussed. The surfaces of CF/PEEK produced by the hot-pressing method, which is widely used in the aerospace industry, were subjected to IR-Yb laser surface pretreatment prior to bonding with the adhesive film. The effect produced by the laser on the surface can be controlled by the value of the released energy, which varies with the laser parameters, including the average power, scanning speed, and frequency. In this study, the effect of changing these laser parameters on the CF/PEEK composite surface was revealed using SEM images, and the appropriate working ranges of the laser parameters were determined for the optimum energy value required to selectively remove the PEEK matrix from the surface without damaging the carbon fiber. Once the working ranges of the laser parameters were determined to obtain the desired surface finishes in the study, single lap shear (SLS), Charpy impact, and double cantilever beam (DCB) tests were performed on the prepared specimens to investigate the effects of the laser parameters on the mechanical strength of the bonded CF/PEEK structures and compared to untreated specimens. An improvement in the mechanical properties of the specimens whose joint surfaces were treated with appropriate laser parameters was achieved. This increase was explained by the values of surface roughness parameters and contact angle measurements.

ÖZET

KARBON FİBER/ PEEK ESASLI TERMOPLASTİK KOMPOZİTLERİN BİRLEŞİM PERFORMANSININ LAZER YÜZEY İŞLEM İLE ARTIRILMASI

Bu doktora tezinin amacı, nanosaniye atımlı IR-Yb (kızılötesi-iterbiyum) fiber lazer yüzey ön işlemi kullanarak karbon fiber/polieter eter keton (KF/PEEK) kompozitlerinin birleşme bölgesi performansını arttırmaktır. Bu amaçla, sıcak presleme metodu ile üretilen, havacılık sektöründe oldukça yaygın kullanılan KF/PEEK termoplastik kompozitlerin yüzeyleri, farklı lazer parametreleri ile yapıştırıcı film kullanılarak birleştirme öncesi işlenmiştir. Ayrıca, ortalama lazer gücü, tarama hızı, frekans gibi değişen lazer parametrelerinin, yüzey yapısı, mikroyapı ve mekanik özellikler üzerindeki etkileri ortaya konmuştur. Lazerin yüzey üzerinde oluşturduğu etki, değişen parametrelere bağlı olarak, açığa çıkan enerjinin değeriyle kontrol edilebilmektedir. Bu çalışmada, bu üç lazer parametresinin değiştirilmesinin KF/PEEK kompozit yüzeyine etkisi SEM görüntüleri ile elde edilmiş ve PEEK matrisinin karbon fibere zarar vermeden yüzeyden seçici olarak uzaklaştırılması için gereken optimum enerji değeri için lazer parametrelerinin uygun çalışma aralıkları belirlenmiştir. Çalışmada istenilen yüzey kalitesini elde etmek için lazer parametrelerinin optimum çalışma aralıkları belirlendikten sonra, hazırlanan numuneler üzerinde tek turlu kesme (SLS), Charpy darbe ve çift konsol kiriş (DCB) testleri hem lazer hem de yüzeyleri lazer ile işlenmemiş referans numuneleri için gerçekleştirilerek, lazer yüzey ön işleminin mekanik özellikler üzerindeki etkileri net bir şekilde ortaya konmuştur. Birleştirme yüzeyleri uygun lazer parametreleriyle işlenen numunelerin mekanik dayanımlarında artış sağlanmıştır. Bu artış yüzey pürüzlülük parametreleri ve temas açısı ölçüm değerleri ile ilişkilendirilerek açıklanmıştır.

TABLE OF CONTENTS

LIST OF FIGURES

Figure **Page**

Figure **Page**

Figure **Page**

LIST OF TABLES

CHAPTER 1

INTRODUCTION

This section provides information on thermoplastic materials and various properties of these materials. In particular, general characteristics of CF/PEEK thermoplastics and laser surface treatment, which is one of the surface treatments required to increase the bond strength of these materials, are given. The purpose of the study, its contribution to the literature and its novelty are given in this section.

1.1. Background

Thermoplastics have become the material of choice for the aerospace industry due to their advantages over thermosets such as end-of-life recyclability, high fracture toughness, improved damage tolerance, corrosion and impact resistance and cost effectiveness. Recent studies show that thermoplastic manufacturing and joining processes reduce the production costs and allow simple structures to be joined to produce large and complex structures. As a result of their rising potential for high performance applications, continuous carbon fiber thermoplastic composites are increasingly being used for structural components.

Nowadays, continuous carbon fiber reinforced polyether ether-ketone (CF/PEEK) composites are increasingly used as structural parts in large-scale industrial fields such as aeronautics and astronautics, due to their excellent impact resistance, unique high-temperature performance, high manufacturing efficiency and recyclability. [1]

This greater interest has led to the need for more complex structures, which makes joining the critical step in their production. Although traditional joining methods are suitable for thermosets and metals, they are not feasible for thermoplastics. Some of the disadvantages of mechanical joining, which is one of the traditional joining methods, can be summarized as follows: it creates extra stress concentrations area in the material, causes weight increase, leads to delamination during drilling, contains fasteners and composite materials with different thermal properties and has the potential for galvanic corrosion to occur. [2]

Adhesive bonding is preferred over mechanical and fusion bonding methods because it has advantages over other conventional joining methods, including lightening of the structure, uniform stress distribution, vibration dampening, reduction of corrosion. However, in order to achieve an effective bond and maximum bond strength, surface treatment is often required in the adhesive bonding process.[2]

One of the innovative methods of surface pretreatment of fiber-reinforced polymer is the application of laser treatment to achieve selective removal of the resin without damaging the fibers. It involves the use of a focused laser beam to selectively heat and melt the surface, resulting in various beneficial effects.[3]

The laser surface treatment process can be used to improve surface roughness, increase surface energy and wettability, and change the chemical composition of the surface. Since there is no mechanical contact in surface pre-treatment with laser, tool wear does not occur. It also provides high flexibility and automation.[3]

Different types of lasers can be employed for materials, such as Nd: YAG, excimer, IR-Yb (Ytterbium), diode, CO2, and UV lasers. Different types of laser sources with different wave and pulse lengths can be used for various purposes. For this reason, it is very critical to determine the purpose of the laser surface treatment and to choose the laser type accordingly.[4]

In laser operation, the appropriate working range of parameters must be set for each different material and these parameters must be optimized. Using the same parameter settings for each material may lead to undesirable results. Therefore, the optimization of parameters for CF/PEEK composite material is very critical for this study.

According to the studies in the literature and the limitations of the nanosecond pulsed IR-Yb fiber laser devices used in our laboratory, three main laser treatment variables must be considered when determining the laser surface treatment process parameters of the CF/PEEK thermoplastic materials to be used in the study. These are output power, scanning speed, and frequency of the laser.

The effects of these parameters on the laser surface treatment are summarized separately below:

- ➢ Laser output power: The higher the output power parameter is set, the greater the effect of the laser system on the material being treated.
- ➢ Scanning Speed: The higher the speed parameter is selected, the less the treating effect of the laser system on the material.

➢ Frequency: The effect of the frequency parameter on treating is similar to speed. The higher the frequency value, the less the treating effect is. This is because fewer scan lines are placed in the treating area.

According to studies in the literature, the effects of a single laser parameter can be summarized as above. However, to achieve the desired surface finish, these three parameters must be varied during parameter selection, and the optimum working ranges must be determined by fine-tuning the laser parameters for each material. For instance, the resistance of thermoplastic materials to laser beam is not as high as metal materials and when such materials are exposed to laser beam, they are affected more than metal materials. For this reason, extreme caution should be exercised when laser treating thermoplastic materials. Shortening the processing time can make it easier to achieve the desired surface finish.

1.2. Aim of the Study

The objective of this study is to improve the joint performance of structural fiber reinforced thermoplastic composite parts used in the aerospace industry. For this purpose, the mechanical strength of the CF/PEEK thermoplastic material in the bonding region is to be increased. In this context, an innovative approach has been taken by applying a laser surface modification prior to the adhesive bonding process. The aim of the laser surface treatment is to achieve maximum surface roughness with minimum fiber damage on the laser treated surface by optimizing the laser parameters. While optimizing the laser parameters, one of the important results of the study is to reveal the effects of changing the parameters on the surface. In order to obtain the desired surface after laser treatment of the CF/PEEK material, it is aimed to determine the optimal operating parameters of the nanosecond pulsed IR-Yb fiber laser and accordingly the required release energy values.

Another critical objective of the study is that the use of epoxy-based film adhesives, which are widely used in the aerospace industry, is limited for thermoplastic materials due to the chemical incompatibility of the matrix material of the thermoplastic composite and the adhesive. By removing the PEEK matrix from the surface with the nanosecond IR-Yb fiber laser surface treatment used in the study, the adhesive contacts the carbon fiber and this chemical incompatibility is eliminated. This expands the

application range of the adhesive, which is widely used in the aerospace industry, and creates more mechanically durable bonded structures.

1.3. Novelty of the Thesis

Nanosecond pulsed laser surface treatment is widely used for fiber reinforced thermoset matrix composites, especially epoxy matrix composites. Furthermore, this thesis contributes to the literature by investigating the nanosecond pulsed IR-Yb fiber laser surface treatment of carbon fiber reinforced thermoplastic matrix composites (CF/PEEK) and the effect of laser parameters to improve mechanical properties prior to adhesive bonding for the aerospace industry.

Another novelty of this study is to reveal the effect of nanosecond pulsed IR-Yb fiber laser on CF/PEEK material, which has not been studied much in the literature. In this study, the effects of parameters that are important in achieving the desired final surface properties in the laser process were investigated. In addition, the incompatibility of the epoxy-based film adhesive, which is widely used in the aerospace industry, with the PEEK matrix limits the application range of this adhesive. In the present study, the PEEK thermoplastic matrix removed from the surface by laser surface treatment made the CF/PEEK composite structure to be bonded compatible with this adhesive. The application range of epoxy-based film adhesive, which is widely used in the aerospace industry, can also be developed for fiber reinforced thermoplastic materials as shown in this study.

In addition, as another new aspect of this study, the optimum range of the released energy value produced on the surface by the nanosecond pulsed laser beam at IR wavelength for CF/PEEK thermoplastics was clearly determined depending on the desired surface quality.

The effect of varying laser parameters and changes in microstructure was clearly seen by SEM analysis, and the optimum operating ranges determined for the laser process parameters were confirmed by mechanical tests and various surface roughness parameters.

In particular, the adhesive bonding mechanism created on the surface by the laser process, which increases the mechanical strength of the bonded area, has been clearly demonstrated.

1.4. Thesis Outline

Chapter I briefly discussed the importance of thermoplastic materials, in particular CF/PEEK thermoplastic composites, and the benefits of using thermoplastics in the aerospace industry, the advantages of adhesive bonding and laser surface treatment. After this brief background information, the aims and objectives of this thesis have been listed. At the end of the chapter, the novelty of the thesis was mentioned.

Chapter II provides general information on composite materials, including their definition and classification. In particular, thermoplastic composites and their manufacturing techniques and applications were mentioned. These general perspectives on thermoplastic composites may be useful to researchers unfamiliar with these fields. In addition, the joining methods used in composite materials, their advantages and disadvantages are given. The adhesive bonding technique and its application, which is also widely used in the aerospace industry, are mentioned. Also included are the joining methods used in composite materials, their advantages and disadvantages are given. The adhesive bonding technique and its application, which is also widely used in the aerospace industry, are mentioned. In particular, surface pre-treatments applied to the surfaces to be joined prior to the adhesive bonding process are explained. Among these treatments, laser surface treatment, which is one of the most suitable surface treatment methods for carbon fiber reinforced PEEK composite, is explained in detail. Different laser light sources, types, and wavelengths used in these studies were reviewed in detail. The studies on these topics, their contents and where there are gaps in the literature are shown. The study was designed with these points in consideration.

Chapter III details the experimental studies and techniques performed for this study. Information was provided on the materials used in the study, the manufacturing techniques, the production of samples, the mechanical tests performed and the standards according to which they were carried out, the analyses applied, and the equipment and apparatus used to perform them. The production of CF/PEEK composite plates was mentioned as one of the thermoplastic composites whose fields of application are expected to expand because it is a sustainable material and is widely used in the aerospace industry. Thermal properties of these produced CF/PEEK plates were determined by DSC analysis. In order to pave the way for more widespread use of these materials in joined structures, the adhesive bonding process and the nanosecond pulsed IR-Yb laser surface

treatment method used to increase the bond strength before the adhesive bonding process are explained in detail. Then, the mechanical properties of the bonded structures fabricated with the film adhesive were revealed by single lap shear test, double cantilever test, and Charpy impact test. The effect of the laser surface treatment process on the surface with changing parameters was investigated using optical microscope and SEM analysis, contact angle analysis, and profilometer.

Chapter IV presents the results of thermal, mechanical, and surface analysis and the effect of laser parameters on the microstructure of the CF/PEEK surfaces. The thermal properties of the fabricated CF/PEEK plate are shown in the DSC thermograph. The influence of the laser surface treatment parameters used to improve the mechanical properties of the joint areas is shown in optical and SEM micrographs for control and laser samples. According to these results, optimal operating ranges for the laser parameters were determined. This chapter also compares single lap shear strength, Mode-I fracture toughness, and Charpy impact energy values for bonded CF/PEEK structures for laser treated and reference specimens. Surface profilometry and contact angle results are given for the laser parameter that gave the highest results in the SLS test and the reference samples. The reason for the increase in mechanical testing achieved by laser surface treatment is demonstrated by these analyses. The results obtained in this section will contribute significantly to the literature, especially on topics such as the energy thresholds required to obtain the desired surface in nanosecond pulsed IR laser surface treatment of CF/PEEK material and the effects of laser parameters on the microstructure.

Chapter V contains the results obtained throughout the study, evaluations of these results, and some important points. In addition, new studies that may be conducted on this topic in the future are given.

CHAPTER 2

FUNDAMENTAL CONCEPTS AND LITERATURE REVIEW

This chapter provides general information about composites. In particular, thermoplastic composites, their classifications, manufacturing techniques, and applications are mentioned. It also includes general information on joining and surface pre-treatment methods for composite materials. In particular, detailed information is given about laser surface pretreatment. Also, adhesive bonding mechanisms of composites are mentioned. Studies on these topics in the literature have been reviewed in detail and the results have been interpreted.

2.1. Definition and Classification of Composite Materials

In ancient times, people discovered that some of their materials had much better properties when they were combined with other materials. For example, mud bricks were strengthened with straw, or in ancient Damascus, warriors strengthened their swords with layers of iron and steel. This was evidence of significant advances in buildings and weapons, respectively. Over time, the search for new materials in every field has paved the way for the development of composite materials.[5]

Composite materials, which have been widely used in recent years, are materials that consist of at least two different components that are physically and chemically separated. However, these materials are combined to achieve specific characteristics and better properties than the individual materials.[6,7]

In addition, as the definition of composites indicates, they are heterogeneous and anisotropic materials, which means that the mechanical properties of composites vary with the direction of loading.[1]

Composite materials consist of two phases: matrix (base material) and reinforcement (filler material).

The matrix is a continuous phase that maintains the geometric arrangement of the fibers, transfers loads between the fibers, and protects them from abrasion. The matrix material used in composite materials can be metals, ceramics and polymers.

Reinforcement is a discontinuous phase that provides strength and stiffness and carries the applied load to the material.[8] Filler or reinforcing material may take the form of natural or synthetic fragments, particles, fibers, or whiskers.[9,10]

Composite materials have been used extensively in recent years because they offer high specific stiffness, high specific strength, and toughness while being lightweight. They are also highly resistant to high temperatures, chemicals, wear, and corrosion.[11–14] Because of these superior mechanical and structural properties, composites are used in a wide variety of industrial applications.

The graph in Figure 2.1 allows for a comparison of composite applications in a variety of industries.

Some of these applications are for the electronics industry, such as insulators, antennas, cable conduits; for construction and public works, such as housing cells, chimneys, concrete forms, etc.; body components, wheels, cabins for road, rail and marine transportation; many aircraft (fuselage, wing and interiors parts) and engine component applications in the aerospace industry; energy fields such as wind turbines and hydrogen tanks; sports and leisure goods such as tennis rackets and bicycles.[1]

Also, Figure 2.1 illustrates that the highest percentage distribution of the total weight (tonnage) of composites according to application areas is civil engineering and transportation.

On the other hand, the graph also demonstrates that the industries with the highest application areas are aviation and space and transportation, with the highest percentage distribution of the total value according to application areas.

Especially in recent years, thermoplastic composites have been widely used in these industries since they are sustainable materials. Furthermore, there has been a rise in interest in composites in industrial sectors such as renewable energy production and storage. As demand for these areas continues to grow, the search for stronger materials with superior properties intensifies. This situation places composite materials in a position of advantage relative to other materials.

Another noteworthy attribute of composite materials is their versatility in terms of material options, which are tailored to specific applications. This allows practitioners to select the most suitable composite material for a given purpose, given the desired properties. In fact, a multitude of materials with varying properties can be produced through diverse joining methods, depending on the desired properties.

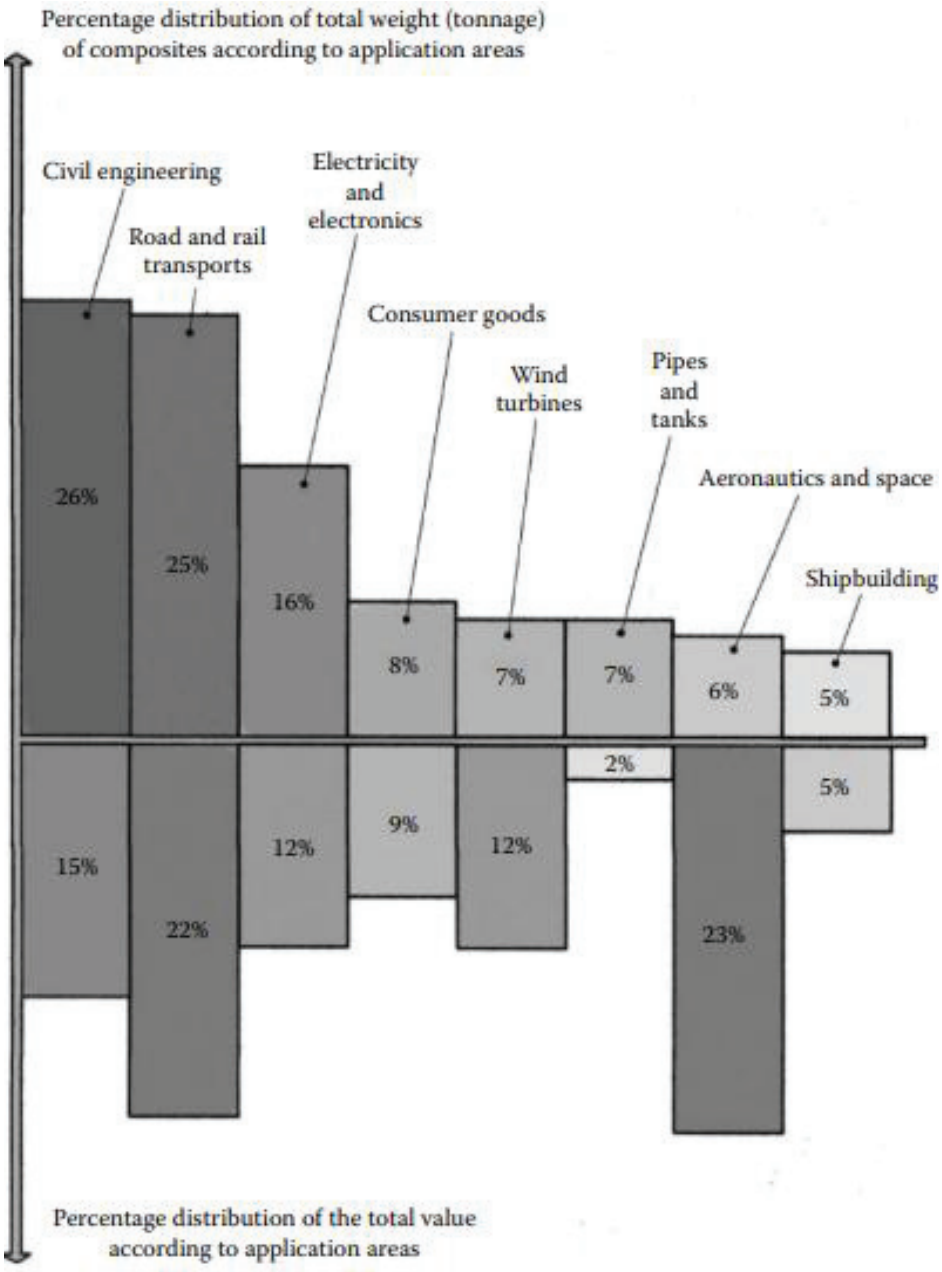

Figure 2.1. Composite applications and their percentage of the total in the various industries.[1]

Depending on the type of constituents and matrix, scale, and whether they are biodegradable, composites can be classified as shown in the Figure 2.2.

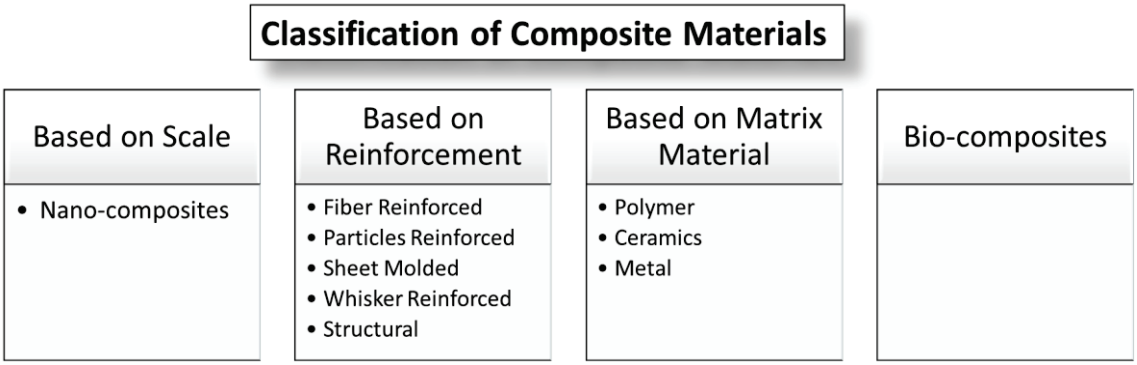

Figure 2.2. Classification of composite materials.[15,16]

Firstly, composites are divided into three main groups based on matrix type which are polymer matrix composites (PMCs), metal matrix composites (MMCs), and ceramic matrix composites (CMCs).

Polymer matrix composites are the most widely used composites due to their low production cost and ease of handling. They can be categorized according to whether the matrix is a thermoset or a thermoplastic polymer. Polymer matrix composites consist of thermoset or thermoplastic matrices usually reinforced with aligned glass, carbon, Kevlar and metal fibers.[17–20] Although thermoset matrix composites have traditionally been more widely used, thermoplastic matrix composites have become the focus of research in recent years. Both thermoset and thermoplastic matrix composites have many advantages and disadvantages depending on the application. For example, thermoplastics have lower manufacturing costs than thermosets. They also have thermal formability, weldability, and better mechanical properties such as high toughness. For this reason, it is very important to select a matrix that is appropriate for the application and intended use of the composite materials.[21]

Metal matrix composites consist of a metal or alloy matrix reinforced with dispersed metallic, ceramic such as oxides and carbides, or organic compounds to improve the tribological properties, high thermal and electrical conductivity, specific strength and stiffness, corrosion, and wear resistance, etc. The most commonly used metal matrices are aluminum (Al), magnesium (Mg), titanium (Ti), and copper (Cu). Although

magnesium-matrix metal composites have many superior properties, they are not as widely used in industry as aluminum-matrix metal composites due to their disadvantages such as low fracture strength and susceptibility to environmental conditions. Aluminum matrix metal composites are preferred due to their light weight, low cost, desired strength and stiffness, resistance to wear and corrosion, and low density.[22] Reinforcements such as SiC, tungsten, and alumina are widely used to further enhance the aforementioned properties of MMCs, reduce density, and control thermal expansion.[15]

Ceramic Matrix Composite (CMC) is a composite material consisting of a ceramic matrix reinforced by fibers, ceramic particles such as silicon carbide (SiC), aluminum oxide (Al_2O_3) etc., whiskers, graphene, and second phases like a metals or polymers. Ceramic matrices can be divided into three groups: oxide matrix (Al_2O_3, ZrO_2, YAG, TiO_2, etc.), non-oxide matrix (SiC, Si_3N, etc.), and glass ceramic matrix (calcium alumina silicate (i.e., CAS), lithium alumina silicate (i.e., LAS), etc. [23]

The most distinctive feature of ceramic matrix composites is that they have high mechanical properties even at high temperatures and excellent thermal shock resistance. In addition, they have excellent wear resistance and high fracture toughness. These features make it widely used in industries like defense, aerospace, automotive, and energy.

On the other hand, composites are classified as fibers, particles, whiskers and structural based on the form of reinforcement in their structure, and as nanocomposites based on their scale. In addition, they can be classified as a bio-composite based on their ability to be biodegradable.[15]

2.2. Thermoplastic Matrix Composites

Polymer matrix composites are classified according to whether the polymer used as the matrix material is thermoplastic or thermoset. Thermoplastics have the simplest molecular structure with macromolecules that are chemically independent of each other. Thermoplastic polymers are polymers that have a high melt viscosity at their melting temperature, and when the polymer matrix used in the composite is selected from thermoplastic polymers such as polypropylene (PP), polyetherketone (PEK), polyamide (PA), and polycarbonate (PC), etc., these materials are classified as thermoplastic composites. Because thermoplastics do not have cross-link, they are recyclable materials

that can be reshaped by applying heat even after they have cured. However, a thermoset polymer is irreversibly cured from a liquid resin when heated. Unlike thermoplastics, thermosets don't melt once cured and cannot be recycled/reprocessed.[24]

Thermoplastics have been used in composite structures since the late 1960s. Due to the increase in demand for advanced materials as technology evolves, thermoplastics have become the material of choice for many industries. Interest in thermoplastics has increased in recent years due to their advantages such as ability to be recycled/reprocess abled, low water absorption, high fracture toughness, high strength to weight ratio, ease of assembly and cost effectiveness. In particular, its recyclability and ease of production have made it a preferred material over thermosets.[25]

Thanks to these properties, thermoplastic composites are widely used in many applications in different industries such as aerospace, automotive, energy and power, transportation, construction, biomedical, sports.[24] The automotive industry, for example, is one of the most important application areas for the thermoplastic composites. Many manufacturers aim to improve fuel efficiency by replacing the metals and steel used in vehicle parts with lighter-weight thermoplastic composites. This reduces the overall weight of the vehicle and improves fuel efficiency.

According to the European Commission[26], the target for cars is to reduce carbon emissions from 130 grams per kilometer to 95 grams per kilometer by 2024. This is to be followed by a further 15% reduction by 2029 and zero carbon emissions by 2035 and beyond. This is expected to increase the demand for thermoplastic composites in automotive manufacturing. In addition, the air transport sector will have to make a contribution to this reduction.[27] It has been observed that the use of thermoplastics in various parts in the aerospace industry has increased, especially after the 2000s. In particular, PEEK and PEKK thermoplastics are the most widely used resin in various applications including aerospace, automotive, biomedical, high temperature electrical structure, helping to produce parts that are a combination of lightweight and strong.[28] Moreover, the cost effectiveness of thermoplastic composites has been proven in many studies to outperform their aluminum and thermoset counterparts. These parts include landing gear doors, ribs, and floor panels.[29]

In addition, the global thermoplastic composites market size is expected to reach approximately USD 64.07 billion by 2032, growing at a compound annual growth rate (CAGR) of 8% during the forecast period from 2023 to 2032 (Figure 2.3).[30]

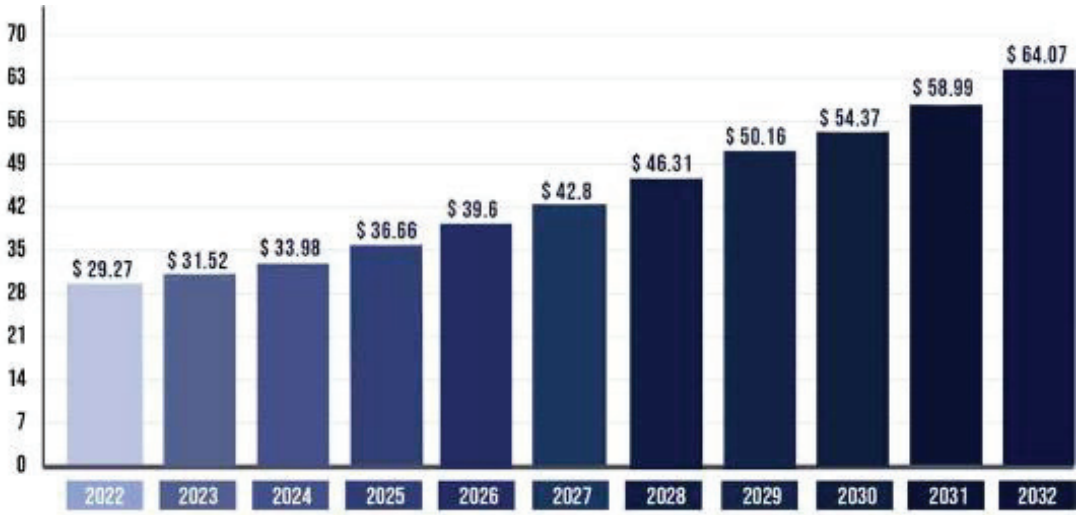

Figure 2.3. Thermoplastic composites market size, 2022 to 2032 (USD billion).[28]

Sudhin A.U. et al.[31] compared the mechanical and physical properties of carbon fiber reinforced thermoplastics (CF/PEK) and thermoset composites (CF/Epoxy) for aerospace applications. According to the tensile test, CF/PEK composite exhibits a tensile strength of 425 MPa, which was much higher than 311 MPa obtained by CF/Epoxy. The Mode-I fracture toughness (K_{IC}) values of CF/PEK composites are observed to be 10% higher than CF/Epoxy counterparts. On the other hand, in accordance with the results of physical properties of both the thermoset and thermoplastic composites, the CF/PEK composites are found to have higher glass transition temperature (Tg), which allows them to be used at elevated temperatures. The examination of flame-retardant properties of the composites is carried out by Limiting Oxygen Index (LOI) test, and the highest value is obtained for CF/PEK composites. As a result, the application range of CF/PEK thermoplastic materials is expanding compared to their thermoset counterparts.

2.2.1. Raw Materials for Thermoplastic Composites

Composite materials, as mentioned earlier, consist of matrix and reinforcement structures. Raw materials for thermoplastic composites are examined under two main topics: matrix and fiber reinforcement. While the reinforcing materials of thermoplastic composites are found in a variety of structures, the matrix material consists of thermoplastic polymers.

2.2.1.1. Matrix Materials

In composites, the matrix material is the component that holds the fibers together, distributes the loads between the fibers, prevents from buckling in compression of the fibers, and ensures interlaminar shear strength. Appropriate matrix material selection is one of the most critical factors affecting material strength and service life.[32]

Thermoplastic matrices do not have the cross-links found in thermoset resins. The strength of these matrices depends on the properties of the monomers that make up the polymer chain and chain entanglement. Thermoplastic resin is available in two types: amorphous and semi-crystalline resin. Amorphous thermoplastics have a high degree of chain entanglement. This can be loosened by heating the material to a viscous liquid, which can then be cooled to form a part. Semicrystalline thermoplastics consist of a crystalline phase with a high level of molecular order and an amorphous phase.

Polyphenylene sulfide (PPS), aromatic polyimides, polypropylene (PP), and poly(ether-ether ketone) (PEEK) are some of the examples of thermoplastic matrix materials. PPS is an aromatic, semi-crystalline polymer with excellent chemical and thermal stability.[33] PEEK is one of the high temperature thermoplastics that has been widely used in the industry due to its superior properties. As this study utilized CF/PEEK thermoplastic material, a detailed examination of its specifications will be presented in the subsequent section.

2.2.1.1.1. Polyether ether ketone (PEEK)

Poly(ether-ether-ketone) (PEEK) is one such polymer, invented in 1978 and considered a super-engineered plastic with a wide range of rather special properties. PEEK started to be used industrially in the late 90's and continues to play an important role in industrial applications such as aerospace, automotive, industrial applications, biomedical.[34] PEEK is a semi-crystalline aromatic polymer with a linear linked structure, the chemical structure of which is shown in Figure 2.4. It is a member of the poly(aryletherketone) (PAEK) family, which includes several variants such as poly(etherketone) (PEK), poly(etherketoneketone) (PEKK), etc. Its superior characteristics include specific strength, low weight, good fatigue and impact resistance, good biocompatibility, excellent thermal and chemical resistance, etc.[35]

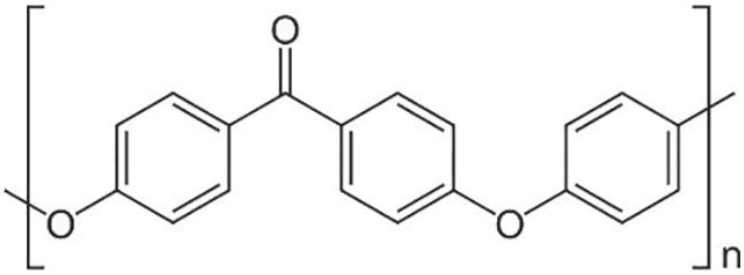

Figure 2.4.Chemical structure of Poly (ether ether ketone).[36]

2.2.1.2. Fiber Reinforcement Materials

In composites, the filler (reinforcement) material is another component in addition to the base material, which is the matrix phase. The filler material or reinforcement is present in the form of particles and fibers (continuous and short), whiskers made of natural or synthetic raw materials.[9,10,37] Continuous fibers can be used as unidirectionally oriented tapes or fabrics. The matrix phase in composites is a relatively softer phase and generally has certain mechanical properties such as formability, ductility, and thermal conductivity.[38] Embedded in the reinforcement of the matrix phase are materials with high strength and stiffness and low thermal expansion. The function of the reinforcement phase is to carry the longitudinal tensile and compressive loads applied to the composite and to increase the mechanical performance of the composite. Therefore, the reinforcement phase in composites is generally stronger and more rigid than the matrix phase.[15]

Fiber-reinforced composites offer many advantages over other reinforcing elements, including ease of structural design and controllability. They can be used in a wide variety of applications. Fiber reinforcement materials can generally be divided into three groups. These are aramid, glass, and carbon fibers. Glass and carbon fibers in particular are extensively utilized in high performance composites.[39] As fiber orientation in composites has a direct effect on mechanical properties, orienting as many fibers as possible in the main load-bearing direction will have a positive effect on the load bearing capacity of the material. Common composite reinforcing fibers and some of their properties are listed in Table 2.1.[32]

Table 2.1. Properties of Typical High Strength Fibers.[40]

Fiber	*Density lb/in.^{3}*	*Tensile Strength (ksi)*	*Elastic Modulus (msi)*	*Strain to Failure (%)*	*Diameter (mil)*	*Thermal Expansion Coefficient 10^{-6} in./in./° F*
E-glass	0.090	500	11.0	4.8	0.36	ρ.8
S-glass	0.092	650	12.6	5.6	0.36	1.3
Quartz	0.079	490	10.0	5.0	0.35	1.0
Aramid (Kevlar 49)	0.052	550	19.0	2.8	0.47	−1.1
Spectra 1000	0.035	450	25.0	0.7	1.00	−1.0
Carbon (AS4)	0.065	530	33.0	1.5	0.32	−0.2
Carbon (IM-7)	0.064	730	41.0	1.8	0.20	−0.2
Graphite (P-100)	0.078	350	107	0.3	0.43	−0.3
Boron	0.093	520	58.0	0.9	4.00	2.5

2.2.1.2.1. Aramid Fibers

Aramid fiber is a type of synthetic fiber containing at least 85% amide bonds between the aromatic rings.[41] The excellent properties of aramid fibers, including high specific strength, high damage tolerans, high specific modulus, and high temperature resistance, have made them a popular reinforcing material in polymer composites. Despite these advantages, the smooth and chemically inert surface of aramid fibers severely restricts their applications. Various surface modification methods can be used to modify the aramid fiber surface to improve chemical bonding and mechanical interlock between fiber and matrix.[39]

2.2.1.2.2. Carbon Fibers

Carbon fibers are known for their high strength, high modulus, and low density. Their tensile strength is up to 7 GPa and Young's modulus is up to E ≤ 900 GPa in case of high-modulus carbon fibers with good creep resistance and an associated density that varies from 1.75-2.00 g/cm^3. Although carbon fibers are resistant to all chemical species, they are not resistant to oxidizing agents like hot air and flames and will self-combust above specific temperatures. The functional importance of carbon fibers is due to their high electrical conductivity. Carbon fibers can be used not only as reinforcements, but also as additives to increase electrical or thermal conductivity, since polymers and

ceramics used as matrix materials in composites have no electrical or thermal conductivity.[21]

Carbon fiber is often delivered in the form of a continuous tow wound on a roll. Tows are bundles of thousands of continuous single carbon filaments held together and shielded by an organic coating or size, such as polyethylene oxide (PEO) or polyvinyl alcohol (PVA). Traditional PAN and pitch-based carbon fibers have been used to improve and optimize the properties of many structures due to their good mechanical, thermal and electrical characteristics.[42]

A carbon fiber is a result of the conversion of a polymer fiber into a carbon fiber. Continuous carbon fiber is typically 7μm in diameter. Controlled by the manufacturing process, a carbon fiber can have different degrees of crystallinity.[21] The commercialization of carbon fiber is growing significantly in several sectors with different applications. Industries such as renewable energy, aerospace and defense, sports and consumer goods are driving total annual carbon fiber production to commercial scale, where growth is expected to reach approximately 142 kilo tons annually in the 2020s. Approximately 96% of all commercially available carbon fiber is made from PAN precursors.[43]

Carbon fiber reinforced composites are used in a wide variety of applications in various industries due to their mechanical advantages despite their high cost. Industries such as aerospace, automotive, energy, transportation and marine are some of these. The use of carbon fiber reinforced composites in place of aluminum alloy parts in the vertical stabilizer of an aircraft results in a total weight savings of approximately 400 kg. Given that a weight reduction of one kilogram is estimated to result in an annual fuel savings of approximately 2,900 liters, the fuel and cost savings realized by using carbon fiber-reinforced parts instead of metal parts in aircraft components are tremendous.[27,44]

While the use of continuous fibers is more common in structural parts, short fibers are also used in the automotive industry in applications such as car body structures (e.g. hood and interior trim), fuel cells.[42] Short fiber reinforced polymers have also been developed to fill the mechanical property gap between continuous fiber laminates, widely used in the aerospace industry, and unreinforced polymers used in non-structural components.[45,46]

2.2.1.2.3. Glass Fibers

Glass fibers are formed from melts and produced in various compositions by changing the amount of raw materials such as sand, clay, calcite and colemanite. Thus, various types of glass fibers have different characteristics.[47]

Glass fibers are among the most widely used reinforcements due to their good combination of mechanical properties and low cost. Glass fibers are available with different properties, including E-glass, S-2 glass, and quartz. E-glass, or "electrical" glass, is the most common glass fiber and is widely utilized in industrial composite applications. S glass and S-2 glass, or "structural" glass, was developed to satisfy higher strength requirements for filament-wound pressure vessels and rocket casings.[48] Glass fiber types and their physical properties are shown in Figure 2.5.[49] The type of fiber should be selected according to the application. It has a density, structural performance and cost that are intermediate between E-glass and carbon fiber. Quartz fiber is one of the most costly glass fibers and is preferred in some electrical applications due to its low dielectric constant.[48]

Woven fiberglass fabrics are useful thermal insulators due to their high surface area to weight ratio. However, their high surface area makes them much more susceptible to chemical attack. With the development of technology, the application areas of these glass fiber reinforced composites with various properties have increased. Electricity, sound and heat insulation, marine industry, renewable energy (especially wind turbines), aviation applications, automotive fields, sports equipment, sheet metal molding applications are some of the usage areas.[50]

Glass fibers are produced in various forms such as longitudinal, woven mat, chopped fiber, and chopped mat, depending on the application, to optimize the properties of composite materials.[49] In terms of energy efficiency, vehicle lightweighting is the most important reason for energy conservation in the transportation industry. In this aspect, the increase in the manufacture of lightweight parts of cars and planes to approximately 50% shows the significance of glass fiber reinforced composites. As a result, glass fiber production has grown and will continue to grow in the future.[47]

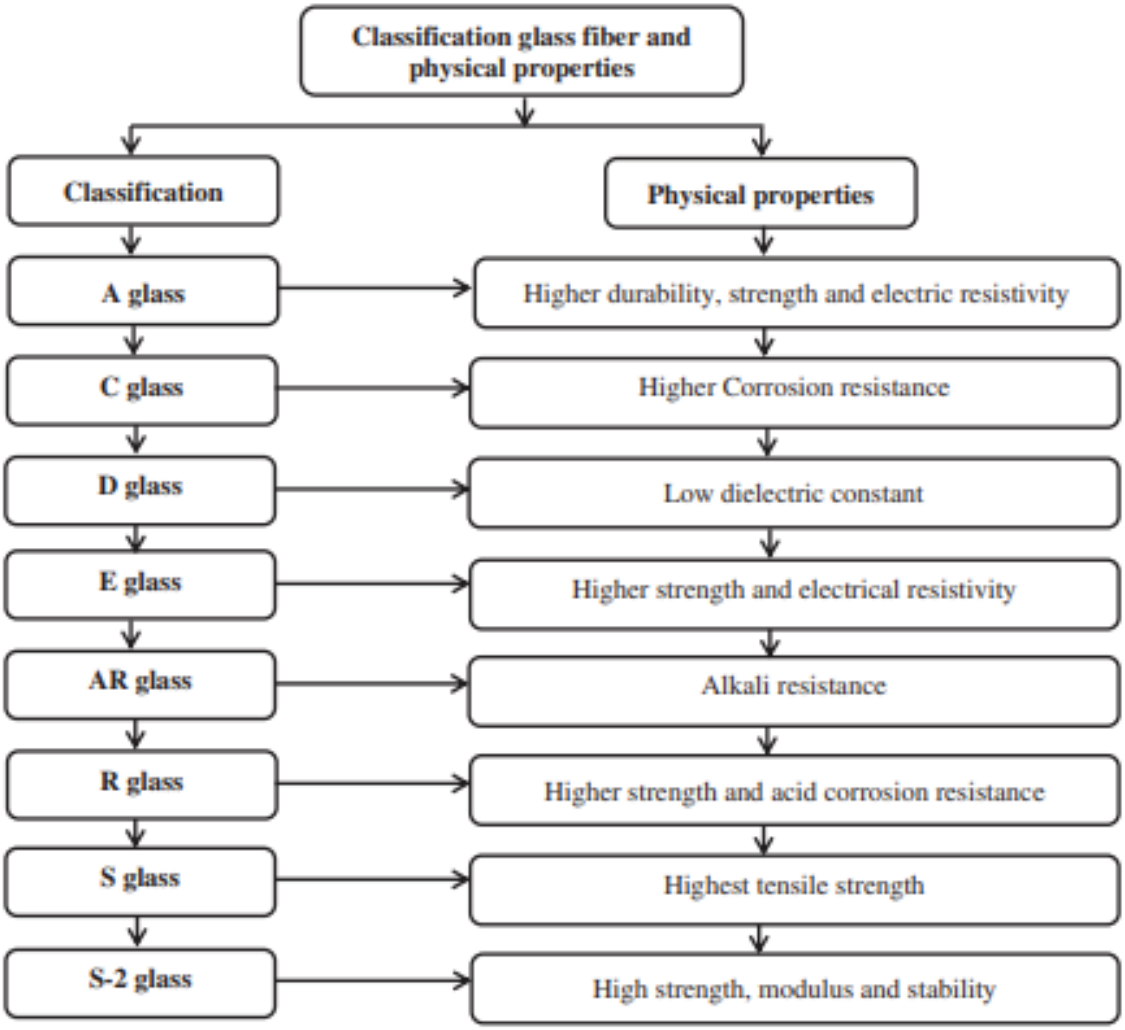

Figure 2.5. Classification and physical properties of various glass fibers. [49]

2.2.2. Manufacturing Techniques for Thermoplastic Composites

Depending on their properties and applications, thermoplastic composite materials require different processing techniques. Determining the process method and parameters suitable for the purpose is very critical.

Based on the type of matrix polymer (thermoset or thermoplastic), the manufacturing techniques used to produce polymer composites can be examined into two groups. Although there are common production methods used in both groups, there are changes in the production parameters depending on the type of matrix to be used. Several manufacturing techniques can be used to produce the polymer matrix composites (Figure 2.6).

Injection molding or screw extrusion is the most widely used process for the production of thermoplastic materials because of its advantages, such as being an automated process that offers the best quality at low cost and the ability to produce customized and complex products with the desired reinforcements in a short time. In addition, this process can be used to recycle non-degradable plastic waste, which is a huge problem today, and use these plastics in many applications. This would lead to sustainable production and lower manufacturing costs. It would also reduce the environmental impact of using waste products.

The diaphragm forming process is specifically used to produce double-curved products, plates, and large-area components. In this method, a laminate is sandwiched between two diaphragms, which are fixed in a mold after the application of vacuum. These are placed in an autoclave and heated at high temperature until a hydrostatic pressure differential is created that forces the laminate/diaphragms into the mold.[51,52]

Autoclave processes are typically used to produce fiber reinforced plastic (FRP) composites for high structural applications.[53] Layers of resin-impregnated fibers (known as prepregs) are layered on a mold to form the required component shape. The mold laminate assembly is placed in the autoclave, which is temperature and pressure controlled. Prepregs are placed in an autoclave where they are cured at a controlled temperature and pressure.[54]

The compression molding process involves preheating metal molds on large molding presses. This process is typically used for complex molded fiberglass components requiring large volume and high compression.[55]

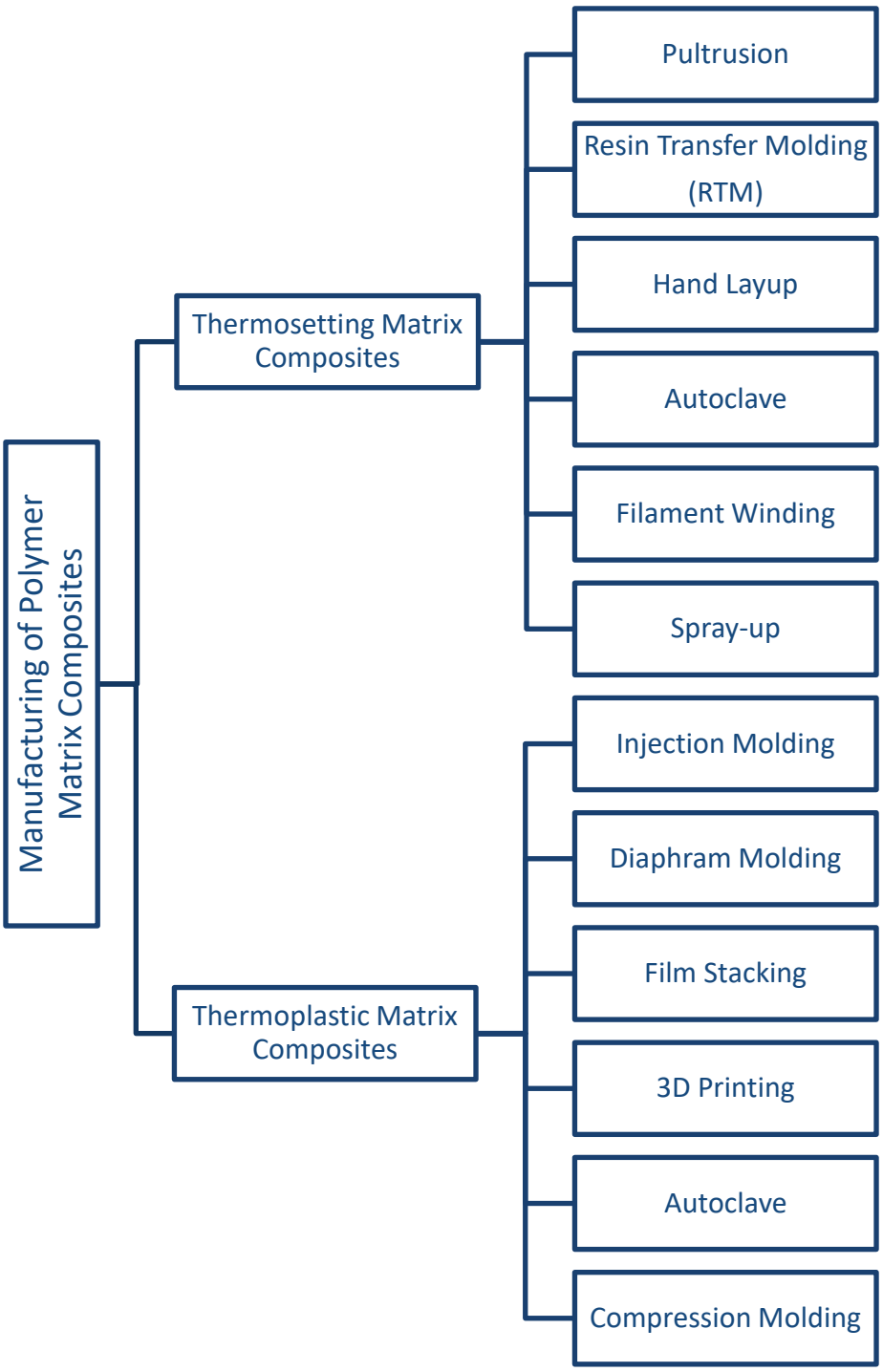

Figure 2.6. Manufacturing techniques of polymer matrix composites. [55]

Reduced material waste, design flexibility, and the ability to produce complex structures have led to widespread acceptance of 3D printing technology in automotive, aerospace, medical, and other engineering applications. An additive manufacturing or 3D printing process that uses inkjet technology to deposit hot, extruded layers of thermoplastic material over a bed of powder in a layer-by-layer pattern to create intricate structures with the desired geometry of 3D parts.

In this study, the hot-pressing technique was used to fabricate carbon fiber-reinforced/PEEK composite laminates. Therefore, this technique will be explained in more detail in the following paragraphs.

Another common manufacturing process to produce thermoplastic composite parts is press forming. The main advantages of the press forming process are:

• Faster manufacturing technique compared to processes such as hand lay-up and the autoclave process,

• Cost effective to manufacture.

• Both UD and woven fabrics can be formed.

• Being a repeatable process.[56]

In this manufacturing process, the composite layers are stacked in molds under specific heat and pressure, and the final thickness of the manufactured part is adjusted by the number of impregnated fabric layers introduced. After heat treatment, the thermoplastic composite part is allowed to cool in the mold under pressure. The schematic image of the hot-pressing machine is shown in Figure 2.7.

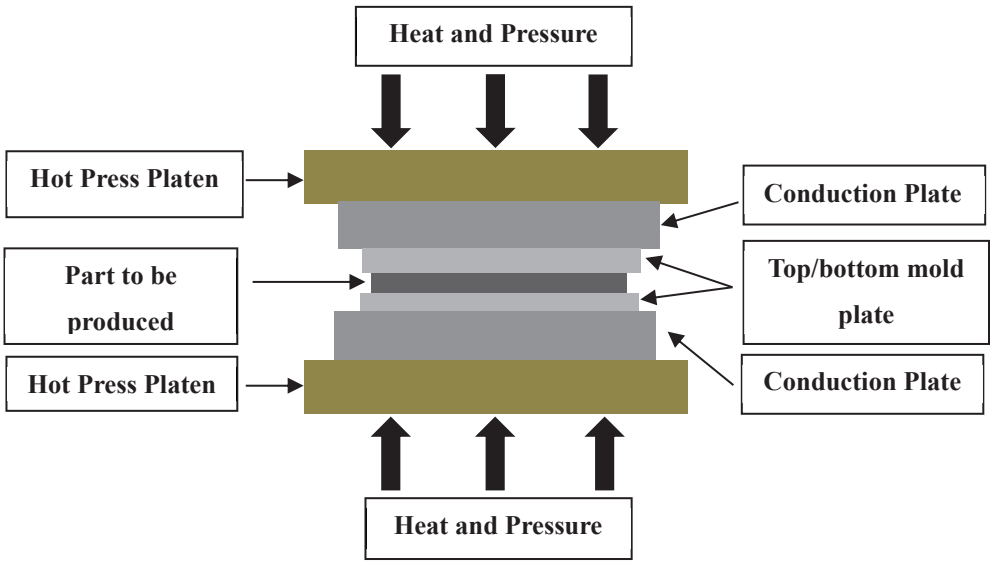

Figure 2.7. Schematic representation of the hot-pressing machine.

Hot pressing thermoplastic composite parts typically have a constant thickness and constant fiber orientation. In press manufacturing, three parameters have a major impact on the quality of the part produced at the end of production. These parameters are process temperature, press pressure, and dwell time.

Before molding, the composite layers must be within the moldable temperature range for the resin to melt. The process starts by heating to a specific temperature above the melting temperature (Tm) of the polymer matrix if the polymer matrix is semi-crystalline, or above the glass transition temperature (Tg) if the polymer matrix is amorphous. Determining this temperature range is very important. This is because temperature can cause various types of damage to the composite material during production. For example, if this temperature range is not selected correctly, the deformation may slip into the plastic region of the resin, causing permanent damage to the resin and the fibers attached to the resin, or thermal decomposition of the resin may occur. The function of the pressing pressure is to improve the bonding between the fibers and the resin and between the layers by compressing the composite sheets. If the press pressure is not well adjusted, poorly bonded areas will occur in the structure, causing voids and fiber fluctuations. All of these defects can lead to a reduction in the mechanical properties of the produced part.[57]

This method is widely used in the production of important parts in the automotive and aerospace industries. Examples include brackets, fasteners, ribs, automotive flex plates, stiffeners, and clips.[58]

2.2.3. Applications of Thermoplastic Composites

With the development of technology in recent years, energy crisis and environmental pollution have become increasingly important problems for humanity. The concept of sustainability has become more important than ever, and many of the strategies advocated in the past have proven to be inadequate. For this reason, energy efficiency, sustainability, and CO_2 emission reduction have become one of the main goals for many industries. The most effective way to achieve these goals is light and high-strength materials and their designs. For this reason, interest in fiber-reinforced plastic composites, which are lightweight and high-strength, has increased in many areas in various

industries. For example, as illustrated in Figure 2.8, they are used in automotive, aerospace, transportation, construction, sports, and other sectors.[59]

Figure 2.8. Some of structural applications of thermoplastics.[60,61]

Composites are widely used in automotive body panels and interior components. In addition, the vehicle body, door, vehicle floor and bumpers, ceiling and trunk panels, and the front of the car, are all made of composite materials. In fact, in recent years, lightweight four-cylinder engine blocks and cylinders have been developed from carbon fiber composites.[62]

The automotive industry's interest in fuel efficiency is growing by the day. By replacing many metal or steel parts used in automobiles with a thermoplastic material, lighter and stronger vehicle parts are produced, thus saving fuel. For example, Oztoprak et. al.[63] fabricated and designed the mono leaf spring component used in the automotive industry using glass fiber-reinforced composites instead of steel. Their prototypes showed a weight reduction of about 80% with improved mechanical properties.

High-performance thermoplastics (PPS, PEEK, PEKK, etc.) are the main materials used in the aerospace industry. These materials are called advanced engineering thermoplastics because they have high strength even at very high temperatures.

Thermoplastic materials commonly used in the aerospace industry and their properties are shown in Figure 2.9.

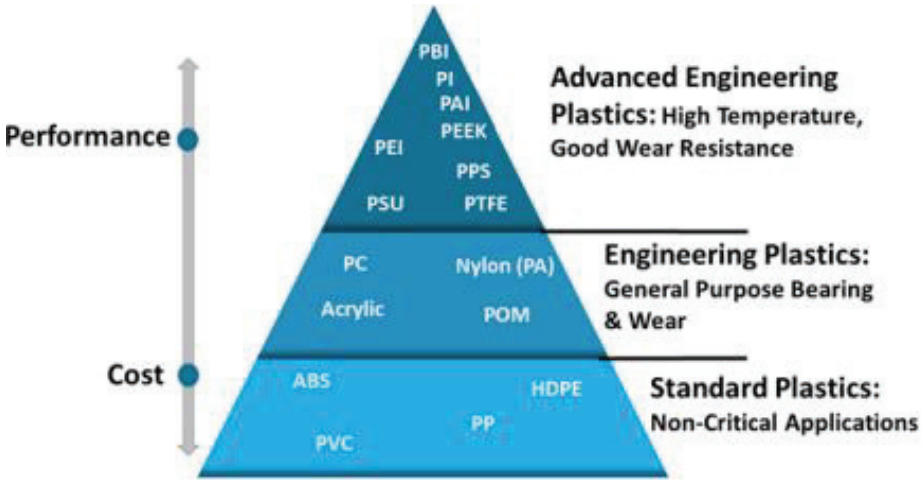

Figure 2.9. Properties and performance of thermoplastics.[64]

In the aerospace industry, high-performance thermoplastics are used in different applications depending on their properties. For example, PPS (Polyphenylene Sulphide) can be used in applications such as thermal protection and electrical connectors where high thermal stability and chemical resistance are required, or PEEK (Polyether Ether Ketone) should be preferred in areas such as connectors, brackets, and electrical insulators where long-term use at high operating temperatures is required without compromising mechanical properties. Also, Polycarbonate (PC) has high flame and impact resistance, excellent optical clarity, and is a lightweight thermoplastic. This makes it ideal for cockpit canopies, aircraft windows, and other components where both lightness and durability are required.

Figure 2.10 shows various aircraft components made from thermoplastic composites. They are used in parts such as seat frames, leading edges, fuselage clamps and cleats, and floor panel profiles.[30]

Carbon fiber-reinforced thermoplastic composite materials are widely used in aircraft fuselages, wing parts and interior parts such as floor panels, rudders and spoilers. For instance, carbon fiber reinforced thermoplastics were used extensively in the fuselage and interiors parts of the new Boeing 787 Dreamliner (2011) and Airbus A350 XWB (2015).[65,66]

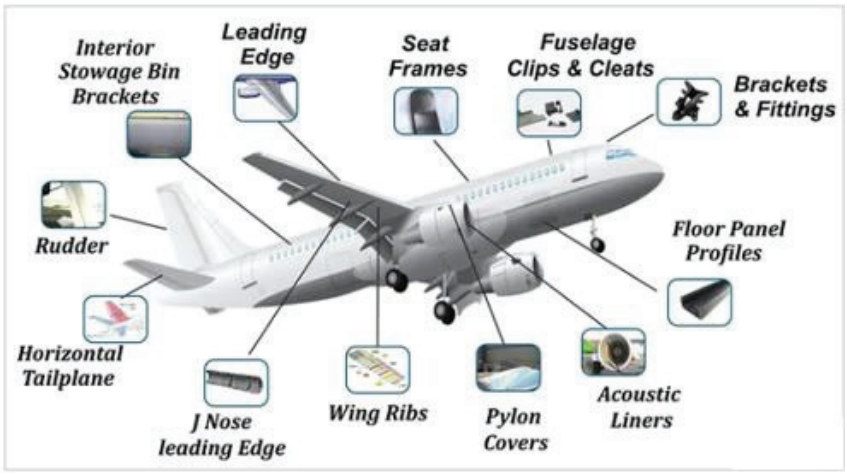

Figure 2.10. Thermoplastic aircraft components.[67]

Abderrafai Y. et al.[68], in their study, show the thermomechanical and microstructural properties of carbon fiber (CF) reinforced polyether ether ketone (PEEK) and polyether imide (PEI) thermoplastics for aerospace applications. The manufacturing process used in the study was fused filament fabrication (FFF), an additive manufacturing (AM) process for potential aerospace applications. In addition to the additive manufacturing process, samples were also produced using injection molding, one of the traditional manufacturing methods for thermoplastics, to determine the effect of the manufacturing process and compare the two manufacturing methods. Their results revealed that FFF printed high-performance thermoplastics are suitable for use in aerospace applications. They observed that the samples produced by this method had better UTS and modulus values in tests performed at room temperature compared to the samples produced by the traditional method. They also contributed to the development of this production method by performing microstructural studies. According to their predictions, once certain developments are achieved for this very new production method, many parts produced with this method can be used in aerospace applications, such as acoustic liners, fan case components, or engine parts.

Mondal M.K. et al.[69] investigated the usability of waste thermoplastics in cement as a building material in their study. For this purpose, three different bricks were produced for experimental studies from three different waste thermoplastics: polycarbonates, polystyrene, and mixed plastics (0-10% by weight). Their results show that the bricks produced were found to have low thermal conductivity and sufficiently high compressive strength. It has been observed that the compressive strength of these bricks is in the upper

half of the strength range specified for bricks in the IS 1077:1992 standard. The high thermal resistance and strength of bricks made from waste thermoplastics can add economic value to brick manufacturers and pave the way for these parts to be used in buildings. Additionally, the recycling and reuse of waste thermoplastics in this study is a commendable endeavour.

A variety of transportation products using thermoplastics, including airplane fuselage and wing parts, bullet train roof structural panels, bus structural panels, bullet train front ends, and interior non-structural panels have been developed and produced.[70] In transportation applications, high stiffness, strength, and resistance to damage combined with low weight are required for structural frame members due to strict design requirements. Thermoplastic polymers play a critical function in serving as the matrix in such composites. Among several potential thermoplastics, such as PPS, polypropylene (PP), and polyamide (nylon), PPS has superior tensile strength, bending modulus and chemical resistance.[71]

Another application for thermoplastics is underground piping. Traditionally, carbon steel is the most commonly used material for pipeline construction. However, steel pipelines have several limitations, including corrosion resistance, weight and cost. In the 1960s and 1970s, non-metallic materials were adopted as pipeline materials to eliminate corrosion problems and were used for low-pressure onshore gas distribution networks.[72]

2.3. Joining Methods of Composite Materials

As technology evolves, the need for materials with different properties increases every day. This means that in many applications, the performance expected from more than one material must be expected from a single part. In addition, if the static structure is too large, the possibility of making it from a single piece decrease as the size increases. In primary manufacturing, there are always size and shape limitations, both static and dynamic. For these reasons, the joining process is required for parts that require different properties and for large parts.[73] Composite joining processes have also promoted their use by reducing production costs and enabling the efficient assembly of simple parts into large and complex structures. There are several methods for joining different parts of composites, depending on the application. Joining techniques can be classified as mechanical, adhesive, and fusion (Figure 2.11).[74]

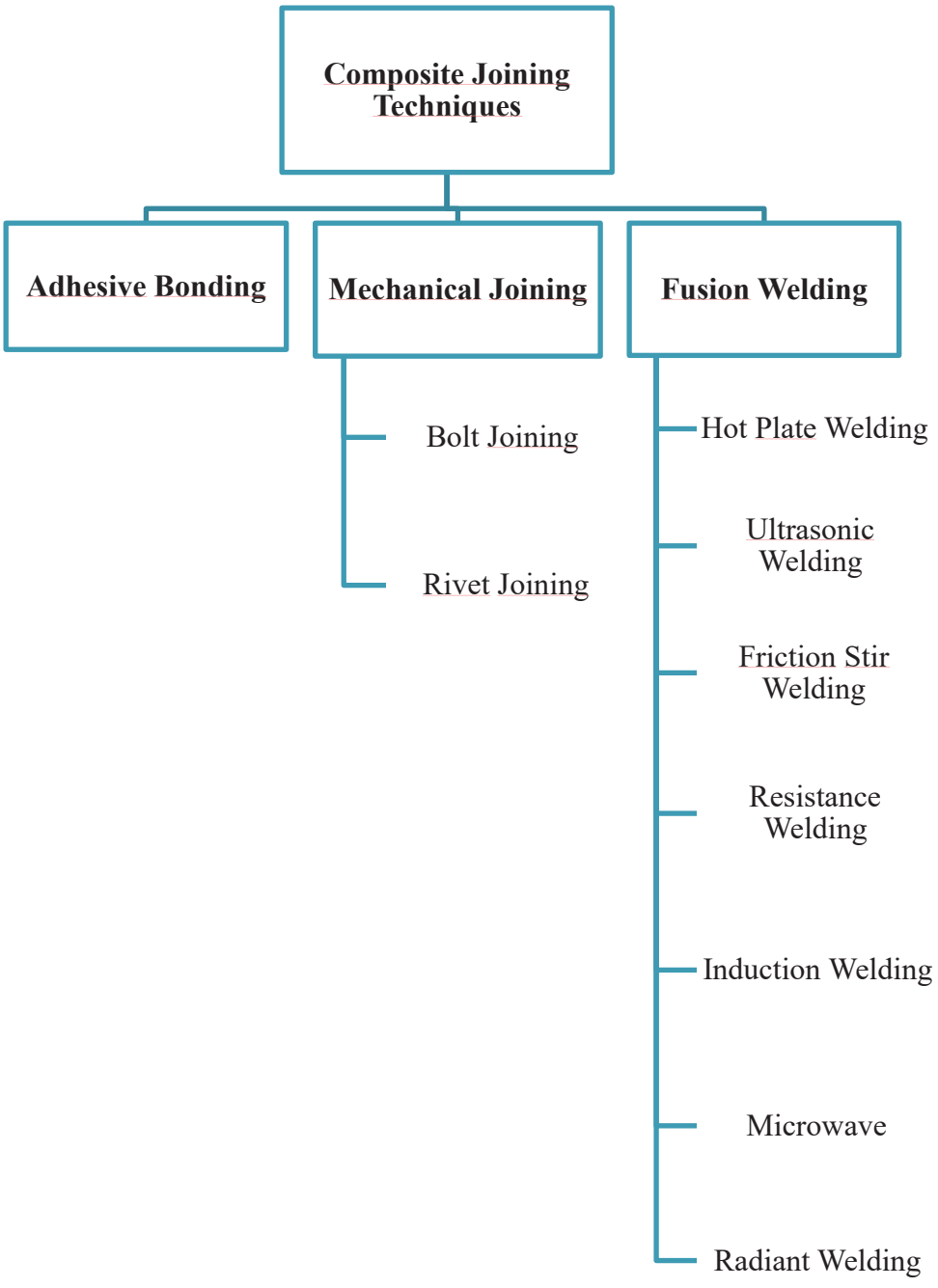

Figure 2.11. Classification of joining techniques.[74]

The mechanical joining method uses fasteners such as rivets, bolts, or screws. This traditional assembly method has advantages such as no need for special surface preparation of the components, less compliance requirements of the surfaces to be joined compared to other methods, and the ability to deliberately disassemble the components without damaging them. In addition to these advantages, it causes additional weight in the joined structure and causes the formation of an extra stress concentration area for the joined structure, which negatively affects the structure mechanically. Therefore, the mechanical joining method should not be preferred, especially for continuous fiber-reinforced composites.[73]

Fusion bonding or welding is generally suitable for joining thermoplastic composites because thermoplastics can be remelted and reprocessed at the required temperatures. The advantages of welding over other joining methods, such as adhesive bonding and mechanical fastening, are that it's a fast process, requires simple equipment, is adaptable to automation and does not require additional surface preparation processes.[74]

The main fusion bonding techniques for thermoplastics are induction welding, resistance welding, ultrasonic welding.

Induction welding (Figure 2.12) produces localized heating by using an induction coil that generates a variable magnetic field in a short time. This is a non-contact welding method. Eddy currents are induced in the electrical conductor placed near the magnetic field, and heat is generated by Joule losses. The high temperature required for welding is easily obtained by using a steel mesh screen placed along the joining line. The process parameters of induction welding are frequency, pressure, power and welding time.[75]

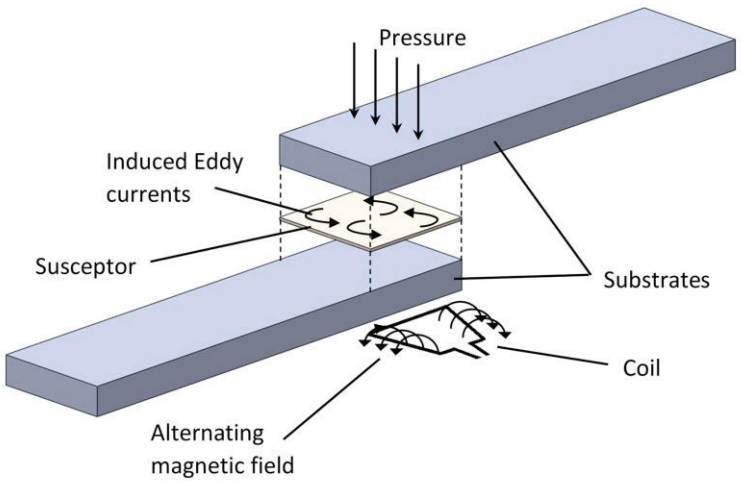

Figure 2.12. Schematic representation of induction welding process.[75]

In ultrasonic welding, the parts to be joined are subjected to ultrasonic vibrations (generally selected between 20 and 50 kHz) perpendicular to the joining area and a certain pressure is applied. The ultrasonic welding process is shown schematically in Figure 2.13.[75]

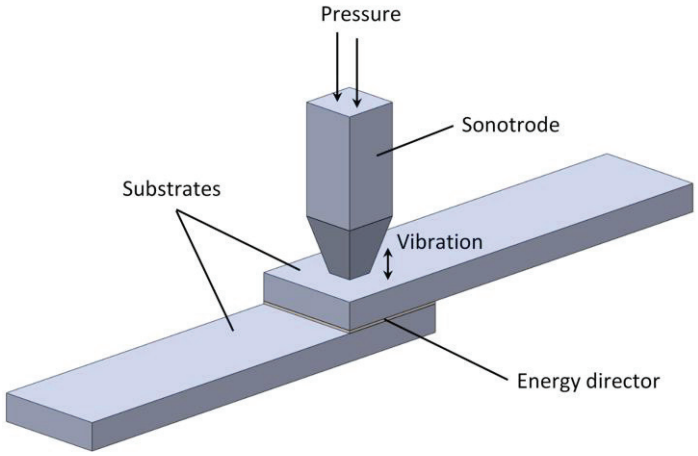

Figure 2.13. Schematic representation of ultrasonic welding process.[75]

The resistance welding process can be briefly summarized as an electric current passing through a resistive element, causing heat and melting through the Joule heating effect. This heating effect generates high temperatures at the joining interface, causing the thermoplastics to melt (Fig. 2.14).[75]

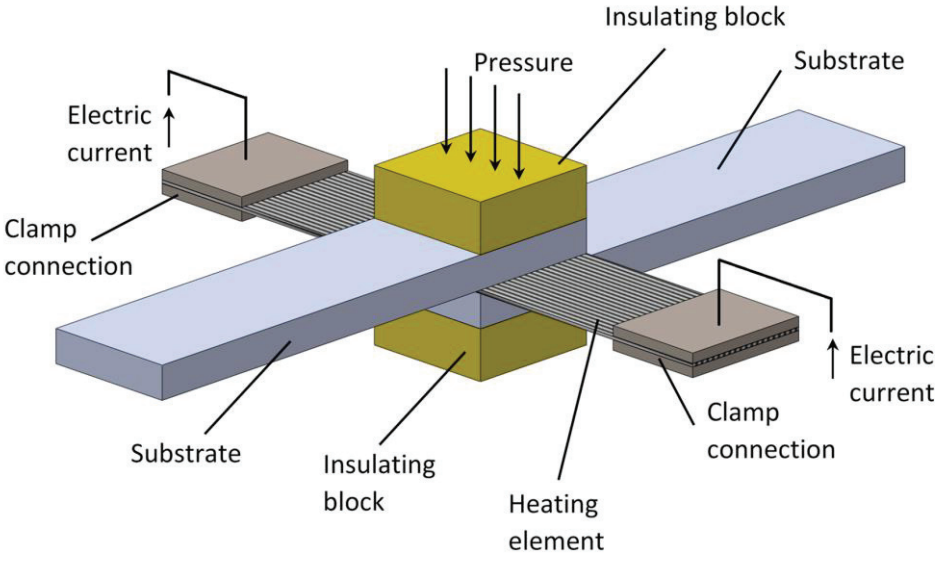

Figure 2.14. Schematic representation of resistance welding process.[75]

The resistance welding process is very advantageous compared to other welding methods in terms of heat generation only on the welded surface, it is the most suitable method for long welded parts because the process time is independent of the weld length and there is no limitation to the thickness of the part to be welded. Similar to induction welding, the resistive element (conductive implant) remains in the structure after welding One disadvantage of resistance welding. Another disadvantage of resistance welding is the risk of heat flow irregularities in thicker layers during the autoclave manufacturing process. For this reason, it has been observed in previous resistance welding experiments that test specimens consisting of thinner laminates gave better bond quality and correspondingly better mechanical test results.[76]

In the resistance welding process, other process parameters that influence the weld quality include welding current, welding time, welding pressure, contact resistance, material properties of the welded parts and heating elements, and geometry and dimensions. In addition, it has been observed that fiber orientation has a direct influence on the homogeneous temperature distribution on the welded surface in the welding process of fiber reinforced thermoplastics.[77]

The applications of the resistance welding process on aerospace industry are increasing day by day. Among these applications, lab-scale sequential welding was used to attach CF/PEEK hinges and CF/PEKK clips to CF/PEEK C-frames in the Clean Sky Eco-Design demonstrator and welded thermoplastic fixed wing leading edge on Airbus A340-500/600, A380 (J-nose, welding jig) can be indicated. Fully welded frames thermoplastic fuselage panel by GKN Fokker and Gulfstream Aerospace features simple “butt-jointed” orthogrid stiffening and fully welded frames (no bolts).

Another joining method that has been widely used in recent years for joining composite materials is adhesive bonding. Since the bonding method chosen in this study is adhesive bonding, it will be discussed in detail in the next section.

2.3.1. Adhesive Bonding Method

Adhesive bonding is a secondary bonding process. In other words, it is the joining of two or more pre-cured composite parts by curing the adhesive through chemical or thermal reactions. In adhesive bonding process a film, liquid or paste adhesive can be placed between adherends and cures to form joint structures, as shown in Figure 2.15.

The most common polymers used in structural adhesives are epoxies, polyurethanes, silicones, phenolics and acrylics, while structural adhesives used in the aerospace industry are generally based on epoxy, bismaleimide (BMI), cyanate ester or hybrid adhesives.[78] Based on their physical state, adhesives can be divided into four groups: liquid, powder, paste, and film. Liquid adhesives typically used in thinner bond lines for direct load transfer. Liquids tend to be more brittle and have lower peel and crack resistance than pastes or film adhesives. Paste adhesives can be used to bond thicker parts than liquid adhesives. Joining rubber, thermoplastics, and metals are the most common applications. Although there is a difference in viscosity between liquid and paste adhesives, many manufacturers categorize most "liquid" adhesives as "paste" without distinction. Film adhesives are high performance adhesives. It should be stored frozen. High bond strength is achieved when a specific temperature is applied to cure the adhesive.[79]

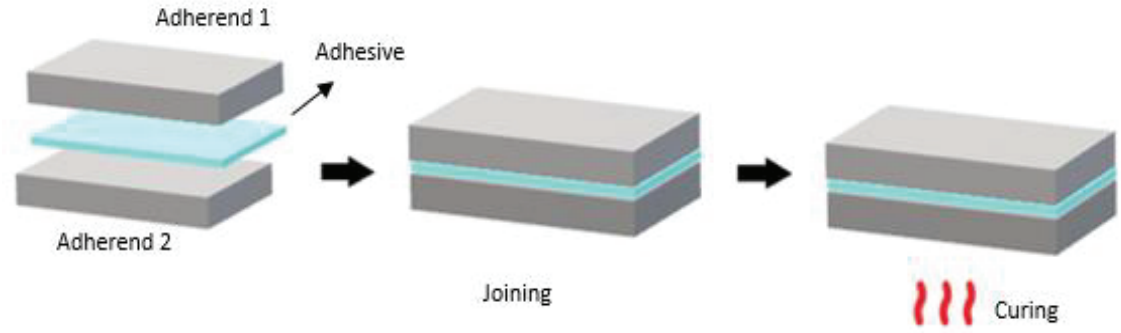

Figure 2.15. Adhesive bonding process.

Considering the structural designs of composite materials, adhesive bonding has been widely used in recent years instead of mechanical and fusion bonding, which are the traditional bonding methods. Adhesive bonding is a method of joining similar or dissimilar materials by the adhesive force generated by the adhesive on the bonded surface. In this process, the materials that are bonded with the adhesive are referred to as the adherend. The forces that provide adhesion to the surface are a combination of chemical bonding, often the result of a chemical reaction, and, in the case of rough or porous bonded surfaces, some mechanical interlock between the adhesive and the adherend.[73,80]

Adhesive bonding offers a number of advantages over other conventional joining methods, including the ability to join of dissimilar materials, uniform stress distribution, capability for damping, and acoustic insulation. Moreover, factors that adversely affect the structure mechanically, such as the additional stress area and weight created by mechanical bonding, are not considered in the adhesive bonding process. In addition, the adhesive used for bonding can effectively prevent cracking and galvanic corrosion between two different materials being joined.[2]

In recent years, there has been a rapid transition from metal to composite materials, especially in the aerospace and automotive sectors. This transition required the existence of hybrid structures (joining dissimilar materials), which further increased the importance of joining methods and enabled the transition from traditional methods to more innovative joining methods. Due to the limited application areas and some disadvantages of other joining methods, such as the fact that welding is not a method that can be used to join two different materials, or the formation of local stress areas in the structure during mechanical joining, and even the damage that can occur during joining, the adhesive joining method is particularly suitable for continuous fiber-reinforced composites.

Figure 2.16. Examples of paste adhesive applications; skin paste bonding and paste bonded fuel floor.[81]

Because of these advantages, adhesive bonding is used in a wide range of applications in industries such as aerospace, rail, automotive and construction. For example, the Boeing 787 Dreamliner and Airbus A350 XWB have miles of bonded surfaces. Another existing example is that more than 60% of the surface area of the Boeing 747 aircraft was produced using adhesive bonding. The main applications of the adhesive in aircraft parts are bonding stringers to skins for both wing and fuselage structures, and bonding metallic honeycomb to skins for ailerons, elevators, flaps, and spoilers as seen Figure 2.16.[82–85]

The factors to consider when selecting an adhesive for composite bonding can be summarized as follows: the type and chemical compatibility of the composite parts to be bonded, the application of the part, its cost, and the environment in which the part will be used. Considering these factors, the temperature resistance, thermal conductivity, mechanical strength, and chemical properties of the adhesive to be used come to the fore.[86]

Scarselli G. et al.[85] investigated the mechanical properties of adhesively bonded UD composite laminates for aerospace industry. In their study, with the addition of nano-graphite to the adhesive to experimentally demonstrate the superior mechanical properties of the adhesive in terms of strength and energy absorption. To this end, two different types of specimens were prepared and compared, one bonded with a conventional epoxy-based adhesive and the other with an adhesive obtained by mixing the same epoxy resin with nanographite particles. The experimental results showed an increase in the mechanical performance of the adhesive regarding shear strength (+18%), elongation at break (+29%), and strain energy at break (+53%) when a nanofilled epoxy resin was used.

Quan D. et. al proposed a high-power UV irradiation technique for surface treatment of PPS and PEEK thermoplastic composites prior to adhesive bonding to achieve high bond strength with epoxy adhesives. As a result of the study, they observed remarkable improvements in the lap shear strength that is, 11.8 MPa to 31.7 MPa for PPS composites and 8.3 MPa to 37.3 MPa for PEEK composites, and Mode-I and Mode-II fracture energy of the adhesive bonded joints.[87]

Luis Valarinho et al.[88] studied the performance of three different types of adhesives (Sikaflex, Sikaforce, and Sikadur) for bonded continuous multi-span composite structural beams. This structure consists of glass fiber reinforced polymer (GRP) and annealed glass panes. According to their results, the specimens bonded with Sikaflex

show the minimum flexural stiffness and strength values compared to other types of adhesives when post-cracking behavior is evaluated. The other two adhesive types showed similar results with higher values.

The optimum for adhesive bonding is that the bonded structures exhibit the desired level of mechanical performance without the need for surface pretreatment. However, to achieve the desired level of durability and mechanical strength in applications, the surfaces to be bonded must be pretreated prior to bonding.[89]

Especially for thermoplastics, surface pretreatment prior to bonding is very significant because, due to their structure, they have a lower surface free energy than thermosets, which reduces the wetting of the adhesive with the joint surface and the desired mechanical performance of the joint cannot be achieved. For these reasons, one of the most critical steps in the adhesive bonding process is surface pretreatment prior to bonding. The most appropriate surface pretreatment method should be selected to achieve the desired mechanical strength and durability of the bonded structure.[90]

2.3.1.1. Failure Modes of Adhesive Bonding

According to ASTM D5573[91], there are seven types of failure modes of adhesive bonded structures for fiber reinforced composites, but these can be grouped under three main categories: adhesive failure, cohesive failure, and adherend (substrate) failure. The main failure modes are shown in Figure 2.17.

Adhesive failure occurs at the adhesive-substrate interface, usually with adhesive remaining on one of the substrate surfaces. These failures are generally associated with the poor quality of the bonding process, environmental factors, and inadequate surface preparation. Cohesion failure, however, is the type of damage that occurs within the adhesive structure. This type of failure is an indication of a successful design, bonding and surface preparation process. After cohesion failure on the bonded surfaces, adhesive material is observed on both surfaces. Substrate or adherend failure occurs when the mechanical strength of the substrate is less than the load-bearing capacity of the bond. This type of failure is more common when thinner and brittle materials are chosen as substrates. Although it shows good bond strength, the substrate is not suitable for the selected adhesive type. In addition, this type of failure indicates that an alternative bonding method should be investigated.[92]

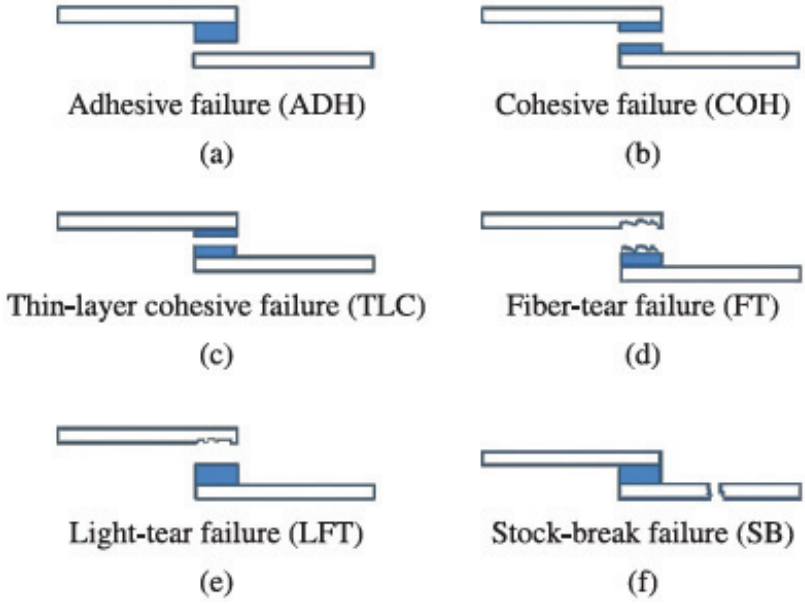

Figure 2.17. Representation of failure modes typical of adhesive joints subjected to shear.[93]

2.4. Surface Treatment Methods of Fiber Reinforced Composite Materials

Preparing the surfaces to be bonded prior to bonding is a very critical process as it directly affects the performance of the bond. In order to achieve maximum strength and more durable bonded structures, surface treatments are applied to the surfaces to be bonded.[94–99] These treatments are designed to remove all surface contaminants, achieve the desired roughness, surface free energy and wettability, and provide a chemically active surface. Also, the benefits of removing the top resin layer prior to bonding have been demonstrated in studies.[100]

Various chemical, mechanical, plasma, laser and other surface treatments are available for different types of adhesives and composite adherends. One of the critical issues in bonding is the selection of the appropriate surface treatment for the adherends and the adhesive. Chemical treatments include acid/alkali etching, solvent cleaning, peeling layers, anodic oxidation, and coupling agents, etc. Mechanical treatments include sandblasting, sandpaper grinding, etc. In addition to these methods, with the development

of technology in recent years, high-energy radiation treatment methods such as laser treatment, plasma and intense pulsed light have become widely used.[101]

Surface treatment methods generally help to increase mechanical strength in the bond area by removing contaminants from the surface, increasing surface roughness, and thus increasing contact with the adhesive. However, each treatment method produces different effects on the surface to achieve the desired surface finish. For example, mechanical treatment methods generally modify the composite surfaces to be bonded by abrading them, while chemical treatment methods mainly include washing and etching the composite surface with chemical reagents and enlarging the contact area. This results in better mechanical interlock between the adhesive and the bonded layer. In addition, the wettability of the adherend surface can be further enhanced by using certain ions or functional groups. Modern high energy radiation treatments are designed to affect the bonded surface of composites by manipulating the energy parameters of the beam and altering the physical or/and chemical characteristics of the composite surface by abrasion.[99]

Grinding, one of the mechanical surface treatment methods, is the simplest, most convenient and economical method that can be applied to obtain the desired surface. This method is generally applied in two ways: polishing and sandpaper grinding. With this method, the impurities and oxide layer produced on the surface are removed from the surface, the required roughness can be provided on the surface, and it provides the formation of free radicals as it breaks the chains on the grinding surface. Sandblasting, another mechanical surface pre-treatment, is the cleaning of the surface to be bonded by contact with sand particles that are applied to the surface at high speed. This method ensures the removal of surface contaminants and also increases the surface roughness, increasing the contact area with the adhesive and thus improving the mechanical properties of the joint structure.[102,103]

Peel ply is a removable surface layer that is a method of composite surface modification. The purpose of peel ply treatment is to remove the surface contaminants, improve the surface roughness and wettability of the composite material. Peel ply surface treatment also produces a uniform surface over a wide area. This provides the desired surface for adhesive bonding. It is mainly applied to glass/epoxy composites, and carbon/epoxy composites, etc.[104]

The effects of three different surface treatments, namely peel ply, grit blasting and plasma surface treatments, on the mechanical performance of the carbon fiber/epoxy composite bonded structures were investigated by Prolongo S. G. et al.[105] Plasma was the treatment method that gave the best results. With plasma surface treatment, a significant increase in the polar component of the composite surface energy was observed, which provided the highest lap shear strength compared to other samples.

Solvent cleaning is one of the chemical surface treatment methods used for the removal of contaminants from the surface and the optimization of surface properties. This treatment does not affect surface roughness. The primary solvents used to clean the surface to be bonded are deionized water, ethanol, methanol, and isopropyl alcohol, which evaporate on the substrate surface, leaving a thin molecular coating on the treated surface to prevent abrasion.[106] In the coupling agent surface treatment method, which is another chemical treatment method, the role of the coupling agent in surface modification is mainly to react with some groups on the surface of the substrate. The strength of the adhesive interface is enhanced by the formation of covalent bonds.[101]

The purpose of acid etching is to create pits on the surface of the substrate through chemical reactions of acidic reagents. This increases the surface roughness and wettability of the part to be bonded, removes the oxide layer on the surface, activates the surface, and creates useful ions or functional groups. The result is an improvement in the mechanical strength of the bond structure.[107]

Nattapat M. et al.[100] etched the CFRP bonding surface with chromic acid and observed an increase in the wettability of the CFRP surface and thus an increase in the bond strength of the joint structure due to acid etching surface treatment.

Zhou L. et al.[108] investigated the effect of several surface treatments on the bond strength between polyetheretherketone (PEEK) composites and two different luting cements. In their studies, the results of the samples bonded after the application of surface treatments such as chemical (sulfuric acid etching, hydrofluoric acid etching), mechanical (air abrasion), and argon plasma were compared with each other and with the reference sample without any surface treatment applied to the bonding surfaces. According to this study conducted for dental applications, the surface treatments that gave the most effective results were determined to be sulfuric acid etching or argon plasma.

Over the years, surface treatments have been developed to improve adhesion based on mechanical or chemical modifications. Although they are widely used and very

effective, these techniques have a number of drawbacks.[89] After the removal of the peel ply, the surface will be covered with a relatively thick layer of resin film, so the adhesive will bond to this layer and not directly to the fibers, resulting in a potentially weak layer and preventing the direct transmission of force into the fibers. The disadvantages of manual mechanical surface treatment operations (abrading, grinding, etc.) include the possibility of damaging the original structure of the substrate surface, which can have a negative impact on the use of the composite structure, the difficulty of the process, as well as the need for secondary cleaning due to the impurities generated during the treatment.[89,109] In addition, cleaning with organic solvents and acid etching surface treatment processes are undesirable because of their impact on the safety of the environment.[89]

Liu J et al.[101] reviewed the effect of different surface treatment process on composite materials. According to their results, mechanical treatment (sandblasting, and grinding) increased the surface roughness significantly. However, the outcome was hard to control and easily damaged the carbon fiber structure of the substrate surface. Chemical treatments such as solvent cleaning, coupling agents, acid and base etching, and anodic oxidation slightly modify the surface morphology of CFRPs and easily achieve a more uniform surface morphology. The aim is the activation of useful ions or functional groups on the substrate surface for better surface wettability. The results of advanced high energy radiation treatments like plasma, laser and intense pulsed light are ideal. Optimization of the surface treatment parameters makes the results ideal and consistent.

Laser surface treatment represents a promising new approach to the surface pretreatment of fiber-reinforced composites to achieve selective resin removal without damaging the fibers.[109] The next section discusses this surface treatment method.

2.4.1. Laser Surface Treatments of Fiber Reinforced Composites

In recent years, laser surface treatment has been used as a new approach in the bonding of fiber-reinforced composites with adhesives because of the disadvantages of mechanical and chemical surface treatments applied to the bonding surfaces of fiber reinforced composites. Laser surface treatment technology has been an effective method for the treating of fiber composite materials. The laser surface treatment process has many advantages, such as the improvement of surface roughness, cleaning the surface, the

increase of surface energy and wettability, and the change of chemical composition of the surface. It also eliminates tool wear because there is no mechanical contact. In addition, it offers a high degree of flexibility and automation.[110]

Considering the laser process for fiber reinforced composites in two different situations, the first is selective matrix removal. Given that the composite material consists of two constituents, matrix and fiber reinforcement, there are two distinct thresholds. Carbon fibers are known to have a higher threshold than the matrix material. If this is not the case, fiber damage is unavoidable during the selective matrix removal process.[111,112] Second, when laser cutting composites process, both components must be removed. Therefore, the laser energy must be set above the higher threshold of carbon fibers.[113]

In particular, laser surface treatment offers the selective removal of matrix from the bond surface without damaging the fibers and represents a promising new method for surface pre-treatment of fiber-reinforced composites. This selective removal allows direct force to be applied to the reinforcements while removing the contaminants. In addition to cleaning and mechanical interlocking, the interactions between the surface and the adhesive at the molecular level play an important role in the adhesion and strength of the bond.[109]

As the technology evolves, the types of lasers are increasing, and several kinds of laser sources are used in the surface treatment of fiber reinforced composites. Commercially available lasers can be classified (accordance with ISO 20473) based on the wavelength of the beam used, such as ultraviolet laser (UV), infrared laser (IR) (near/mid/far infrared), and so forth. They can also be classified according to the beam output mode in the lasers, as continuous wave (CO_2, diode, and CW fiber) long pulse (microsecond, millisecond), short pulse (nanosecond), and ultrafast lasers (picosecond and femtosecond). Pulsed lasers are more commonly used in applications where ablative etching is needed, due to the well-controlled localized delivery of energy to the substrate. Figure 2.18 represents the effects of continuous and short pulsed laser irradiation on the surface of the target material.

As illustrated in Figure 2.18, the effect of continuous lasers on the surface is much greater than that of pulsed lasers. The heat affected zone (HAZ) is much larger. For different objectives, several types of laser sources with different wavelengths and pulse lengths have been used. Depending on the intended use of the laser and the expected effect, the type of laser should be selected correctly.[3]

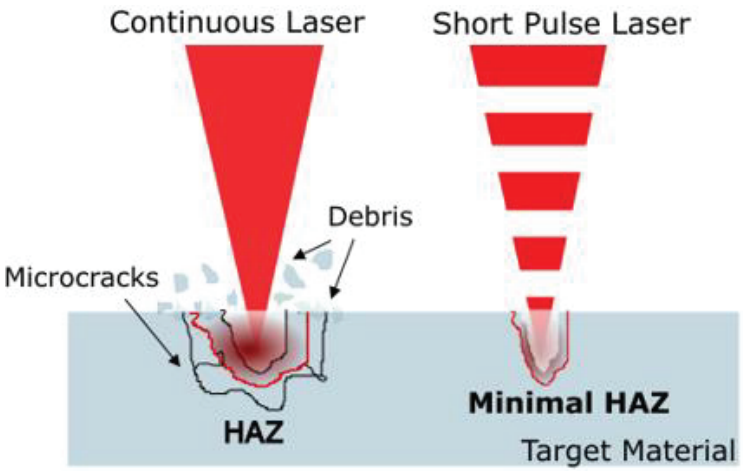

Figure 2.18. Differences between the effects continuous and short pulsed lasers.

Once the laser energy has been deposited inside the material, the modification of the material is controlled by the way in which this energy is diffused. The main ablation mechanisms used to dissipate energy are thermal, mechanical, chemical and electrical.[114] Due to the difference in wavelength and operating mode, the ablation mechanism of the laser process is distinct. Besides the thermal effect on the material surface, photochemical effects are also observed during UV (wavelength range from 200 nm to 400 nm) laser ablation mechanisms due to the high photon energy. This effect causes the breaking of chemical bonds on the polymer surface and a series of chemical reactions. For this reason, the UV absorption on the treated surface is very high, which reduces the laser's effect on the surface, i.e. the penetration depth is less. Therefore, UV laser treatment has been used for mechanical improvement prior to adhesive bonding to remove impurities on the composite surface, change the chemical properties of the surface, and increase the surface roughness. UV lasers reduce damage to the fibers on the treated surface. However, treating a large composite surface takes a long time and requires dozens of shots per unit area. This results in higher energy consumption and increased costs.[3] CO_2 and IR (wavelengths between 780 nm and 1 mm) lasers, which have become more widely used in recent years, have a photothermal ablation mechanism on the surface due to their low photon energy, unlike UV lasers.[112] These lasers can be used to selectively remove matrix material from the surface. During this photothermal ablation mechanism, the energy generated by the laser at the surface is absorbed by the fibers and transferred to the bulk material. This surface temperature creates the heat affected zone. Due to the difference in thermal properties between the polymer matrix and the carbon fiber, the weakened

polymer matrix undergoes thermal degradation and moves away from the surface, producing pyrolysis gas, while the carbon fibers remain on the surface undamaged. Thus, IR laser processing offers great advantages over UV laser processing with respect to energy efficiency and process speed.[3]

In addition to the advantages of laser surface treatment of composite materials mentioned above, there are also some challenges. The heat generated during the laser process causes various thermal damage to the surface due to these differences in the physical and thermal properties of composite materials. Due to the thermal nature of the interaction between the laser radiation and the material, thermal and thermo-mechanical decomposition of the material is to take place. For example, fiber pull-out, fiber thinning, fiber thermal degradation, laminar delamination, the most common being heat affected zone (HAZ).[115] In carbon fiber-reinforced composites, the fibers transfer heat to the bulk of the material, resulting in a large heat affected zone (HAZ) where the matrix-fiber interface weakens due to thermal decomposition of the polymer.[116] In fiber reinforced composites, the HAZ is also dependent on the direction of the fibers. According to studies, the most important factor affecting the mechanical properties of composite materials in the laser surface treatment process is the formation and extension of the HAZ region.[117]

The most important factor in the formation of this heat affected region is the difference in the physical properties of the polymer used as resin and the fiber. For instance, while carbon fibers have a very high vaporization temperature around 3300°C, resin decompose at around 500°C (Table 2.2).

Table 2.2.Thermal Properties of the Fibers and the Matrix.[109]

Material	Conductivity (W/(m.K))	Density (g/cm^3)	Specific Heat (J/kg.K)	Diffusivity (cm^2/s)	Vaporization Temperature (^0C)
Epoxy resin	0.1	1.21	1884	0.0004	400-500
Polyphenylene-sulfide (PPS)	0.29	1.66	795	0.0022	350-500
Polyetheretherketone (PEEK)	0.25	1.32	320	0.0059	350-500
Carbon fiber T300	50*	1.85	710	0.66*	3000-3300

* Along fiber axis

Carbon fiber thermal conductivity (50 W/mK) is several times higher than that of epoxy (0.1 W/mK) and other matrix materials such as PPS (0.29 W/mK) and PEEK (0.25 W/mK). Moreover, the carbon fibers exhibit three times higher thermal conductivity in

the longitudinal direction (4.9 W/mK) than in the transverse direction (1.7 W/mK).[113,118] In addition to the thermal properties, the optical properties of both the polymer and the fiber used in the composite are important in selecting the wavelength of the laser to be used. Optical parameters of carbon for a variety of wavelengths were shown in Table 2.3.

Table 2.3. Optical parameters of carbon at various wavelengths.[119]

Wavelength (nm)	355	532	1064
Reflectivity R (%)	19	21	25
Absorption coefficient α (1/μm)	33	20	14
Absorption length l_α (nm)	31	50	74

Also, Fischer et al.[109] investigated the transmission (%) of epoxy, PEEK and PPS polymer matrices for different wavelengths in their studies. Also, they investigated the light penetration depth (1/ α) of ultraviolet UV (355 nm) and near- infrared NIR (1064 nm) laser for two different polymers which are epoxy and PEEK (Table 2.4).

Figure 2.19 represents the percent transmission of various thermoplastics as a function of incident laser radiation. It is evident that the absorption is notably low for wavelengths within the near-infrared (NIR) range, particularly for PEEK matrices.

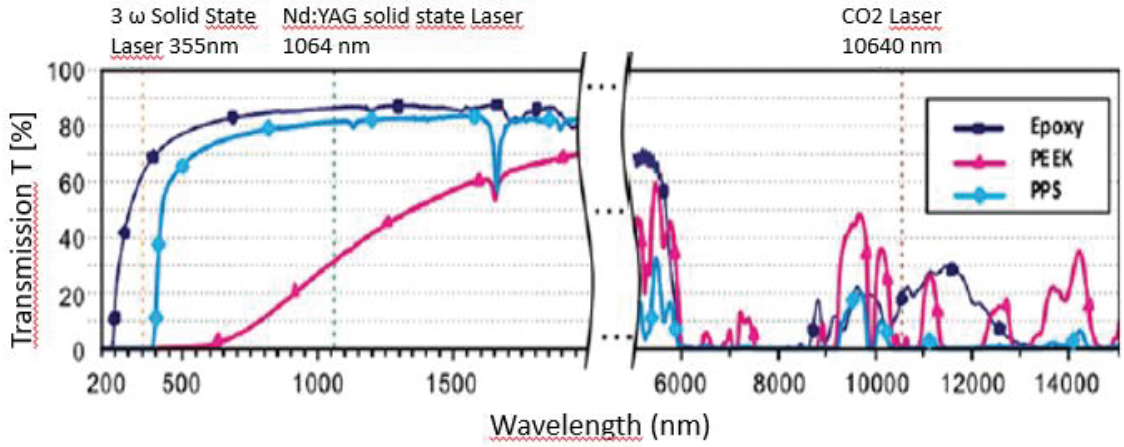

Figure 2.19. Transmission spectra of various polymers.[109]

Their results showed that the level of absorption is very low at near infrared (NIR) wavelengths and the surface pretreatment of polymer materials with NIR laser radiation involves the heating of fibers and the explosion of the upper matrix layer mechanism due

to thermal stress, resulting in the risk of thermal degradation of the fibers. When working with this type of laser, the risk of thermal fiber degradation should be considered. This can negatively affect mechanical strength.

Table 2.4. Depth of Light Penetration of UV and NIR Laser in Two Common Polymers.[109]

λ (nm)	PEEK		Epoxy	
	α	1/α (m)	α	1/α (m)
355	29826.6	3.4×10^{-5}	2231.4	4.5×10^{-4}
1064	3809.8	2.6×10^{-4}	1.001	0.9

Herzog D. et al.[116] investigated the achievable HAZ of CFRP composites cut by pulsed Nd:YAG, CW Nd:YAG and CO_2 lasers and found that the HAZ expanded up to 0.6, 1.2 and 1.4 mm, respectively. They also found that the decrease in tensile strength was in proportion to the HAZ area.

In laser surface processing, the heat-affected zone has become a criterion for determining the bond quality of fiber-reinforced composites. In order to keep the effects of the HAZ at the desired level and improve the quality of the resulting structures, laser parameters such as laser wavelength, laser light source, scanning speed, and beam diameter should be optimized.[111,120]

For example, Wolynski et al.[118] studied the ablation thresholds of carbon fibers in an epoxy matrix for three various wavelengths using a picosecond laser. According to their results, the thresholds were 0.216 J/cm^2 for the laser wavelength of 355 nm, 0.284 J/cm^2 for the laser wavelength of 532 nm, and 0.410 J/cm^2 for the laser wavelength of 1064 nm. Epoxy matrix ablation threshold value is assumed to be much lower than carbon fiber and is not taken into account.

In another study, Fischer F. et al.[109] compared the PEEK film and carbon fiber ablation thresholds value shown in Figure 2.20. The results indicate a threshold value for PEEK that is about two orders of magnitude lower than that for carbon fibers.

However, due to thermal effects, matrix degradation and fiber delamination may be more common during the IR laser process than with the UV laser. Therefore, in IR laser processing, controlling the extent of the heat-affected zone (HAZ) is very

critical.[3,118] On the other hand, thermal effects and thermal damage can be minimized by using shorter laser wavelengths and narrower pulse widths during the laser treatment process. The reduction of the laser-surface contact time has a positive effect on HAZ. However, the thermal damage area is large for continuous laser processing and millisecond or nanosecond short pulse laser processing. As a new laser processing technology, ultrashort pulse laser processing, such as picosecond and femtosecond lasers, has high controllability, environmental friendliness, no restriction of material types, and no transmission of heat.[110] Akman et al.[112] studied the nanosecond pulsed UV laser and the microsecond pulsed CO_2 laser for the selective removal of the matrix. For both lasers, differences in ablation results have been observed because of the different ablation mechanisms. The CO_2 laser left ablation products, whereas the UV laser left no residues.

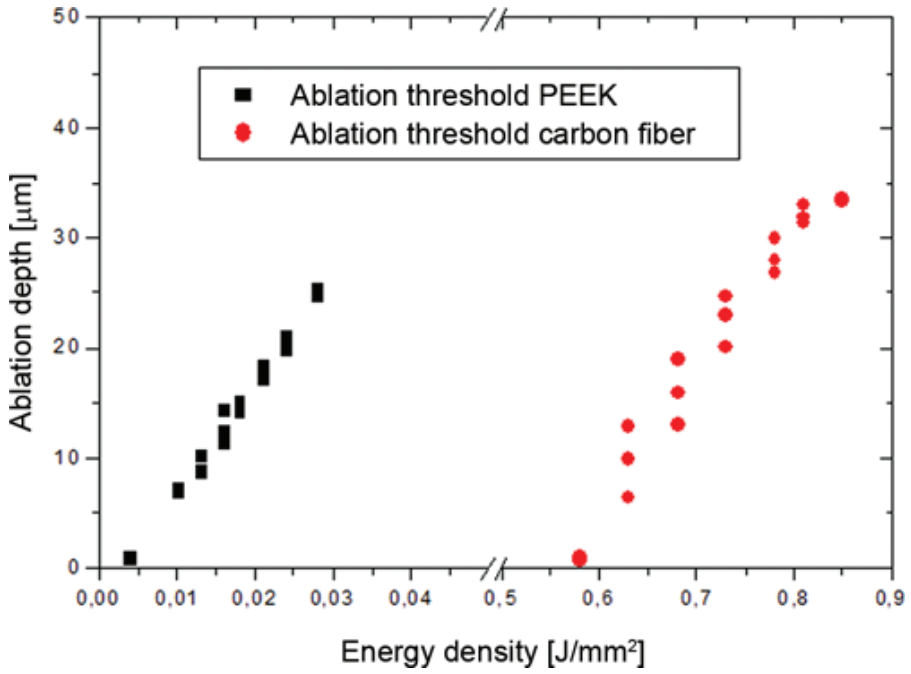

Figure 2.20. Ablation depth on PEEK film and carbon fiber lamina vs. energy density.[109]

Fischer F. et al.[109] examined the effect of laser surface pretreatment of CFRP on the absorption behavior. For this purpose, the results of untreated specimens were compared with the results of specimens whose bonded surfaces were treated by peel ply, abraded, and various type of laser treatment (UV and CO_2) methods. Compared to the untreated specimens, an increase in mechanical strength was observed for all specimens whose surfaces were treated, and it was observed that the UV-laser treated specimens had

the maximum shear strength value. Also, they showed that the CO_2 laser system generated more heat on the treated surface than the UV laser system, increasing the risk of damage and delamination.

The IR-Yb fiber nanosecond laser was used in this study. Therefore, this type of laser will be discussed in the next section.

2.4.1.1. IR-Yb Fiber Lasers

Fiber lasers almost always use optical fibers doped with laser-active rare earth ions as the gain medium. Some rare earth elements commonly used in these lasers are ytterbium (Yb^{+3}), erbium (Er^{+3}), neodymium (Nd^{+3}), and thulium (Tm^{+3}). The Yb-doped fiber laser has many advantages over other laser active rare earth doped fiber lasers. The main advantage is that it has an emission bandwidth ranging from 975 to 1200 nm, which is very convenient for laser amplifying. The Yb-doped fiber laser is particularly well suited for the generation of high-power lasers. It also has high quantum transformation efficiency and low thermal impact. It has a various pump source and a wide absorption band (800-1064 nm). Yb-doped fiber laser is commonly employed in ultra-short pulse amplification and high-power continuous laser output.[121–124]

Because UV lasers cannot be guided by an optical fiber, their use in automation processes is limited. The infrared (IR) laser, on the other hand, can be directed through an optical fiber and is therefore well adapted to automation.[125] Other encouraging applications of IR laser surface treatment in recent years include studies to increase the bond strength of fiber-reinforced thermoplastic matrix composites.[89,126] While interest in IR wavelength lasers has increased in recent years, fiber laser applications are rapidly expanding in all areas of medicine, communications, and directed energy.[127]

Yang Z. et al.[128] modified the surface wetting characteristic of Inconel 718 ((IN718)- nickel chrome alloy) by using the Ytterbium nanosecond pulsed fiber laser with three various patterns (line, grid, spot). They observed that the laser-treated surfaces of IN718 showed very high hydrophilicity in contact angle results measured immediately after laser treatment in ambient air. And this hydrophilic nature quickly changed to very high hydrophobicity in about 20 days. The reason for this was revealed by XPS analysis. The results showed that the change in wettability from hydrophilic to hydrophobic over

time can vary depending on the change in surface chemistry, especially the carbon content.

Effect of IR-Yb laser surface treatment on morphological and adhesion properties of scarfed carbon fiber reinforced epoxy surfaces examined by Harder S. et al.[129] They applied solvent cleaning and laser surface treatments to the joint surfaces and compared the results. According to their results, an increase of approximately 5% was observed in the bonding performance of laser surface treated CFRP specimens.

In another of our studies, we demonstrated the effect of IR Yb nanosecond laser parameters on the surface modification of carbon fiber-reinforced epoxy. While low laser power partially damaged the epoxy surface, high power damaged the carbon fibers. A super-hydrophilic surface was created by determining the optimal laser parameters for the material.[130]

Genna S. et al. used a Q-switched Yb:YAG fiber laser to enhance the bonding properties of carbon fiber-reinforced PPS thermoplastic composites. They performed laser scanning using three different strategies to observe the effect of fiber orientation. These are shown in Figure 2.21.[89]

According to the mechanical test results, while all laser samples increased their shear strength compared to samples with untreated surfaces, the sample with the highest apparent shear strength result was determined to be the sample treated in the 45^0 fiber direction (B strategy).

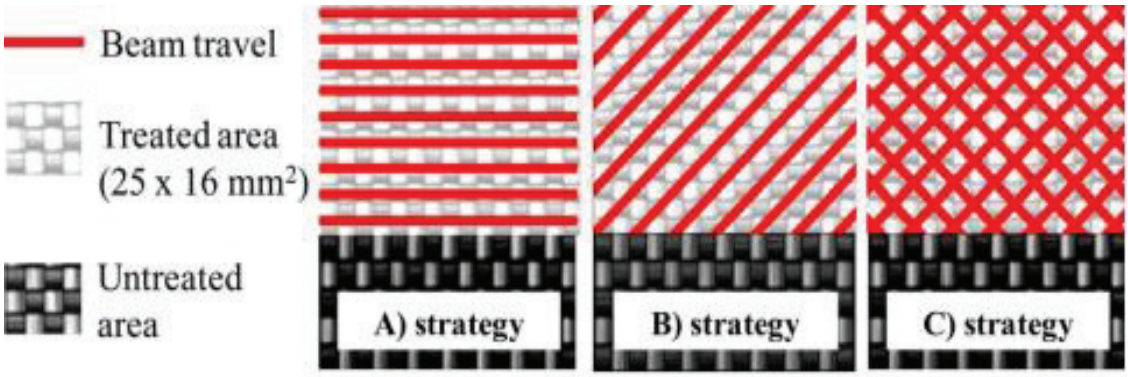

Figure 2.21. Schematic of the adopted scanning strategies. (a) A strategy (lines at 0^0); (b) B strategy (lines at 45^0); (c) C strategy (lines at $\pm45^0$).[89]

2.5. The Role of the Surface Treatment Strategy in the Adhesive Bonding Mechanism

An adhesive bonded structure consists of three components: the substrate, the adhesive layer, and the interfaces between the substrates and the adhesive. Since the strength of these structures depends on the different physical and chemical properties of these three components, there is no one theory or model that can describe all the adhesion mechanisms in adhesive bonding. The most common bonding mechanisms are:

- Adsorption theory
- Mechanical interlocking theory
- Diffusion / multi diffusion theory
- Chemical bonding theory
- Electrostatic theory

Adsorption theory holds that the material will adhere based on the formation of interatomic and intermolecular forces following intimate contact between the atoms and molecules on the surface of the adhesive and the surface of the substrate. These adhesive-to-substrate forces include primary bonding (ionic, covalent, metallic), secondary bonding (hydrogen bonding, van der Waals), and donor/receptor interactions.[131,132] In addition, according to adsorption theory, if a material is to have a high adhesion force, the surface free energy must be higher. This indicates a stronger bond to other materials. For this reason, many researchers have concentrated on improving the bond strength of substrates by increasing their surface energy.[133,134]

The surface roughness and structure of the material are also factors that directly affect the spread and penetration of the adhesive into the material.[131,135] The mechanical interlocking theory also states that the primary source of adhesion is the imperfection of the mechanically interlocked adhesion surfaces, meaning that adhesion results from the mechanical interlocking of the adhesive with the pores, roughness, and other surface defects of the substrate (Figure 2.22).[101]

In addition, the mechanical interlocking theory explains that after the adhesive penetrates the substrate surface, the cured adhesive forms interlocking bonds with the irregular topography of the substrate surface.[131] However, mechanical interlocking is not a mechanism at the molecular level. It is just a technical way to improve the amount of adhesive adsorption on the substrate.[137] Experimental studies have shown that mechanical

locking, which is very significant to the strength of the joint, is the dominant adhesion mechanism for the Mode I fracture toughness test.[138]

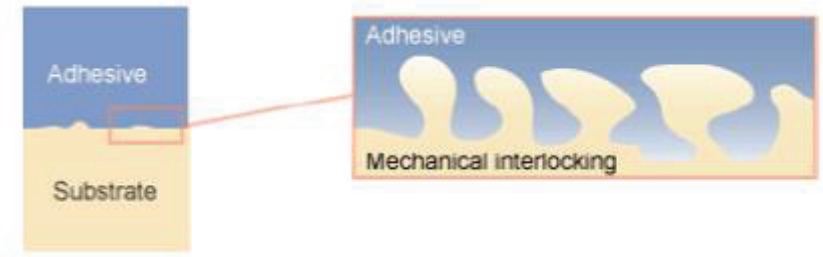

Figure 2.22. Illustration of mechanical interlock.[136]

Diffusion theory (Figure 2.23) is valid when both the adhesive and the substrate are polymers and long-chain molecules can move.

The occurrence of diffusion due to mutual Brownian motion of macromolecules as a result of the intimate contact of two polymers at the adhesive-substrate interface is called mutual diffusion or diffusion theory. This diffusion causes the adhesive interface to disappear and a transition zone to form. Polymer interdiffusion across an interface is feasible when polymers are at temperatures above their glass transition temperatures (Tg). Through diffusion, molecular interlocking occurs, and adhesion is achieved.[139]

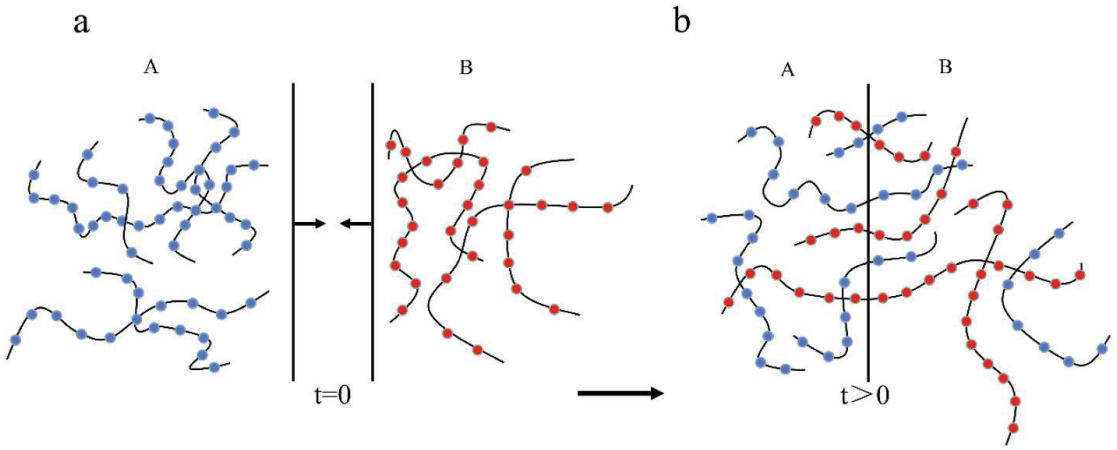

Figure 2.23. Diffusion theory of adhesives. a) adhesives; b) mutual diffusion of substrate molecules.[101]

Chemical bonding mechanism refers to the formation of an adhesion due to surface chemical forces between the adhesive and the surface molecules of the substrate.

There are several intermolecular forces between the adhesive and the substrate interface. These include chemical bonding (i.e., ionic, covalent, and metallic bonds), dipole-dipole interactions, and van der Waals forces.[140] The adhesive strength of the structure is increased by various surface treatments to ensure chemical bonding on the surface to be joined, or by chemical processes such as creating a dipole on the surface. For example, plasma treatment attempts to functionalize the adherend to a higher surface energy, which promotes adhesion by creating interactions across the adhesive-adherend interfaces.[98]

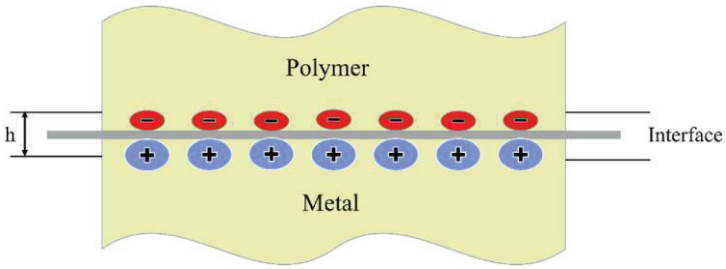

Figure 2.24. Electric double layers at the polymer-metal interface.[101]

According to electrostatic theory, electrostatic forces form at the adhesive/adherent interface in the formation of an electrical bilayer. These forces account for the resistance to release, such as the electrical discharges that occur when an adhesive is peeled from an adherend surface, and the direct contact electrostatic charge due to formation of thin films of metals deposited on polymer surfaces.[140] That is, if the adhesive and the adherend are an electron acceptor-donor combination, electrons are transmitted from the donor to the acceptor, creating an electrical double layer on both sides of the interface, causing electrostatic attraction, as shown in Figure 2.24. This theory only works for non-compatible materials such as polymers and metal substrates.[131]

CHAPTER 3

EXPERIMENTAL METHOD AND INSTRUMENTATION

This chapter presents the experimental studies and techniques performed for this study. Information has been provided on the materials used in the study, the manufacturing techniques, the preparation of specimens, the mechanical tests performed and the standards according to which they were carried out, the analyses applied, and the equipment and apparatus used to carry out these analyses.

3.1. Materials

The base material used in this study was PEEK (Toray Cetex TC1200; melting point of 343 ^{0}C and glass transition temperature of 143 ^{0}C). In addition, its carbon woven prepreg has a fiber content of 58% by weight.[141]

The properties of FM®300K film adhesive, used in the adhesive bonding process and widely used in the aerospace industry, are shown in Table 3.1.[142]

Table 3.1 FM 300K film adhesive properties.

Adhesive	Nominal Weight (gsm) (±25)	Nominal Thickness (mm)	Carrier
FM 300K	244 391	0.20 0.33	Wide Open Knit

3.2. Manufacturing of CF/PEEK Thermoplastic Composite Plate

CF/PEEK composite laminates with a unit weight of 485 g/m^2 were fabricated by stacking arrays of 8-layer CF/PEEK prepregs $[45/0/45/0]_s$ using the hot-pressing technique, followed by a cure step performed at 385 °C and 1 MPa under pressure. These productions were carried out at Turkish Aerospace Industries (TAI), the industrial partner of the study. The manufactured plate thickness was determined to be 2.46 mm. The CF/PEEK laminates manufacturing steps are shown in Figure 3.1.

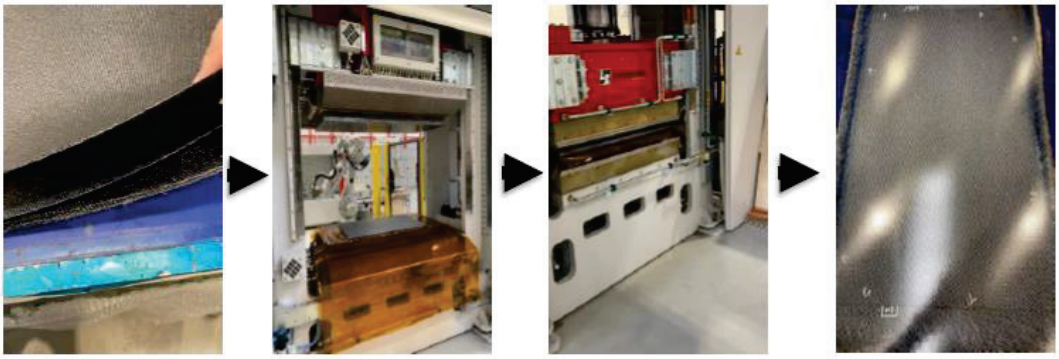

Figure 3.1. Manufacturing steps of CF/PEEK laminates.

3.3. Laser Surface Treatment

In order to increase the mechanical performance of the joint area of the manufactured CF/PEEK thermoplastic composite plate, laser surface treatment was applied to the sample surfaces prior to bonding with the adhesive film. An IR-Yb (Ytterbium) fiber nanosecond pulsed laser (FLAST-NanoMARK Energy-50w) was used in this study (Figure 3.2) with the following parameters: wavelength of 1064 nm, spot diameter of 30 nm, and pulse width of 100 ns.

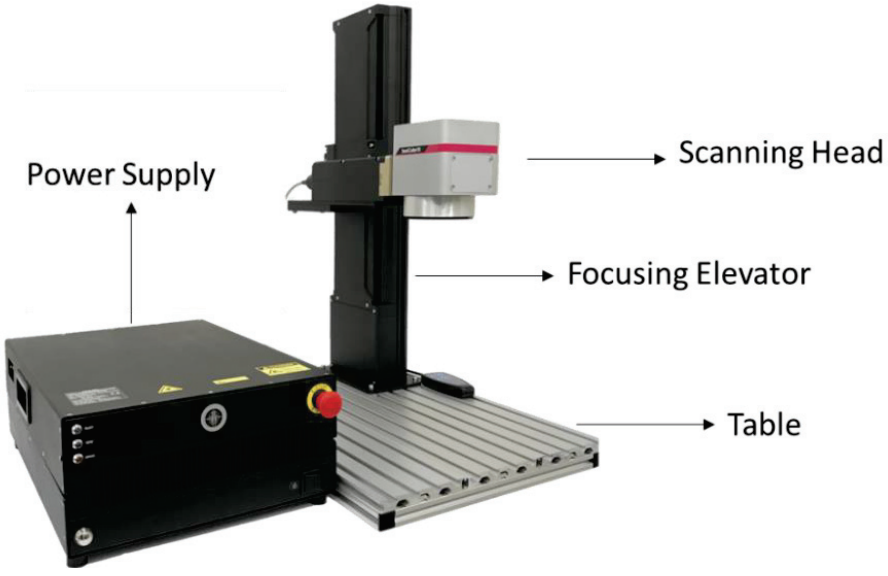

Figure 3.2. The fiber laser system.

As shown in Figure 3.2, the laser system that used in this study consists of a scanning head, a table, a focusing elevator, and a power supply.

The laser surface treatment process was performed using different laser parameters on CF/PEEK samples whose surfaces were cleaned and prepared to the desired dimensions prior to bonding with adhesive. The most crucial step in the laser process is the determination of the optimal laser working parameters for the CF/PEEK material that was used in the study.

3.3.1. Determining Optimum Laser Parameters

CF/PEEK composite plate surfaces were treated with laser in a square shape (25*25 mm^2) and fiber direction (45^0) (Figure 3.3).

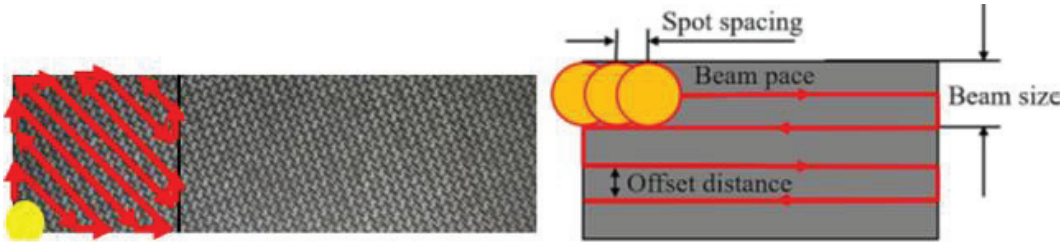

Figure 3.3. a) Laser principle: ablation by treating in fiber directions (45^0) and b) laser spot distribution parameters.[143]

Depending on each surface to be treated, the focus point of the laser device was adjusted with the help of the focusing elevator. The area that the laser optical head can move for focusing is limited by the movement distance of the focusing elevator. This movement distance is 64 x 140 x 610 mm.

There are some critical parameters and limitations that we will focus on in the experimental setup and processing strategy for the laser ablation process. One of the most critical points to consider is to obtain maximum surface roughness with minimum fiber damage. In addition, it is very important to fine-tune the focus of the laser to obtain the desired laser-treated surface. By changing the height of the laser optic head used in the laser setup, the focus point was adjusted for each surface to be treated.

In order to achieve maximum surface roughness with minimum fiber damage, the optimum values of some parameters used during the laser process are very critical. To this end, this study attempts to obtain the desired surface by varying the average laser

power, frequency and scanning speed. The values applied to the surface to optimize the laser parameters are shown in the Table 3.2.

Table 3.2 Experiment parameters for the laser treatment process.

Parameter	Values
Power (W)	5 8 10 12 20 30
Scan Speed (m/s)	0.1 0.5 1 5 10 20
Frequency (kHz)	100 and 200

The laser power was varied between 5-30 W and the frequency values were varied between 100-200 kHz, while the application speed of the laser optic head was varied between 0.1 and 20 m/s. Laser offset distance values of 0.03 mm were chosen. The reason for working over such a wide range of laser parameters to be applied is that it is desired to achieve optimum values by defining boundary conditions. The operating range of these three parameters selected at the beginning of the study was also determined by considering the limits of the laser device. To achieve the desired surface finish and maximum mechanical performance of the bonded structure, the operating range for the given parameters must first be determined.

After laser treatment, the samples were first exposed to air at a pressure of 7 bar, then placed in an ultrasonic bath for 2 hours to clean the surface and dried in an oven for approximately 2 hours. In this way, contaminants, fibers, and resin residues that may have accumulated on the surface during the laser process were removed from the surface.

3.4. Fabrication of Adhesive Bonded CF/PEEK Plates

In the study, the joint structures of laser-treated and untreated (reference) CF/PEEK specimens were fabricated using FM®300K adhesive film. The production steps of adhesive bonded CF/PEEK structures are shown in Figure 3.4. According to Figure 3.4, the plates produced in TAI were scaled to the desired dimensions with a diamond saw and, after cleaning their surfaces in an ultrasonic bath and with compressed air at 7 bar, the laser surface treatment process was applied. The reference samples do not include the laser process step. The surfaces prepared for joining were joined directly with

the adhesive film, without laser application, under the same joining conditions as the laser-treated samples. Bonding was performed under the conditions specified in the adhesive's technical data sheet. Accordingly, the parts to be bonded were held under a hot press at 180 ^{0}C for 1 hour and then allowed to cool to room temperature under pressure. The thickness of the bonded plate was determined to be 5.26 mm. Test coupons sized according to the relevant standards were cut and prepared from these CF/PEEK bonded plates.

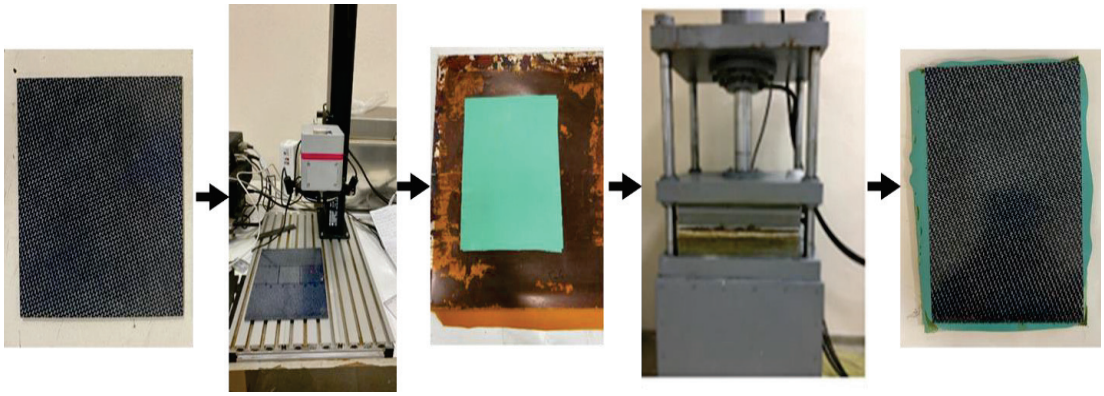

Figure 3.4. Manufacturing steps of adhesive bonding CF/PEEK plates.

3.5. Instrumentation and Testing

This section provides information on the samples prepared, the analyses and tests performed, and the standards used for these tests to determine the thermal, mechanical, surface, and microstructural properties of the samples produced. In addition, the equipment used for these analyses and tests is specified.

3.5.1. Differential Scanning Calorimetry (DSC) Analysis

The crystallization and melting behavior of the composites was investigated by Differential Scanning Calorimetry (DSC) using a TA Instruments Q10 Differential Scanning Calorimeter, operating under a nitrogen flow. Approximately 10 mg samples were weighed and sealed in aluminum specimen pans. The DSC analysis was performed in two runs. First, it was increased from room temperature to 400 ^{0}C at a rate of 10 ^{0}C/min and decreased to 50 ^{0}C at the same rate. Then it was increased from 50 ^{0}C to 380 ^{0}C, again

at a rate of 10 ^{0}C/min. In the calorimetric curves, the transition temperatures were taken as the peak maximum or minimum.

3.5.2. Mechanical Characterization of Adhesively Bonded CF/PEEK Composites

Single Lap Shear (SLS), Charpy Impact, and Double Cantilever Beam (DCB) tests were performed on the specimens prepared according to appropriate standards to determine the mechanical performance of the joint region of the specimens whose surfaces were treated with the selected laser parameters and the reference (non-laser treated) specimens. The effects of the laser surface treatment process were obtained comparatively.

As a result of these tests, the behavior of the bonded CF/PEEK structures under various loads has been studied in detail. The effect of laser surface treatment on the interface was clearly demonstrated.

3.5.2.1. Single Lap Shear Test

The reference and laser treated adhesive bonded plates were prepared for the single lap shear test accordance with ASTM D5868[144] standard. Single-lap shear test used to determine the bond characteristics of laser-treated and reference specimens and to determine the shear strength of the bond. According to ASTM standard, the specimen loading rate was set to 13 mm/min. A minimum of five lap shear specimens were prepared and tested for each group.

During the preparation of the test coupons, the test specimens were joined using 3 layers of FM300K adhesive film. Each sample surface was subjected to surface cleaning processes before joining with adhesive. For this purpose, 7 bar compressed air was applied to both the reference sample surfaces and the laser treated sample surfaces, and then the specimens were kept in an ultrasonic bath for approximately 2 hours. Finally, they were kept in an oven at 50 ^{0}C for 2 hours to remove moisture. The specimens, whose surfaces are prepared, were then bonded according to the adhesive bonding process conditions. After that, specimens scaled with a diamond saw and the channel opening

process was performed with a Maintek CNC router (Figure 3.5) to measure the strength of the joint area.

As a result of the test, strain versus stress graphs were obtained and standard deviations were calculated, and comparisons were made. Also, the single-lap shear strength results obtained from the test were calculated and compared for the laser and reference specimens.

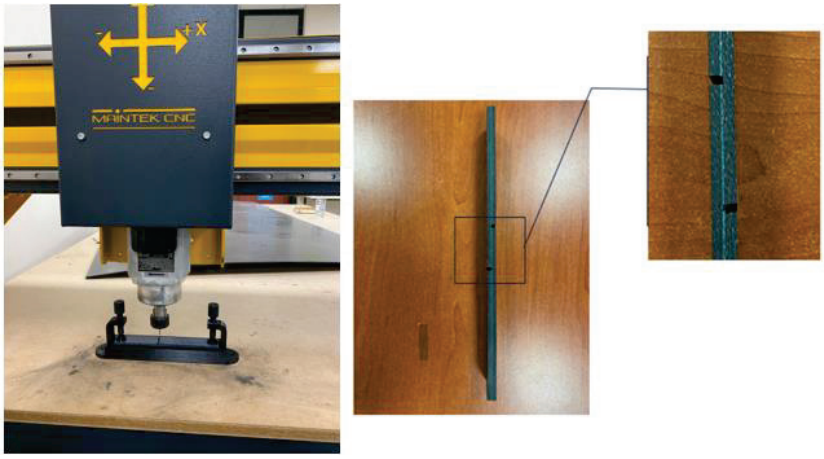

Figure 3.5. CNC router device and bonding region of single lap shear specimen.

An illustration of the prepared lap shear specimens is shown in Figure 3.6. As shown in Figure 3.6, the specimens are 180 mm long and 25 mm wide with a bonded area of 25 × 25 mm^2.

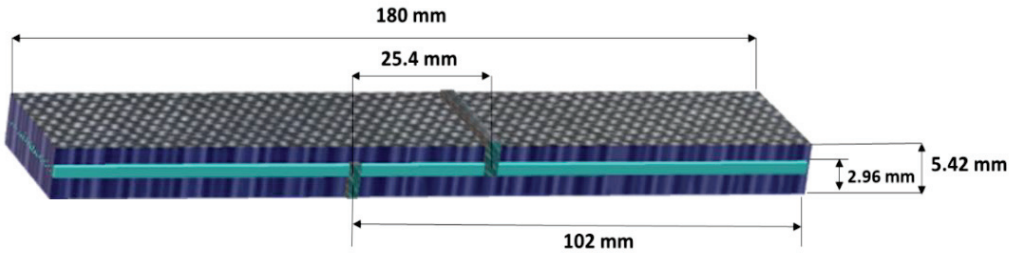

Figure 3.6. Illustration of dimensions of test specimens.

The prepared CF/PEEK single lap shear test coupons and an MTS Landmark^{TM} Servohydraulic Test System was used for single lap shear test are shown in Figure 3.7.

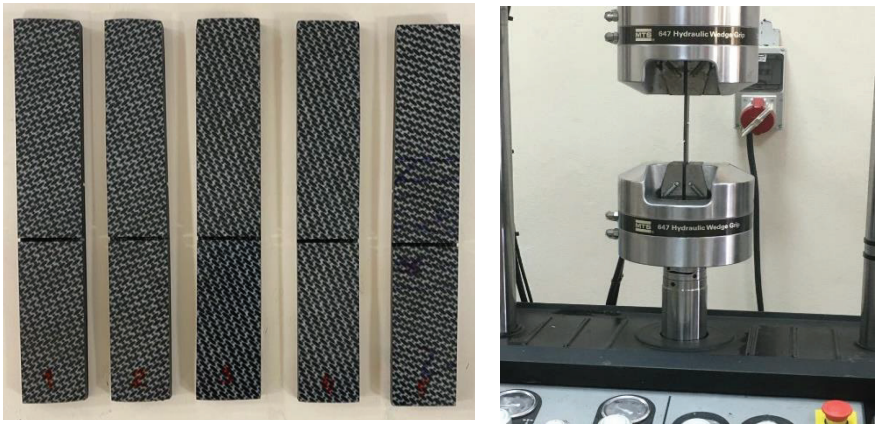

Figure 3.7. Single lap shear test coupons and test specimen during testing.

3.5.2.2. Charpy Impact Test

The Charpy impact test was performed on laser treated and reference specimens prepared (Figure 3.8) in accordance with the ISO 179-1 standard using the CEAST ® Resil Impactor device with a maximum energy of 15 J pendulum (Figure 3.9).

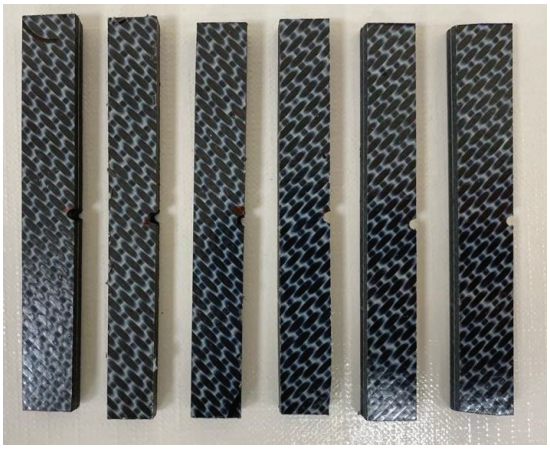

Figure 3.8. Charpy impact test specimen.

The Charpy impact test is performed on a specimen to measure the amount of energy required to break a specimen in Joules (J). This involves measuring the potential energy before and after the pendulum strikes the sample. The energy absorbed in the fracture of the test specimen is equal to the change between the energy of the pendulum hammer at the moment of impact and the energy which remains in the pendulum hammer

after the fracture of the test specimen. To obtain the impact energy in kJ/m^2, this value must be divided by the cross-sectional area at the notch.

In the Charpy impact test, laser-treated surfaces with the parameter that gave the best strength result according to the lap shear test results and reference samples with untreated surfaces were bonded with 3 layers of FM300K adhesive in a hot press under the bonding conditions specified in the data sheet. Before bonding with adhesive, all surfaces were subjected to the previously described surface cleaning process. A minimum of 6 specimens were then prepared by cutting 10 x 80 mm rectangles and notching 2 mm. During specimen preparation, the V-notch was opened on the specimens using a notch opening machine as specified in the standard. This test method also provides information about the toughness of the specimens.

Figure 3.9. Charpy impact test device.

3.5.2.3. Double Cantilever Beam (DCB) Test

The Mode I interlaminar fracture toughness of the specimens was determined by double cantilever beam (DCB) testing. The DCB test is commonly used to determine the initiating and propagating values of Mode I fracture energy under load.

In the DCB test, load is applied to specimens at the same crosshead speed in opposite directions (i.e., tensile load) and is applied to a DCB specimen with a through-width insert embedded in the specimen center plane. The crack tip progression in a DCB specimen can be observed with a CCD camera, microscope, or crack gauge. At the end

of the test, the critical energy release rate was determined as a function of delamination length.[146]

Standard Test Method for Mode I Interlaminar Fracture Toughness of Fiber-Reinforced Polymer Matrix Composites 1, n.d. (ASTM D5528[148]) is used to investigate mode-I interlaminar fracture toughness of fiber-reinforced polymer matrix composites. Fracture toughness is the ability of a material to withstand the initiation and growth of cracks. In accordance with ASTM D5528-13, three types of data reduction methods are used to calculate G_{Ic} values. These are a compliance calibration (CC) method, a modified compliance calibration (MCC) method, and a modified beam theory (MBT) method. Because the MBT method is more consistent, it is the preferred approach for calculating G_{Ic} values. The dimensions of the test specimens prepared in accordance with the specified standard are shown in Figure 3.10.

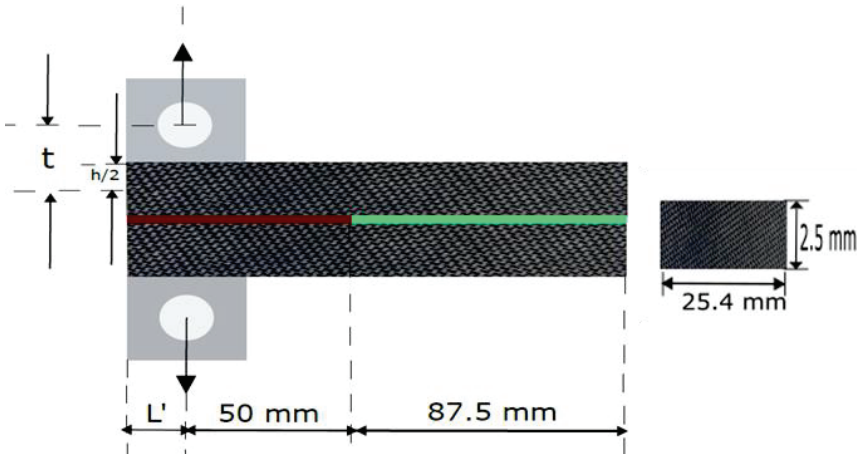

Figure 3.10. Dimension of DCB test specimen.

A minimum of 6 samples were prepared for both laser-treated and reference samples. The sample preparation steps are shown in Figure 3.11.

During the preparation of the DCB test coupons, laser treated surfaces, and reference samples (untreated surfaces) with the parameters that gave the best strength results, as indicated by the lap shear test results, were bonded separately with 3 layers of FM300K adhesive in a hot press using the bonding conditions specified in the data sheet, i.e. it was heated to 180 ^{0}C under pressure, held at that temperature for 1 hour, and then cooled to room temperature under pressure. As shown in Figure 3.11, the specimens were cut with a diamond saw to a width of 25.4 mm and a length of 150 mm. The initial

delamination length, a_0, was approximately 50 mm. Kapton film was used as a crack starter.

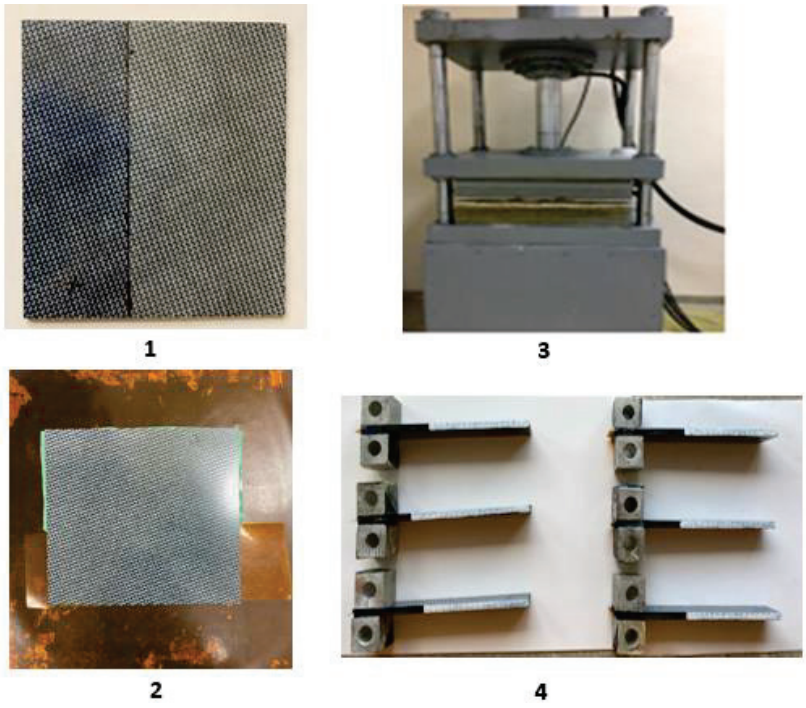

Figure 3.11. DCB test specimen production steps.

The DCB test is carried out on test specimens as follows: First, the specimens are loaded, and the crack is allowed to propagate approximately 5 mm. The specimens are then unloaded. Finally, the specimen was again loaded until the crack had propagated to a distance of approximately 70 mm from the beginning of the crack. During this test, the crosshead speed was set to 1 mm/min.

Figure 3.12 represents a DCB test specimen undergoing Mode-I testing. The specimen load, crack length, and displacement values were all collected during the test to calculate the Mode-I interlaminar fracture toughness (G_{Ic}). DCB test is examined as initiation and propagation according to crack length. The Mode-I interlaminar fracture toughness values for initiation and propagation were also determined and compared for both laser and reference specimens. The Modified Beam Theory (MBT) data reduction approach was used to calculate the G_{Ic} in this study as follows (Eqn 3.1):

$$G_I = \frac{F}{N}\frac{3P\delta}{2b(a+|\Delta|)} \tag{3.1}$$

where G_I is the Mode-I interlaminar fracture toughness, F and N are the correction parameters.

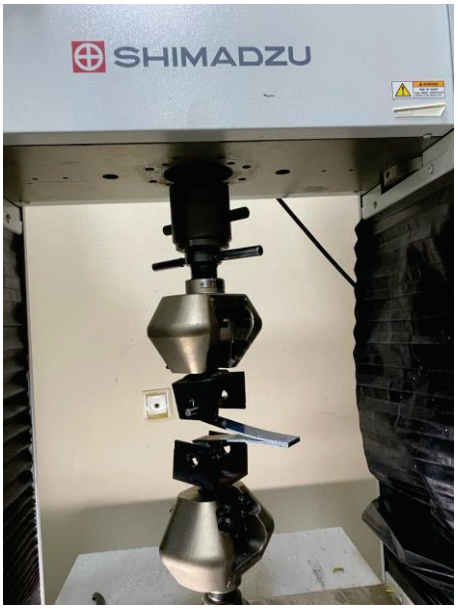

Figure 3.12. DCB test specimen during test.

These correction parameters can be obtained using Eq.(3.2) and Eq.(3.3), where P is the load, is the load point displacement, b is the specimen width, a is the delamination (crack) length, which is determined experimentally by making a least squares plot of the cube root of the compliance ($C^{1/3}$) as a function of the delamination length. The compliance, C, is the ratio of the load point displacement to the applied load, and t and in the equations are shown in Figure 3.10.

$$F = 1 - \frac{3}{10}\left(\frac{\delta}{a}\right)^2 - \frac{3}{2}\left(\frac{\delta t}{a^2}\right) \tag{3.2}$$

$$N = 1 - \left(\frac{L'}{a}\right)^3 - \frac{9}{8}\left[1 - \left(\frac{L'}{a}\right)^2\right]\left(\frac{\delta t}{a^2}\right) - \frac{9}{35}\left(\frac{\delta}{a}\right)^2 \tag{3.3}$$

3.5.3. Methods for Determination of Laser Surface Treatment Effects

In order to reveal the effects of laser surface treatment parameters on CF/PEEK interface surfaces, the samples were examined by optical microscopy and SEM. After the optimal laser parameters were determined by microscopic examinations and then by

mechanical tests, the roughness profile and contact angle values of the selected surface were given in comparison with the reference sample.

3.5.3.1. Optical Microscopy Analysis

In preliminary studies, CF/PEEK surfaces that were laser treated prior to bonding were examined under an optical microscope to determine the effect of the laser on the surface.

The goal of this investigation is to determine how the laser pulse shape and surface patterning change with varying laser parameters. For this purpose, the samples, whose surfaces were treated with different laser parameters, were made ready for examination with an optical microscope by holding them at 7 bar of compressed air and in an ultrasonic bath for 2 hours to clean their surfaces. The samples were then placed in an oven to remove any moisture from the samples. The study was conducted using a Leica DM2500 M branded light microscope.

3.5.3.2. Scanning Electron Microscopy (SEM) Analysis

CF/PEEK surfaces that were laser treated prior to bonding were prepared for SEM analysis to determine the effect of the laser on the surface. Prior to SEM analysis, the samples were exposed to air at 7 bar pressure and kept in an ultrasonic bath for 2 hours to remove any contaminants on the surface. The specimens were then placed in an oven to remove any moisture. In addition, scanning electron microscope (SEM) images of the fractured surfaces of the CF/PEEK composites were taken to determine failure modes and to evaluate strengthening mechanisms after mechanical testing. The specimens were sputter coated with a thin layer of gold for 90 seconds and examined under a Quanta 250FEG SEM and ZEISS EVO10 at various magnifications.

3.5.3.3. Surface Roughness Analysis (Profilometer)

One of the parameters that increases the strength of the joint area of specimens whose joint surfaces are laser treated prior to bonding is the increase in surface roughness

caused by the laser process. Surface topography must be obtained to measure surface roughness.

A BRUKER DektakXT profilometer (Figure 3.13) was used to obtain the surface topography of the reference and laser treated surfaces. An area of 12*12 mm^2 was scanned with profilometer and a surface profile was obtained for both samples. As a result of the analysis, the roughness values of both surfaces were determined. The correlation between the obtained surface roughness values and the effect of the laser surface treatment process on the mechanical strength of the bonded CF/PEEK structure was demonstrated.

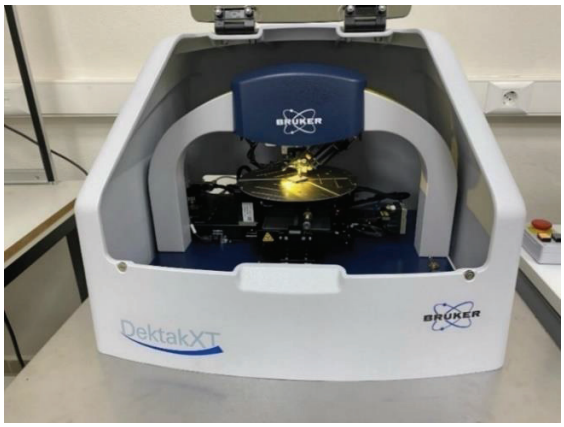

Figure 3.13. Profilometer device.

3.5.3.4. Contact Angle Analysis

Contact angle analysis was performed using pure water to determine the wettability of the laser-treated and reference samples. This analysis was conducted using the KSV Attension Theta instrument as shown in Figure 3.14.

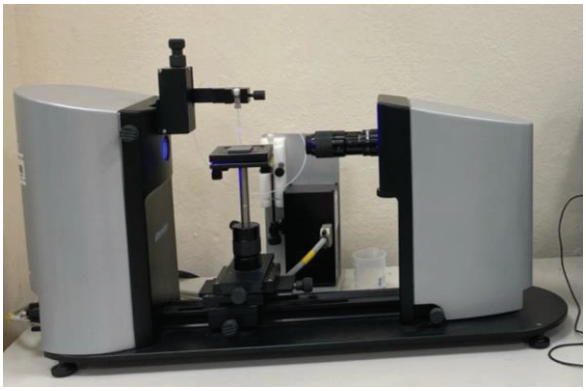

Figure 3.14. Contact angle measurement device.

Figure 3.15 shows the sample prepared for 20*20 mm^2 contact angle analysis and the sample during the analysis.

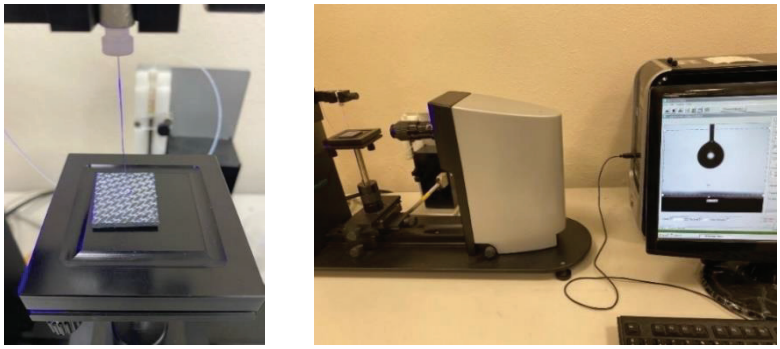

(a) (b)

Figure 3.15. a) Contact angle test sample b) Sample undergoing contact angle measurement.

Three measurements were taken from different points on each surface. A 5 µL droplet is carefully placed on the surface to be analyzed and the CCD camera captures one snapshot of the droplet per second. The wettability (contact) angle of both surfaces was compared and the effect of laser surface treatment on the wettability property was investigated.

The static sessile drop method was used for the determination of the contact angle at room temperature (23°C). The procedure used to calculate the contact angle of the drop with the surface after it touches the surface is shown in Figure 3.16.

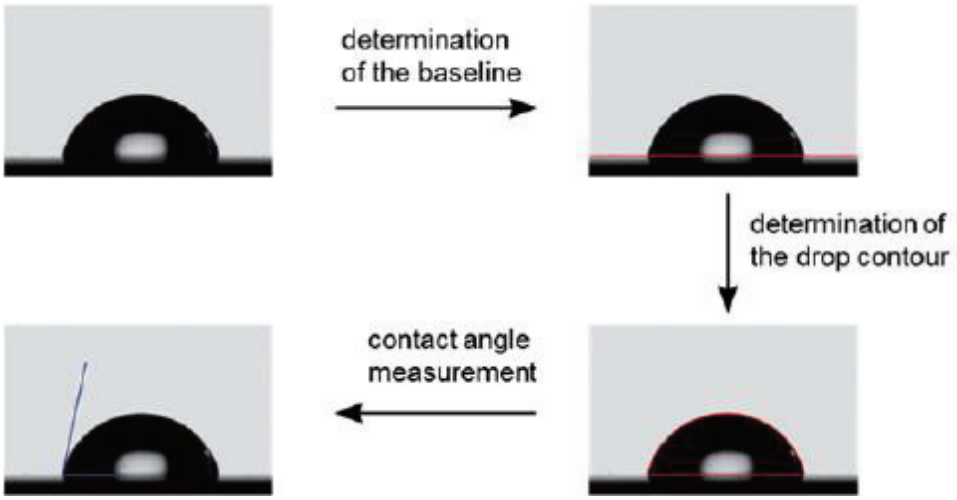

Figure 3.16. Procedure for the determination of contact angles with the sessile drop method.[149]

In the Sessile Drop Experiment procedure, the needle adjustment is used to place a drop of pure water on the surface. A drop of appropriate size (5µl) is lowered from the needle onto the surface of the sample. It is often useful to start imaging as soon as the drop touches the surface, so it is possible to set a trigger and ROI (Region of Interest) to do this before the drop is dispensed. ROI means that a region of interest is created around the drop. The contact angle formed by the drop on the surface and the surface is calculated from images taken at regular intervals. In this study, 15 images were taken at 1 second intervals.

According to Figure 3.16, the static contact angle was determined by drop shape analysis. First, the contact line of the drop with the surface, i.e., the baseline, the drop contour, and the image clarity are adjusted. The instrument then automatically calculates the contact angle value using the ellipse fitting mathematical method. In this method, the droplet on the surface is completely surrounded by an elliptical line. The contact angle is determined as the slope of the contour line at the three-phase contact point on the left and right sides of the drop. Contact angle results are measured for these two intersection points (right and left).[150]

.

CHAPTER 4

RESULTS AND DISCUSSION

This section reports the results of the thermal properties of the CF/PEEK plates, the effect of the laser parameters on the microstructure of the CF/PEEK surfaces, and the mechanical properties of the bonded CF/PEEK structures. The influence of the laser surface treatment parameters on the improvement of the mechanical properties of the bond regions are illustrated by optical and SEM images of control and laser specimens. Optimal operating ranges for the laser parameters were determined from these results. This chapter also compares single lap shear strength, Mode I fracture toughness, and Charpy impact energy values for bonded CF/PEEK structures for laser-treated and reference samples. In addition, the bonding mechanism created by the laser treatment process on the CF/PEEK surface was determined by SEM, surface roughness and contact angle analyses. Surface profilometry and contact angle results are shown for the laser parameter that gave the highest results in the SLS test and the reference specimens. These analyses highlight the reason for the increase in mechanical testing achieved by the laser surface treatment.

4.1. Thermal Properties

Important temperature values (melting, crystallization, and glass transition temperatures) of the PEEK matrix were determined by Differential Scanning Calorimetry (DSC) analysis. The thermal properties obtained from DSC analysis are of great significance for the determination of the production parameters and the conditions of use of the material (service temperature).

4.1.1. Differential Scanning Calorimetry (DSC) analysis

DSC analysis was performed to determine the glass transition temperature (T_g), crystallization temperature (T_c) and melting temperature (T_{melt}) of the CF/PEEK prepreg. In the calorimetric curves, the transition temperatures were considered to be the peak maximum or minimum. DSC heating curves of PEEK material are shown in Figure 4.1.

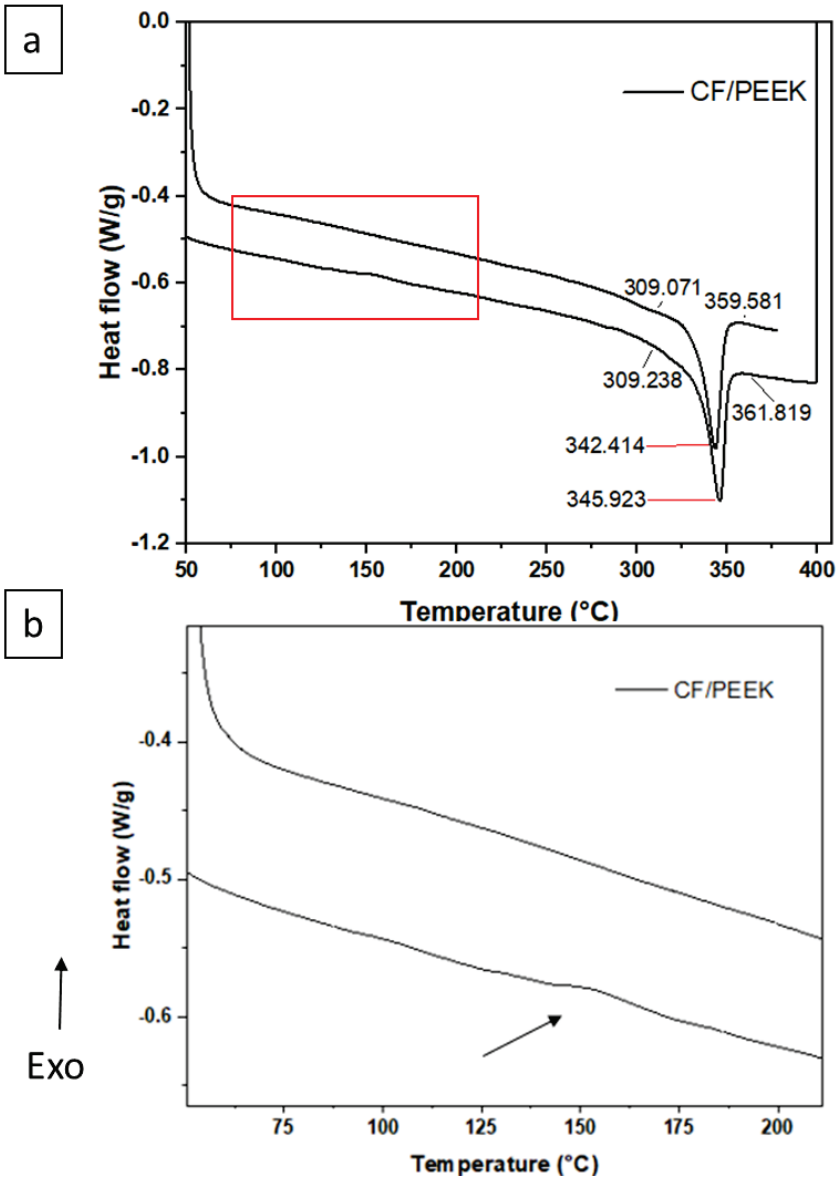

Figure 4.1. DSC scans of a) CF/PEEK prepreg b) high magnification of the red area in Figure 4.1a (the arrow indicates the glass transition of the PEEK matrix in the composite).

In the case of the melting process, the DSC heating curves are shown in Figure 4.1a. A small variation in heat flow associated with the glass transition temperature of PEEK is shown in Figure 4.1a at about 149 ^{0}C, and a magnified view of the area where Tg appears on the DSC graph is shown in Figure 4.1b. The PEEK polymer matrix has a semi-crystalline structure. The glass transition is related to the mobility of the chain in the amorphous regions in the polymer structures. For this reason, the glass transition temperature did not give a sharp peak. Figure 4.1a also shows an endothermic peak for PEEK at 345.92 ^{0}C, which corresponds to the melting temperature Tm.

The crystallization temperature of PEEK, the point at which the exothermic peak is observed, is approximately 302.44 ^{0}C, as shown in Figure 4.2.

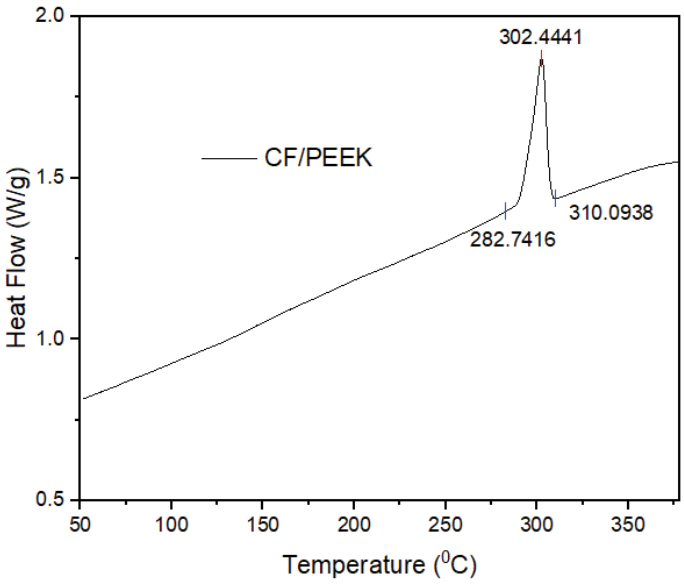

Figure 4.2. The crystallization peak of CF/PEEK prepregs in DSC analysis.

PEEK is a high temperature semi-crystalline thermoplastic known for its excellent thermal and chemical stability. In thermoplastic composites, parameters such as melt temperature, dwell time, fiber volume percentage, and shear deformation history have a strong influence on the crystallinity of the final part. Without proper crystallization, thermoplastics tend to have amorphous properties, which typically result in much lower mechanical properties and low chemical resistance.[151] For this reason, it is necessary to determine its chemical and especially thermal properties before starting work. For example, in the hot-pressing process used in this study, the process temperature must be

above the melting temperature to produce CF/PEEK composite plates. The results of these pre-production analyses were also used to determine the production process parameters.

4.2. Determining Optimum Laser Parameters

In order to achieve maximum surface roughness with minimum or no fiber damage, and to increase the mechanical performance of the adhesive bonded structure, studies have been conducted to determine the optimum values of some parameters used during the laser process, taking into account the limitations of the laser device. These parameters are laser power, frequency and scanning speed. In this study, hatch distance values of 0.03 mm were set. The laser power was varied between 5-30 W, the frequency values were varied between 100-200 kHz, and the application scanning speed of the laser optical head was varied between 0.1 and 20 m/s.

The surfaces of the CF/PEEK plates to be laser processed were prepared in a square shape to determine the optimum values of the laser parameters. In order to determine the effect of the laser parameters on the samples whose surfaces had been prepared, an optical microscope examination was performed first, followed by a surface examination by SEM.

4.2.1 Optical Microscopy Examination

First, the optical microscope image of the sample whose surface was not laser treated (reference) is shown in Figure 4.3.

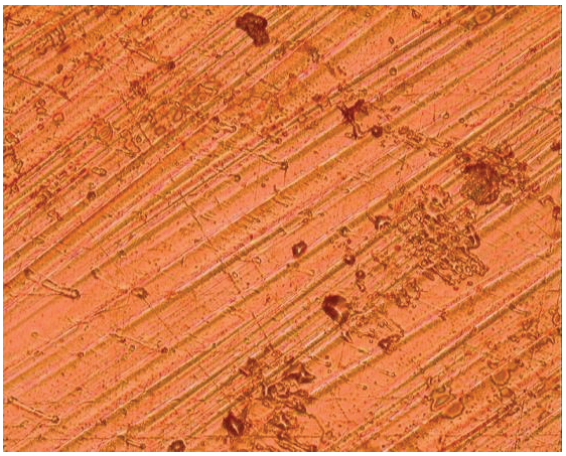

Figure 4.3. Optical microscope image of the reference sample (10x magnification).

The first step was to determine if there was a correlation between the laser treating direction and the fiber direction. For this purpose, the surfaces were treated with two different strategies in the 0^0 direction and in the 45^0 (fiber) direction and the results were examined with an optical microscope. Optical microscope images of these surfaces are shown in Figure 4.4.

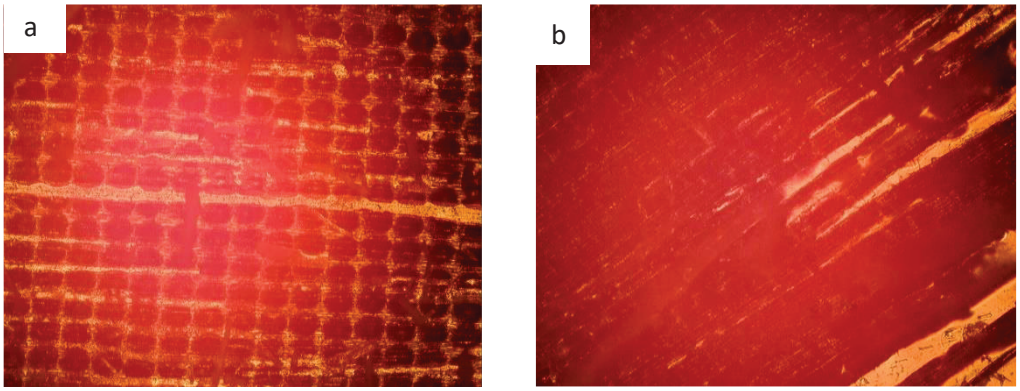

Figure 4.4. Optical microscope images of laser treated CF/PEEK in different scanning angles: a) 0^0 direction b) 45^0 (fiber) direction.

According to the optical microscope results, it was seen that scanning the surfaces in the fiber direction (45^0) gave better results (Figure 4.4b). In other words, it was observed that the laser has a greater effect on the surface in the scans made in the fiber direction, so it can remove more matrix material from the surface. The reason for this is that carbon fibers transmit the energy received from the laser beam to the matrix material more easily by scanning in the fiber direction. (Figure 4.5).

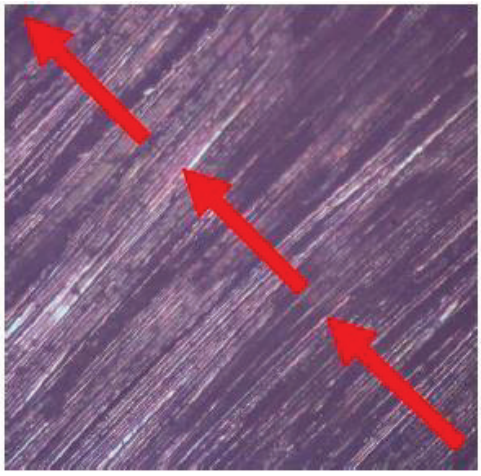

Figure 4.5. Direction of the laser beam (45^0).

The first results of the optical microscope analyses showed how the laser pulse traces formed on the surface changed with the three parameters mentioned above. For example, Figure 4.6 shows optical microscope images of laser pulse traces formed at the same average laser power and scanning speed, but at different frequencies.

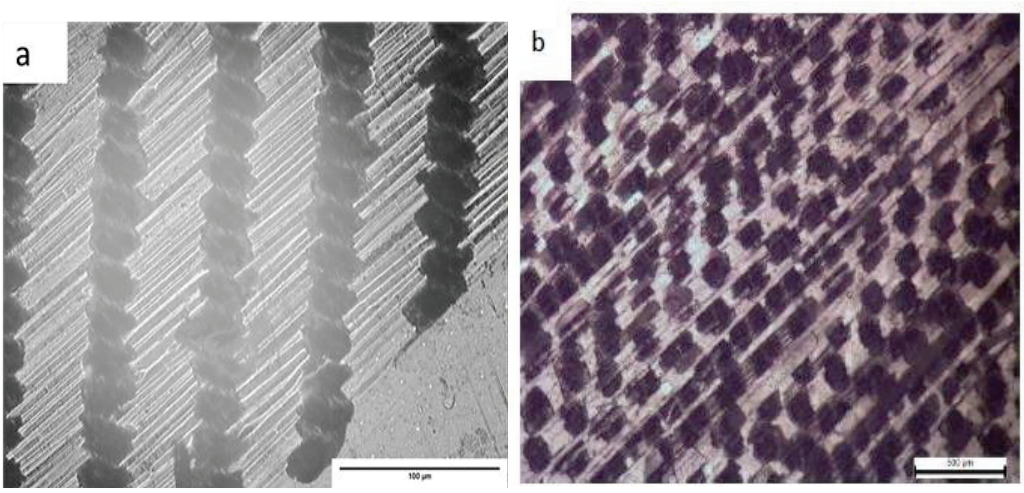

Figure 4.6. Optical image of CF/PEEK with surfaces treated by laser with different parameters a) 20 W, 20 m/s, 100 kHz b) 20 W, 20 m/s, 200 kHz (10x magnification).

Figure 4.7 shows optical microscope images of laser pulse traces at the same power and frequency, but at different scanning speeds.

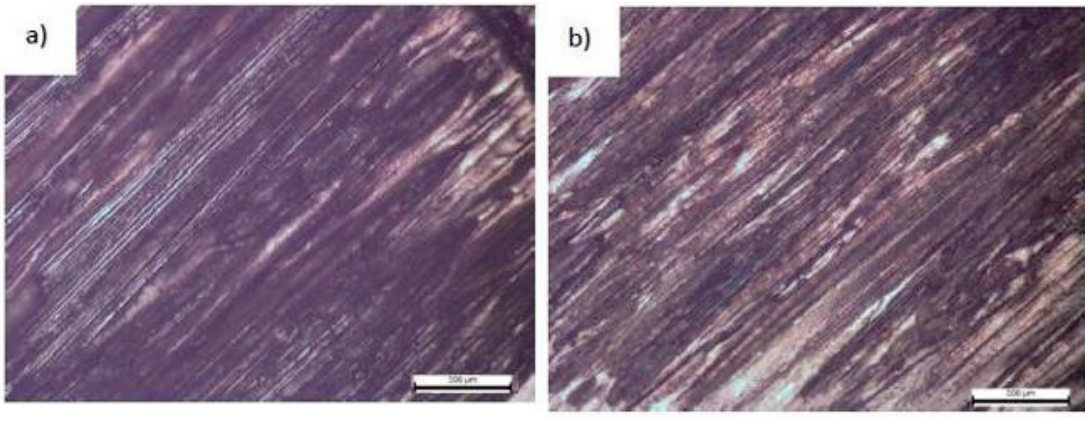

Figure 4.7. Optical image of CF/PEEK with surfaces treated by laser with different parameters. a) 10 W 0.5 m/s, 200 kHz, b) 10 W, 1 m/s, 200 kHz (20x magnification).

Laser pulse traces at the same power and scanning speed but at different frequencies are given in Figure 4.8.

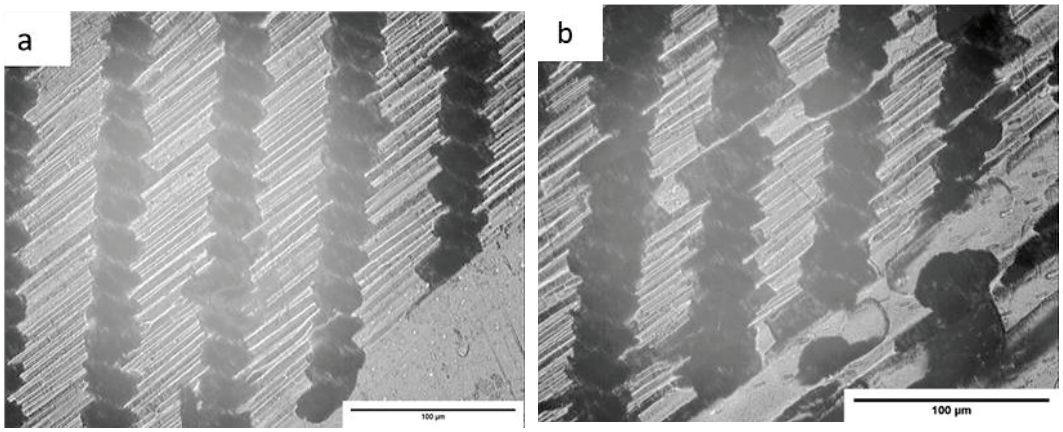

Figure 4.8. Optical image of CF/PEEK whose surfaces are treated by laser with different parameters a) 20 W, 20 m/s, 100 kHz, b) 30 W, 20 m/s, 100 kHz.

Based on these optical microscope images, the marking pattern on the surface changes with the laser pulse as the frequency and scanning speed parameters change. It was observed that the laser power parameter has no effect on the marking style on laser-treated surfaces.

In order to better observe the effects of laser power, scanning speed and frequency parameters on the CF/PEEK bond surface, they were investigated by SEM analysis prior to bonding. According to these effects, optimal laser parameters were determined to obtain the desired surface.

4.2.2. Effect of Laser Frequency Parameter on Microstructure of CF/PEEK Plates

In the process of selectively removing the matrix material from the surface by laser surface treatment, it was found that the effect of the frequency and scan speed values on the microstructure changes the laser pattern formed on the surface, according to optical microscope examinations. The reason why the pattern on the surface changes with the laser frequency and laser scanning speed parameters is that the distance between the laser pulse points changes with these two parameters. In the study, the hatching distance value was set to 0.03 mm. The power parameter has no effect on the distance parameter between

two laser points formed on the surface. As the distance value between points decreases, areas of overlap occur on the surface, and these areas cause the HAZ effect to increase. In order to prevent the negative effect of HAZ, it is necessary to minimize the overlap on the surface and keep it at the desired level according to the power parameter. The parameter to be examined is the distance between laser pulse points on the surface. Distance values between points for different speeds and parameters are given in Table 4.1.

Table 4.1 Point distance values for various frequency and scan speed parameters.

Frequency (kHz)	Scan Speed (m/s)	Point Distance (mm)
100	0.1	0.001
	0.5	0.005
	1	0.01
	5	0.05
	10	0.1
	20	0.2
200	0.1	0.001
	0.5	0.003
	1	0.005
	5	0.025
	10	0.05
	20	0.1

While the distance between points increases with increasing speed, the frequency value decreases with increasing frequency. Therefore, in order to clearly examine the effect of the frequency value on the microstructure, the maximum value of 20 m/s was selected in the instrument to prevent the laser scanning speed from causing overlapping. At this speed value, the distance between the laser points is at its maximum. The overlapping seen in the microstructures and the resulting HAZ regions are structures formed only by frequency change. Thus, the effect of the frequency value on the microstructure is clearly shown in this study. The frequency values of the laser device used in the study vary between 100 kHz and 200 kHz. Surface examination studies for these two frequency values were carried out by SEM analysis.

SEM images of the changing surface pattern for laser surface treatments at different frequencies at the same power and scanning speed are shown in Figure 4.9.

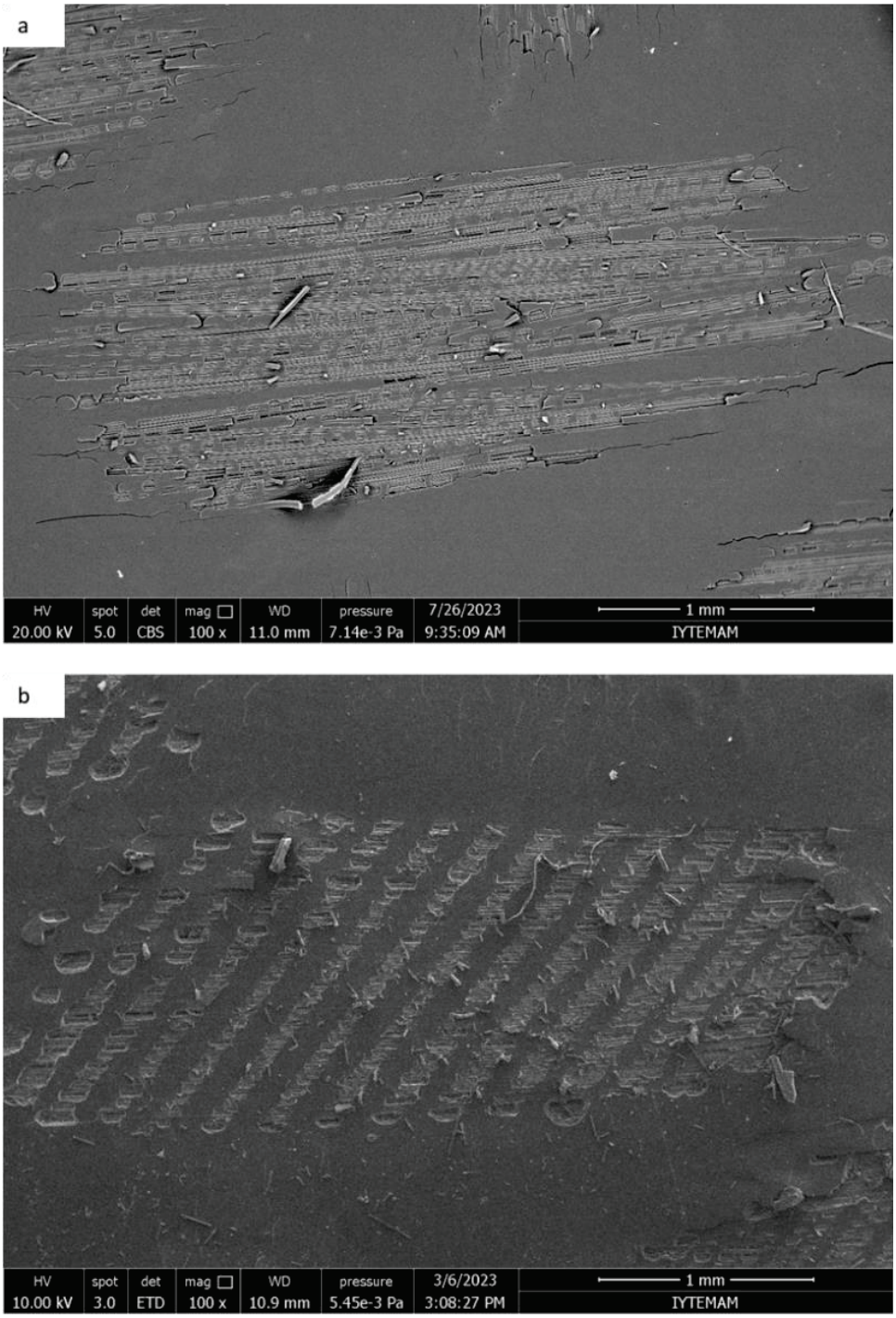

Figure 4.9. SEM images of laser treated surfaces with following parameters: a) 20 W, 20 m/s, 100 kHz b) 20 W, 20 m/s, 200 kHz.

As shown in Figure 4.9, the laser tracks that change as the frequency changes can be clearly seen on the surface. Depending on the change in pattern shape, overlapping occurs in some areas on the surface. This situation can increase the effect of the HAZ formed on the surface and lead to fiber damage, depending on the effect of laser power and speed.

Figures 4.10(a) and 4.10(b) show higher magnification micrographs of the SEM images of the surfaces in Figures 4.9(a) and 4.9(b), respectively. The surface in Figure 4.10(a) is very close to the desired surface. At the point of the laser pulse, the matrix material has been removed and the fibers are visible on the surface without damage. As shown by the red area in Figure 4.10(b), even if the same values of speed and power are used, a change in the frequency value can result in undesirable areas (fiber damage and matrix residue) on the surface. This will negatively affect the mechanical performance of the joint area. Therefore, this situation should be taken into consideration when selecting the frequency value. At the same time, it can be seen that the CF/PEEK plates whose interface areas between the two surfaces are treated with a high-frequency (200 kHz) laser parameter are closer to the desired surface.

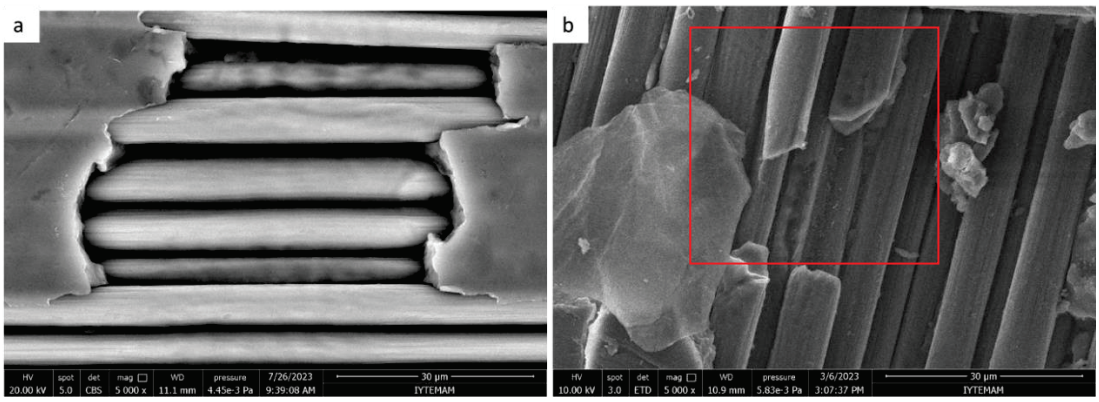

Figure 4.10. Higher magnification SEM images of laser treated surfaces with the following parameters: a) 20 W, 20 m/s, 200 kHz b) 20 W, 20 m/s, 100 kHz.

Figure 4.11 shows images of the laser treatment performed at different frequencies with the same power and speed, this time with lower laser power to avoid fiber damages that negatively affects the mechanical strength in the joint area.

According to Figure 4.11(a), the high-frequency laser treatment did not remove matrix material from the surface to the desired extent. This resulted in matrix residue on

the surface, which would reduce mechanical performance. Low frequency (100 kHz) SEM images (Figure 4.11(b)) gave results closer to the desired surface. At the points of the laser pulses, matrix material was removed from the surface without damaging the fibers.

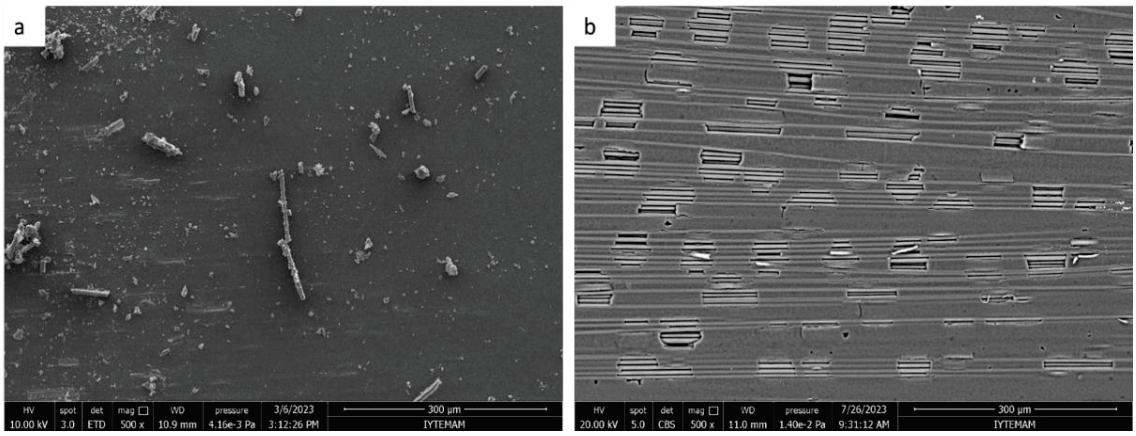

Figure 4.11. SEM images of laser treated surfaces with the following parameters: a)10 W, 20 m/s, 200 kHz b) 10 W, 20 m/s, 100 kHz.

In conclusion, regardless of the speed parameter, laser surface pre-treatments with IR-Yb fiber laser should be used at high frequencies (200 kHz) to minimize the negative effect caused by HAZ when high laser powers are used to enhance the mechanical performance in adhesive bonding.

At lower laser powers, low frequency (100kHz) laser treatments gave results close to the desired surface for CF/PEEK composites. Considering the laser scanning speed parameter, the distance value between laser pulse points should be increased to reduce overlap and heat affected zone on the treated CF/PEEK surfaces. This value also increases with increasing scanning speed.

4.2.3. Effect of Laser Scan Speed Parameter on Microstructure of CF/PEEK Plates

Another important parameter in the laser surface treatment process is the scanning speed. The scanning speed parameters for the IR-Yb laser used in the study vary from 0.1 m/s to 20 m/s.

As mentioned previously in Table 4.1, the space between the laser points increases as the scanning speed increases for the same values of frequency. Therefore, working at high scan speeds reduces the HAZ. Since the scan speed also affects the contact time of the laser with the surface, the HAZ can be reduced by shortening the contact time at high laser power values, i.e., by working at high scan speeds. In low power studies, low speeds should be used to increase the contact time and increase the effect of the laser on the surface. However, it is very important to determine the optimum speed value to obtain the desired surface and to ensure that the HAZ is not higher than desired.

In order to determine the effect of laser scan speed on microstructure, surfaces with different scan speeds are shown in Figure 4.12 for the same power and frequency parameters.

The effect of the scan speed parameter is shown for both high laser power (Figures 4.12(a) and 4.12(b)) and relatively low laser power (Figures 4.12(c) and 4.12(d)).

As can be clearly seen on the surfaces scanned at high laser power in Figure 4.12(a) and 4.12(b), as the laser scan speed decreases, the effect of the laser on the surface increases and more matrix can be removed from the surface. A similar effect was seen in Figures 4.12(c) and 4.12(d). However, if this effect is too great, the HAZ expands and can damage the fibers.

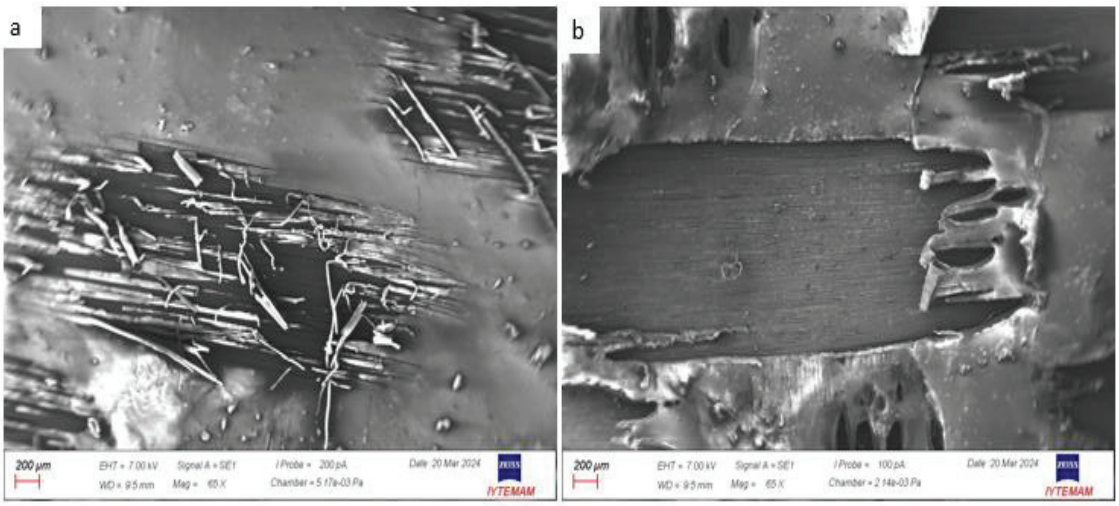

(cont. on next page)

Figure 4.12. SEM images of laser treated surfaces with the following parameters: a) 20 W, 5 m/s, 200 kHz b) 20 W, 1 m/s, 200 kHz c) 12 W, 5 m/s, 200 kHz d)12 W, 10 m/s, 200 kHz.

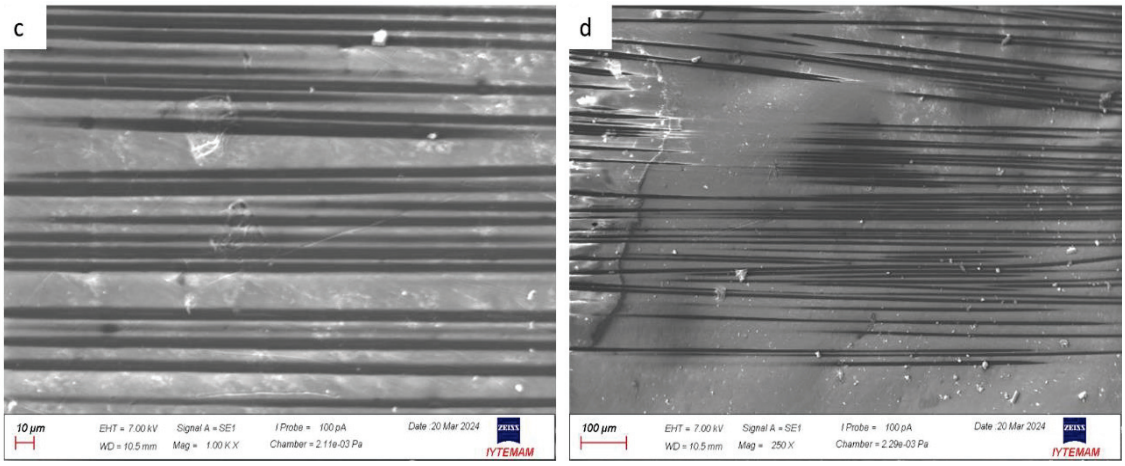

Figure 4.12 (cont.).

For example, a higher magnification image of the same surface in Figure 4.12(b) is shown in Figure 4.13, and the expanding HAZ resulting in fiber fracture, fiber thinning and matrix debris surrounding the fibers are clearly visible. In other words, the scan speed has the same effect on surfaces scanned at high power as it does on surfaces scanned at low power. The HAZ should be taken into consideration when determining the speed range that should be used for the applied power. These microstructures are undesirable and are considered to negatively affect the mechanical strength of the CF/PEEK bonded area. Since the load-bearing parts in composite structures are fibers, if the fiber is damaged, the mechanical performance will be negatively affected.

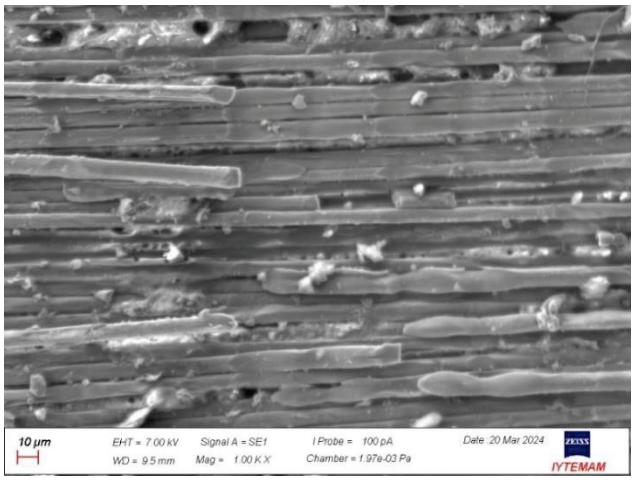

Figure 4.13. Higher magnification SEM images of laser treated surfaces with the following parameters: 20 W, 10 m/s, 200 kHz.

4.2.4. Effect of Laser Power Parameter on Microstructure of CF/PEEK Plates

The other parameter that affects the surface properties of CF/PEEK plate surface treatment with IR-Yb laser prior to adhesive bonding is the laser power parameter. Equipment limitations for the power parameter can range from a minimum of 1W to a maximum of 50W. In the study, laser power values between 5W and 30W were tested for different scanning speeds and frequencies to find the optimal power value.

In order to observe the effect of the power parameter, the frequency and scan speed parameters were held constant and the optimum operating range for the power parameter was determined. In this section, the effect of the laser power parameter on the junction area was examined by SEM analysis.

The study began with an initial trial of low power levels in order to find the minimum power level that could be used.

As the effect of the speed parameter was determined, it was observed that working at lower speed values was more effective at removing the matrix material from the surface at low power values because it increased the laser-surface contact time. However, as shown in Figure 4.14, even when the speed value was at the minimum value, power parameters of 7 W and below were not sufficient to remove the matrix material from the surface.

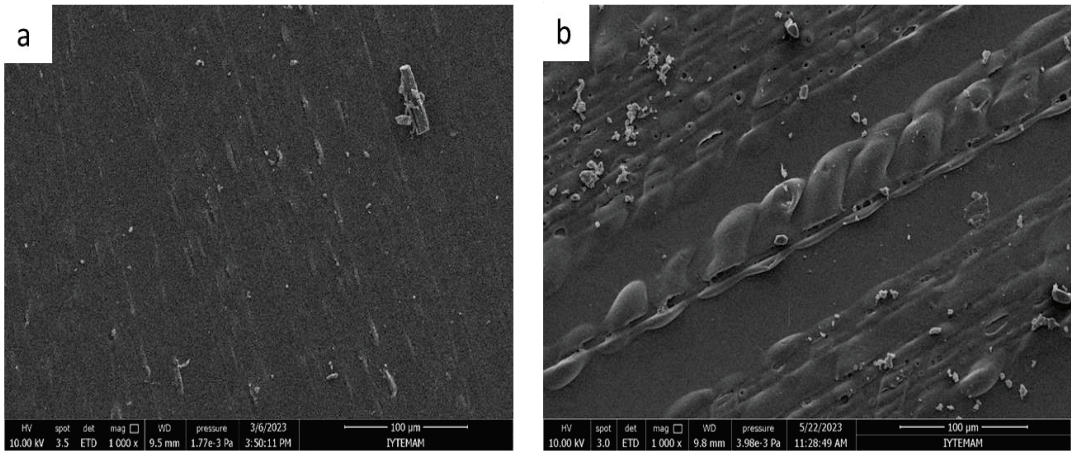

Figure 4.14. SEM images of laser surface treated CF/PEEK surfaces with the following parameters a) 7 W, 1 m/s, 200 kHz, b) 7W, 0.1 m/s, 200 kHz.

The surfaces treated with 10 W and 12 W laser power at the lowest speed parameter, 0.1 m/s and 200 kHz frequencies, are shown in Figure 4.15(a) and 4.15(b), respectively.

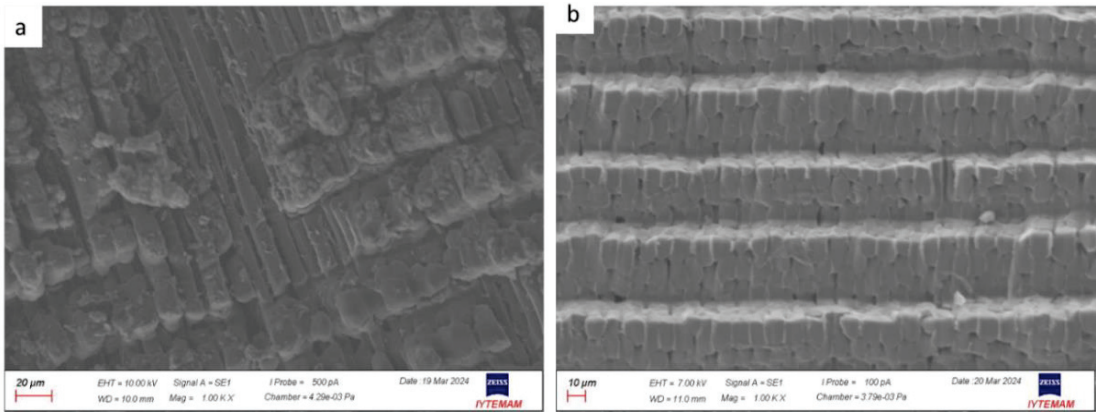

Figure 4.15. SEM micrographs of laser treated CF/PEEK surfaces with the following parameters a) 10 W, 0.1 m/s, 200 kHz, b) 12 W, 0.1 m/s, 200 kHz.

According to Figure 4.15, the desired surface could not be obtained on either surface. The matrix material was left on the surface. The fiber structure is not visible on the surface. Power levels above 8 W did not produce the desired surface results at this speed value.

Another important results from the SEM images, the effect of laser power on the average scan speed values as seen in Figure 4.16.

In order to examine the effect of laser power on the average scan speed values, the surfaces scanned with 200 kHz fixed frequency value and 10 W, 20 W, 30 W laser power values for 1 m/s speed are shown in Figure 4.16(a-c), respectively. The surfaces scanned with 10 W, 20 W and 30 W power values for a speed of 10 m/s are shown in Figure 4.16(d-f), respectively.

According to Figure 4.16(a), it can be seen that 10 W power at 1 m/s speed is not sufficient to remove the matrix material from the surface. However, for the same scanning speed value, it was observed that the 20 W and 30 W laser powers shown in Figures 4.16(b) and 4.16(c), respectively, caused fiber damage on the surface and occasionally caused contamination of the surface with matrix and broken fiber debris. This is because increasing laser power causes the HAZ to expand. At 10 m/s, three different laser power levels produced results closer to the desired surface.

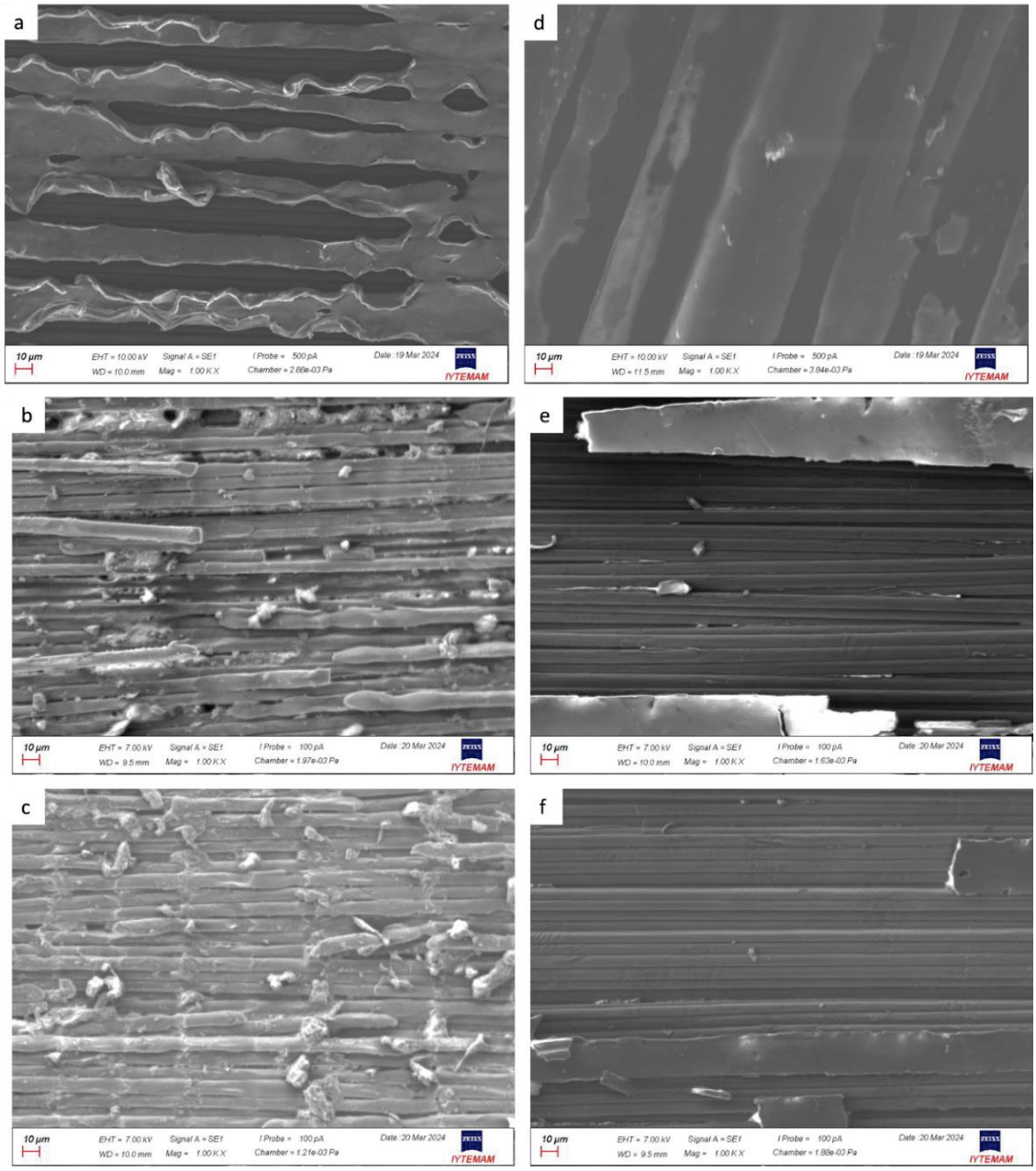

Figure 4.16. SEM images of laser treated CF/PEEK surfaces with the following parameters a) 10 W, 1 m/s, 200 kHz b)20 W, 1 m/s, 200 kHz c) 30 W, 1m/s, 200 kHz, d) 10 W, 10 m/s, 200 kHz e) 20 W, 10 m/s, 200 kHz f) 30 W, 10 m/s, 200 kHz.

In particular, the surfaces in Figures 4.16(e) and Figure 4.16(f) clearly show the fibers on the surface. Residual matrix material can be seen in places and between the fibers.

In addition, for optimal results, a power value of 20 W, 30 W, or a power value in between can be determined for a laser scanning speed of 10 m/s. In order to prevent fiber damage on surfaces treated with high laser power parameters, the effect of the laser on the surface should be reduced by increasing the scanning speed, considering the negative effect caused by HAZ. Then, the CF/PEEK surfaces were treated with different laser power parameters, keeping the frequency value constant at 200 kHz for the maximum scanning speed of 20 m/s, and the effects of the laser power parameter on the microstructure were observed. SEM images of this speed and frequency are shown in Figures 4.17(a-c) for 10 W, 12 W, and 30 W, respectively.

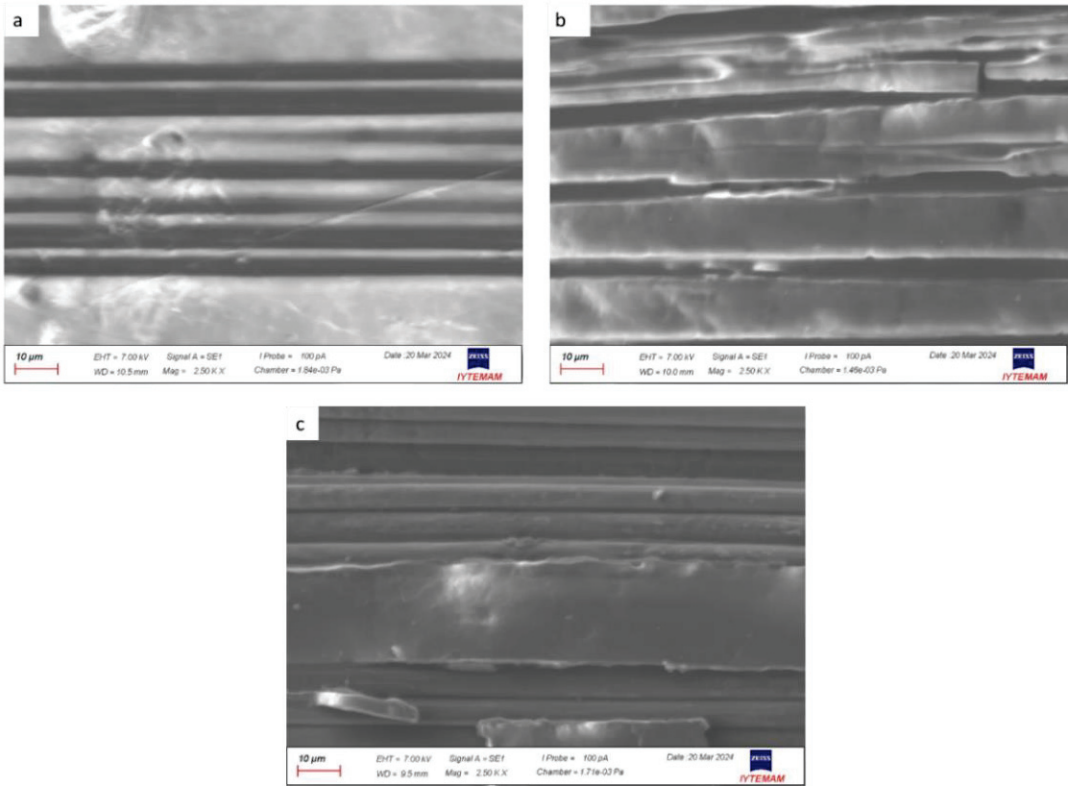

Figure 4.17. SEM micrographs of laser treated CF/PEEK surfaces with the following parameters a) 10 W, 20 m/s, 200 kHz b)12 W, 20 m/s, 200 kHz c) 30 W, 20 m/s, 200 kHz.

As can be seen in Figure 4.17, laser powers of 10 W (Figure 4.17(a)) and 12 W (Figure 4.17(b)) at a speed of 20 m/s are not effective in removing enough matrix material from the CF/PEEK surface. Similarly, Figure 4.17(c) shows that as the laser power

increased (30 W), the amount of matrix removed from the surface also increased and a surface closer to the desired surface was obtained. In other words, for optimal results, the power value should be between 12 W and 30 W for a speed of 20 m/s.

In this study, SEM microstructure analysis was performed to selectively remove matrix from the CF/PEEK composite surface without damaging the fiber to improve the mechanical strength of the joint area. For the laser power parameter, if you want to work at a low scanning speed, you should work at low power values (10 W and below). However, at 7 W and below, the PEEK matrix could not be removed from the surface even at the lowest scan speed (0.1 m/s). Higher scan speeds gave better results than lower scan speeds. However, if high scanning speeds are to be used, high laser powers should be used. Based on these results, different optimal operating ranges were determined for three laser parameters.

For the laser surface treatment, SEM images of the three surfaces (Sample 1, Sample 2, and Sample 3) closest to the desired bond surface, based on criteria such as selective removal of matrix material from the surface, no fiber damage, and no debris on the surface where the laser pulse is generated, are shown in Figure 4.18(a), Figure 4.18(b), and Figure 4.18(c), respectively.

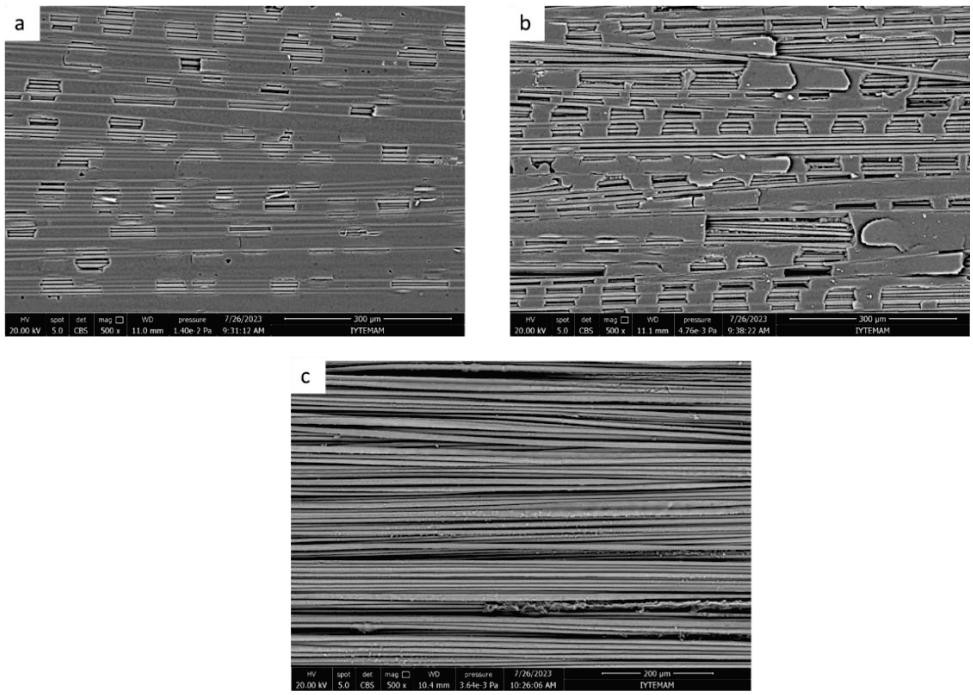

Figure 4.18. SEM micrographs of laser treated CF/PEEK surfaces with following parameters at 500x magnification: a) 10 W, 20 m/s, 100 kHz, b) 20 W, 20 m/s, 200 kHz, c) 8 W, 0.1 m/s 200 kHz.

According to the SEM images in Figure 4.18, there is a significant difference between Figure 4.18(a), Figure 4.18(b), and Figure 4.18(c). On the surfaces in Figure 4.18(a) and Figure 4.18(b), the matrix material has moved away from the surface only at the points where the laser pulse is applied, and the remaining matrices provide roughness on the surface. At the points where the pulse is applied, the area around the fibers is clean and no matrix residue is visible.

On the other hand, as shown in Figure 18c, not only at the points where the laser pulse is applied, but also because the scanning speed is very slow in this parameter, the HAZ has expanded considerably, and the matrix has been removed from the surface along the fibers. Fiber structures are much more abundant on the surface compared to the other two images. However, matrix remnants can be seen between the fibers in some places, and it is thought that these structures may be causing contamination on the surface.

At this point, two different laser strategies have been tried on CF/PEEK surfaces where the bonding surfaces are laser treated for mechanical testing. While the first two samples removed the matrix only at the point where the laser beam was applied, the last sample removed the matrix material from the entire area where the laser beam was applied. Higher magnification images of the surfaces shown in Figure 4.18 are shown in Figure 4.19.

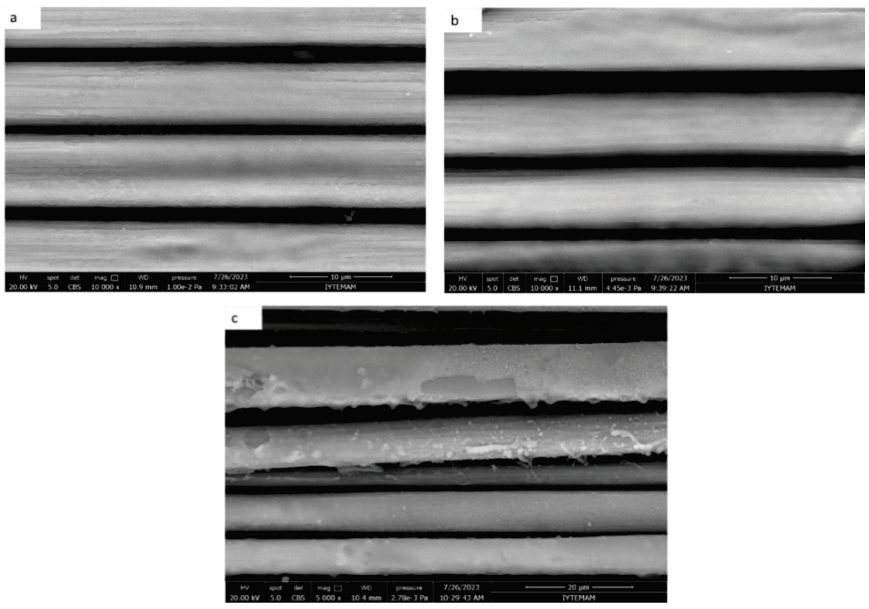

Figure 4.19. SEM micrographs of laser treated CF/PEEK surfaces with following parameters at higher magnification (5000x): a) 10 W, 20 m/s, 100 kHz, b) 20 W, 20 m/s, 200 kHz, c) 8 W, 0.1 m/s 200 kHz.

On the surfaces in Figure 4.19(a) and Figure 4.19(b), the area around the fibers has been cleaned of matrix material, and on the surface in Figure 4.19(c), the remaining matrix residue is clearly visible around the fibers. No fiber damage was observed on any of the three surfaces.

In conclusion, according to SEM analysis, four different possible situations have been observed on laser treated CF/PEEK surfaces. These are:

1) Incomplete matrix removal: The CF/PEEK surface is clean and the fibers are still covered with matrix. There are no fibers to be observed on the surface.

2) Partial removal of the matrix with fiber damages: A portion of the matrix material has moved away from the surface, but the fibers are partially decomposed, burned, or broken. In addition, residual fibers and matrix can be seen in many places.

3) Partial matrix removal without fiber damage: CF/PEEK surface is partially clean, fiber surroundings are clean and fibers are not damaged and matrix material is visible where there is no laser pulse.

4) Complete matrix removal with little matrix residue around the fibers: In some places, the matrix material is still visible around the fibers, even though it has been largely removed from the surface. There is no fiber damage. However, at some point, thermal degradation of the fibers was observed.

All of these cases are affected by laser process parameters such as scan speed, frequency, laser point spacing, laser power, hatch distance, and scan strategy. To understand the interaction, the thermal effect on both the matrix and the fiber must be considered. The matrix is nearly transparent at the chosen wavelength, while the fiber acts as a black body absorbing all radiation. As a result, the heat will be absorbed by the reinforcing material and transferred to the matrix. This means that when the matrix material is heated, various damages are introduced into the structure, causing HAZ formation and expansion. Therefore, the correct selection of the operating range of the most appropriate laser parameters is very important.[89]

In the laser surface treatment process, all microstructures of CF/PEEK seen in SEM analyses are controlled by the energy released per unit area (E_{spec}). The amount of energy released onto the surface varies with the parameters of the laser process. The energy per unit area is calculated using the following Eqn. (4.1) for selected three specimens:[152]

$$E_{spec} = \frac{P_a.r}{Ss.Hd} \tag{4.1}$$

where P_a is the average power of the beam, r is the number of repetitions, Ss is the scan speed, and Hd is the hatch distance. Changing the amount of energy produces different microstructures.

According to this equation, the parameters that give the desired and near desired surfaces in the study and the energy values calculated for these parameters are given in Table 4.2. In this study, the number of laser repetitions is set to 1 for all three of the samples.

Table 4.2. Selected laser parameters and their released energy values

	Power (W)	Scan Speed (m/s)	Frequency (kHz)	Hatch Distance (mm)	Released Energy (J/mm^2)
Sample1	10	20	100	0.03	0.016
Sample2	20	20	200	0.03	0.033
Sample3	8	0.1	200	0.03	2.66

According to Table 4.2, the amount of energy on the surface of sample 3 is significantly higher than that of the other two samples. As clearly seen in the SEM surface analysis and as mentioned above, the surfaces scanned with two different mechanisms (sample 1, sample 2 with same mechanism, sample 3 with different mechanism) are mechanically tested and the results are compared.

Another conclusion from the microstructure analysis results is that there is no single exact value for the parameters whose optimum values are studied in order to obtain the desired surface. It was found that there is an optimum working range for the parameters. For each parameter, the value that gives the desired surface can be found by changing other parameters. Therefore, optimum working ranges were found and for these three selected parameters in IR-Yb laser surface treatment of CF/PEEK composite plates.

In Table 4.3, four different surface structures obtained from SEM images for the laser power and scanning speed parameters investigated in this study are shown in different colors, and the energy amounts (J/mm^2) corresponding to each laser power and scanning speed are shown. The frequency value is fixed at 200 kHz.

The areas shown in red in the table are the areas where the energy level is high and fiber damage is observed as the partial matrix is removed from the surface. The cream area is the parameter where the matrix cannot be removed from the surface. The blue area shows the parameters where the matrix has been almost completely removed and although

there is no fiber damage, small amounts of matrix residue remain around the fiber at some points. The green areas show the parameters where partial matrix is removed with no fiber damage. The amount of energy in this region is also lower. The parameters where the desired final surface is seen in the study are in this area.

Table 4.3. Structures formed on the bond surface for different laser power and scan speed values and their corresponding released energy values.

Scan Speed (m/s)						
	20	0.013	0.017	0.02	0.033	0.05
	10	0.027	0.033	0.04	0.066	0.1
	5	0.053	0.067	0.08	0.133	0.2
	1	0.267	0.333	0.4	0.667	1
	0.1	2.66	3.333	4	6.667	10
		8	10	12	20	30
		Power (W)				

	incomplete
	partially w/o fiber damages
	Partially w/fiber damages
	Complete w/matrrix cluster

According to Table 4.3, at power levels of 10 W and above, if the Espec value is greater than 0.1 J/mm^2, unwanted fiber breaks and surface contamination are observed. In other words, for this study, the maximum energy value should be 0.1 for laser power parameters of 10 W and above. This value is the threshold at which fiber damage begins to occur. In this case, this energy level should be lowered as it will negatively affect the mechanical strength of the joint area. Previously, it was observed that the laser could not affect the CF/PEEK surface even at the slowest speed with a power of 7W and below. In addition, it was observed that the energy value for the matrix burned away from the surface at 8 W laser power and 0.1 m/s scan speed parameters was quite high. This indicates that the matrix ablation observed in this sample occurs by a different mechanism compared to other surfaces. However, since it provides a surface result close to the desired one in the SEM images, the sample preparation will be done with these parameters for mechanical tests. The energy values confirmed that it should be worked at low speeds with low laser power parameters and at high scanning speeds with high laser power values (10W and above).

According to these results, the green areas in the table represent the optimal operating range for IR-Yb fiber lasers on CF/PEEK surfaces.

4.3. Single Lap Shear (SLS) Test Results of Adhesive Bonded Specimens

According to the SEM images, the joint surfaces were laser treated with different parameters and the 3 parameters that gave the best results were selected for the single lap shear test application. The laser process parameters for laser samples 1, 2, and 3 are as follows, respectively; 10 W, 20 m/s, 100 kHz; 20 W, 20 m/s, 200 kHz; 8 W, 0.1 m/s, 200 kHz. Then, the single lap shear test was applied to the specimens prepared with these three different parameters and the reference specimens according to the corresponding ASTM standard. The results of these specimens, i.e., average shear strength, standard deviation, and improvement, are shown in Table 4.4.

Table 4.4. Single lap shear test results of laser treated and reference specimens.

Test Sample	Avg. Shear Strength (MPa)	Standard Deviation (±)	Improvement (%)
Reference	4.859	0.479	-
1	6.783	0.708	39.596
2	11.760	0.880	142.02
3	9.948	0.368	104.733

According to Table 4.4, while the average shear strength value of the reference specimen was found to be 4.86 MPa, this value was found to be 6.78 MPa for specimen number 1, 11.76 MPa for specimen number 2, and 9.95 MPa for specimen number 3. The specimen with the highest shear strength value is the specimen whose surface was laser treated with parameter number 2.

Li W. et al.[153] in their study, laser surface treatment of FDM-printed PEEK/CF composites increased the shear bond strength from 3.28 to 6.42 MPa compared to untreated samples.

In addition, an increase in mechanical strength was observed for all samples whose joint surfaces were treated with different laser parameters compared to the reference sample. This indicates that laser surface treatment is an effective method for increasing the strength of the joint area of CF/PEEK material. This increase is clearly

illustrated in Figure 4.20. The effect of the applied laser is directly influenced by the selection of the correct laser parameters.

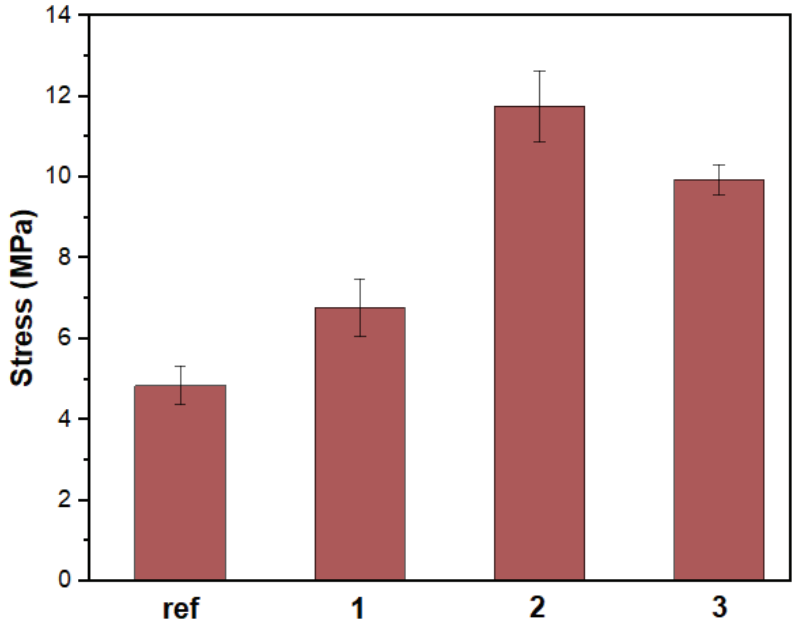

Figure 4.20. Single Lap Shear test results for both reference and laser treated specimens.

The reason for this increase in mechanical strength in the joint area of all samples whose joint surfaces were treated with IR laser prior to adhesive bonding, compared to the reference sample, is that the PEEK matrix material, which is not compatible with the adhesive, is removed from the surface, the fibers emerge to the surface and the surface is roughened, mechanical interlocking at the micro and nano scale is more evident on the laser treated surface.

The reason why the increase seen in Sample 1 is not as great as that seen in Sample 2 is that, as can be seen from the SEM images (Figure 4.18 and 4.19), more matrix material remains on the surface of Sample 1. Although the remaining matrix pieces created roughness on the surface, they were not able to bond properly with the adhesive because they were in large quantities, thus preventing the mechanical strength value from increasing as much as in Sample 2. The reason why the strength value is not as high as Sample 2, even though more matrix is removed from the surface in Sample 3, is the thermal degradation that occurs in the fibers due to high energy, as seen in the SEM images (Figure 4.19). Figure 4.21 shows the stress-strain curves of the reference and laser treated specimens.

Compared to the reference specimens, both strength and strain increased with laser surface treatment for the specimens whose bonding surfaces were laser treated prior to bonding. This shows that the laser surface treatment allows the bonded CF/PEEK to withstand higher loads for longer periods of time. As expected, the force increased until it reached its maximum and suddenly failed for all specimens. The samples with the highest increase are the laser Specimen2, as mentioned previously. On the other hand, the sample with the lowest lap shear strength is Specimen1. As can be seen from the SEM images (Figure 4.18 (a)) of this sample, the reason is that it is the sample with the most matrix on its surface compared to the other two laser samples. The matrix layer, which could not be removed from the surface, prevented contact between the adhesive and the fibers, resulting in lower bond strength.

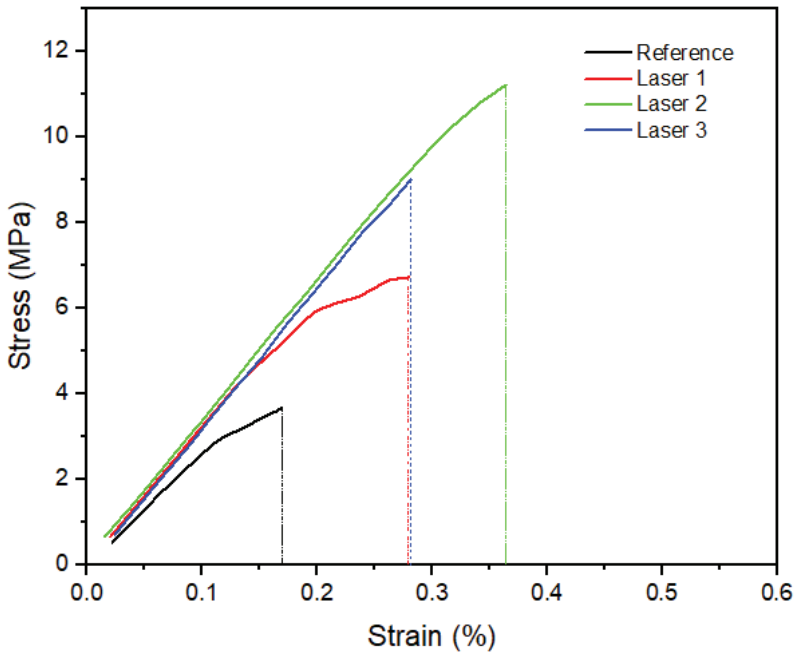

Figure 4.21. Single lap shear strength vs. strain curves for reference and laser-treated specimens.

It is also noteworthy that the tensile behavior of Specimen1 in the single pass shear test is different from the other specimens. While the other laser specimens have a linear curve up to the moment of failure, the curve of specimen1 shows that it enters the plastic deformation region (out of linearity) at a much lower strain value. These load value fluctuations show that laser Specimen1 began to suffer permanent damage at lower load values compared to the other laser specimens, delaying delamination, and suppressing its

growth until the moment of fracture of Specimen 3. However, as a result, neither Specimen1 nor Specimen3 could reach the load amount and strain value as much as laser Specimen2.

4.4. Charpy Impact Test Results of Adhesive Bonded Specimens

According to the result of the single lap shear test, the parameter with the highest increase was selected (Sample 2), specimens were prepared according to the previously mentioned standard, and Charpy impact tests were performed on both the laser specimens and the reference specimens.

Figure 4.22 shows the prepared Charpy impact test samples before and after testing.

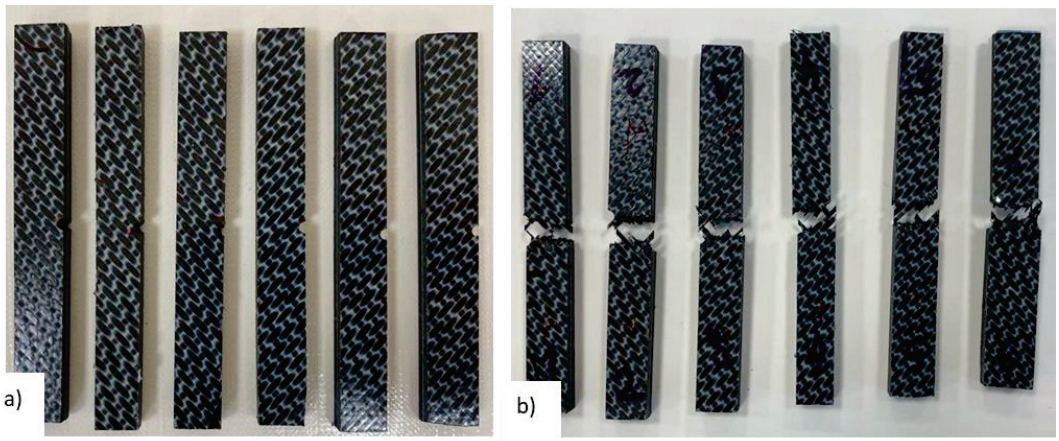

Figure 4.22. Charpy impact test specimens a) before testing, b) after testing.

According to the Charpy impact test results, it was clearly observed that the impact strength was significantly improved by the laser, reaching 4.6 kJ/m^2. Accordingly, while the Charpy impact value for the CF/PEEK reference sample was 2.55 kJ/m^2, this value was 4.60 kJ/m^2 for the CF/PEEK samples prepared by laser scanning the interface surfaces.

An 80% increase in the Charpy impact value was observed with the laser surface treatment.

The test results are presented in Table 4.5.

Table 4.5. Charpy impact test results.

	Reference	Laser Treated
Charpy Impact Strength (kJ/m^2)	2.55	4.60
Min Absorbed Energy (kJ/m^2)	2.07	3.7
Avg. Absorbed Energy (kJ/m^2)	2.26	4.05
Std. Deviation (±)	0.18	0.36

The comparative results of the reference and laser samples are also shown in Figure 4.23. The Charpy impact test results indicated that the impact energy of the existing CF/PEEK and adhesive interface could be significantly improved using the laser surface treatment technique. The fracture surfaces examined by SEM after the Charpy impact test revealed the reason for the increased impact energy value with the laser surface treatment process. These micrographs (Figure 4.29) clearly showed that there was poor interfacial bonding between the CF/PEEK and the adhesive in the reference sample.

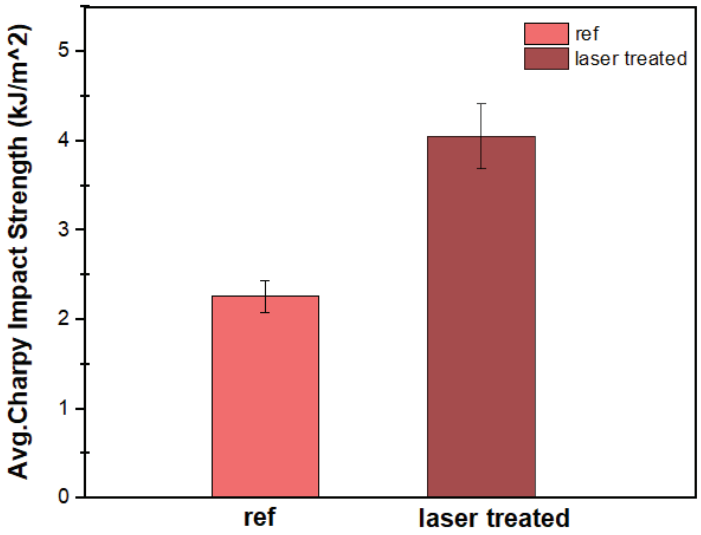

Figure 4.23. Average Charpy impact strength results for reference and laser specimens.

4.5. Double Cantilever Beam (DCB) Test Results of Adhesive Bonded Specimens

Mode-I fracture toughness values (G_{Ic}) are shown in Figure 4.24(a) and 4.24(b) for the reference and laser treated specimens (sample 2), respectively.

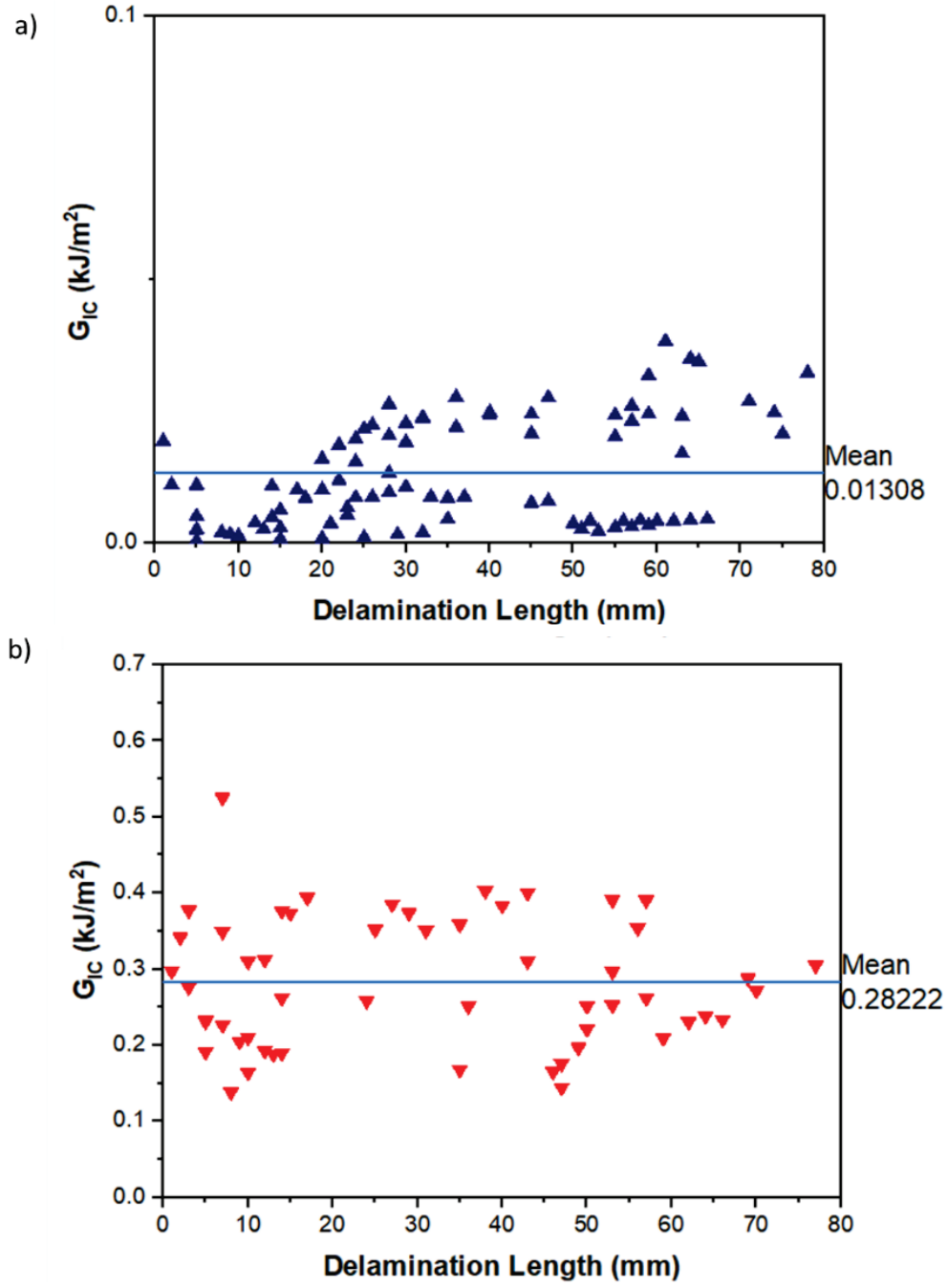

Figure 4.24. DCB test results of (a)reference, (b) laser treated specimens.

As can be seen, the G_{Ic} of the reference specimens was in the range between and 0.000404 and 0.03824 kJ/m^2 0.13854 and 0.40305 kJ/m^2 for the laser treated specimens. The average Mode-I fracture toughness value was found to be 0.013 kJ/m^2 for the reference specimens and 0.282 kJ/m^2 for the laser treated specimens. According to these results, the Mode-I fracture toughness values increased with laser surface treatment prior to the adhesive bonding process.

According to the Mode-I fracture toughness results, it was observed that the mechanical strength values of the PEEK matrix material and the adhesive in this loading direction were quite low for the reference sample. This is due to the chemical incompatibility of the epoxy-based film adhesive, which is widely used in the aerospace industry, with the PEEK matrix.

The laser surface treatment performed to eliminate this incompatibility removed the PEEK matrix material from the surface and allowed the fibers to come to the surface. For this adhesive, which is widely used in the aerospace industry, it is noteworthy that the laser surface treatment improved the adhesion between the adhesive and the fiber in the Mode I loading mode, increasing the strength value by approximately 22 times.

In addition, considering the increase in surface roughness and wettability values with laser surface treatment, this increase in $G_{ıc}$ value observed in the laser samples is thought to be due to mechanical interlocking at the interface with the laser surface treatment. This increase in fracture toughness value under Mode-I loading is indicative of good adhesion due to mechanical interlocking at the interface of CF/PEEK and adhesive with laser surface treatment.

In order to reveal the formation and progression of the crack in the adhesive bonded structure under Mode-I loading, the results were examined as initiation parts covering the beginning of the crack and the delamination length up to 5 mm, and propagation parts covering the progression of the crack in the structure (after 5 mm delamination length). These results are shown in Figure 4.25 for reference and laser specimens.

According to these results, it was observed that the toughness value of the laser specimens in the crack initiation part increased 50 times compared to the reference specimen. In the propagation part, an increase of about 21 times was observed. This indicates that the bond strength at the CF/adhesive interface is much higher than at the PEEK/adhesive interface and the laser surface treatment was successfully applied to the CF/PEEK interface prior to adhesive bonding. Another important point to note is that

while the fracture toughness value was higher in the propagation portion of the reference specimen, higher toughness values were achieved in the initiation region of the laser treated specimen.

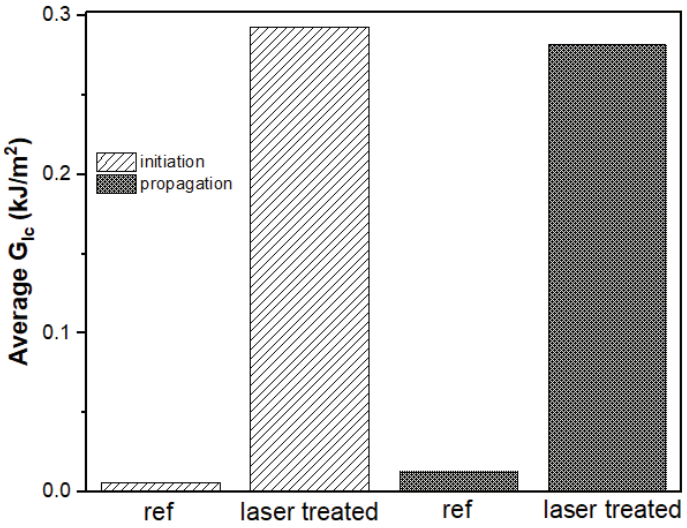

Figure 4.25. The averaged initiation and propagation mode-I fracture toughness for reference and laser treated specimens.

The reason for this decrease in the laser treated specimen was that the crack encountered a relatively weak CF/adhesive interface and jumped into this weak interface. It then continued to propagate in this relatively weak interface (seen in Figure 4.26). Much more energy was absorbed in the crack plane and released into the weak carbon fiber/adhesive interface of the composite compared to the reference specimens.

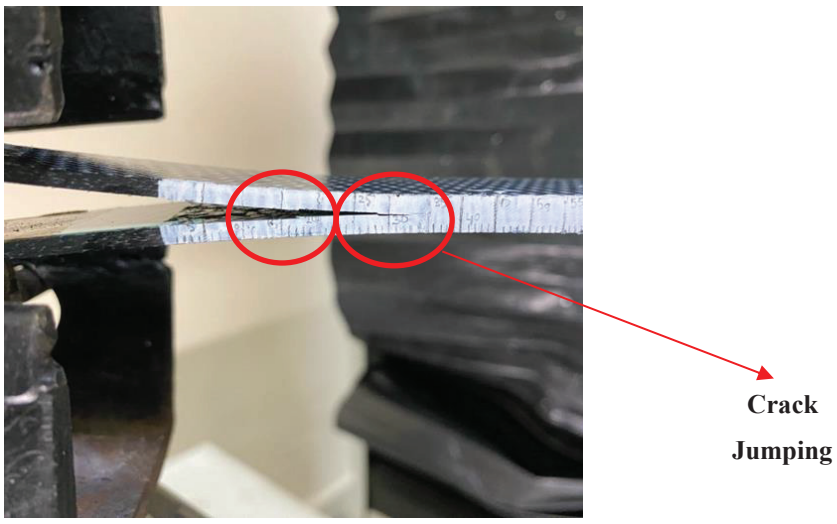

Figure 4.26. Crack jumping phenomena during DCB testing in laser treated specimens.

4.6. Surface Characterization

In order to analyze the bonding surfaces, SEM micrographs were obtained to determine the failure modes occurring on the bonding surfaces after mechanical testing, and to determine if proper adhesion had been achieved. Then, to reveal the effects of laser surface treatment, the surface topography and wettability properties of laser-treated and reference samples were compared. Thus, the reasons for the results obtained in the mechanical tests were sought to be revealed through surface characterization together with the effects of laser surface treatment on the joint area.

4.6.1. Failure Mode Analysis

After the single lap shear test, the fracture surfaces of the reference and laser specimens were examined to determine the failure mode that occurred on the surface. Images of the CF/PEEK fracture surfaces of the reference and laser treated specimens are shown in Figure 4.27(a) and Figure 4.27(b), respectively. The same surfaces were examined by SEM and are shown in Figure 4.28.

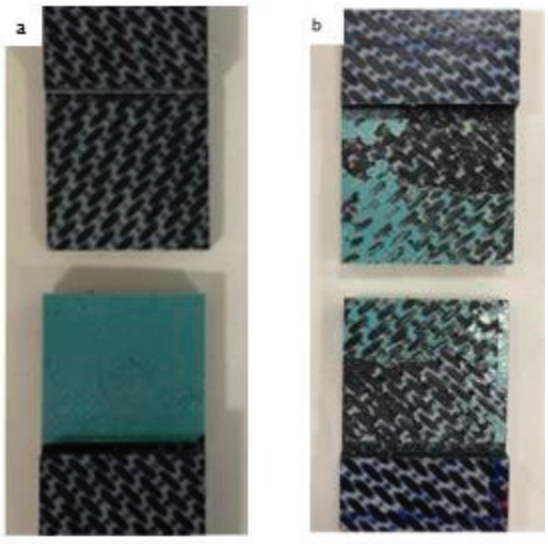

Figure 4.27. After single lap shear tests, bonding surface of a) reference, and b) laser treated CF/PEEK specimens.

As shown in Figure 4.27, adhesive failure was observed on the fracture surface of the reference specimens. In other words, all the adhesive remained on a single adherend

surface and no residue of the other adherend was seen on the adhesive surface. This situation indicates that the interface between the CF/PEEK plate and the adhesive, i.e. the PEEK matrix and the adhesive, does not adhere very well. This is the reason why the mechanical strength of the reference specimens obtained in the single lap shear test is lower than that of the laser specimens. The problem of poor adhesion to the adhesive in the reference samples resulted in low strength in the single lap shear test.

On the other hand, when the fracture surface of the laser specimens was examined, cohesive failure was observed on the surface. In other words, adhesive residues and fiber fractures on these adhesive residues are clearly visible on both adherend bonding surfaces. This indicates that the specimens with laser treated joint surfaces had good adhesion. This good adhesion surface is evidence of the much better mechanical strength result of the carbon fiber/adhesive interface obtained from the single lap shear test.

With the increasing use and popularity of composite materials, it is essential to investigate the behavior of these materials in the event of a crash, depending on the location of use, especially with regard to their properties when exposed to damage, the associated failure modes, and the analysis of fractured materials.[154]

According to the SEM images (Figure 4.28(a)) taken from the fracture surface of the reference specimen, the adhesive remained on only one adhesive surface and no fiber residue was found on this adhesive surface. This situation shows that the adhesion is not sufficient and there is an adhesive failure mode on the surface.

On the other hand, the SEM images of the fractured surface of the laser specimen (Figure 4.28(b)) showed that the adhesive on the bonding surface was visible on both joined substrate surfaces, and that there were quite a few fiber fractures on both surfaces. The presence of adhesive residue on both surfaces indicates that the failure in these specimens was cohesive failure.

Cohesive failure is a type of failure observed in adhesive bonded structures where adhesion is well established. In this way, the single-lap shear strength was higher in specimens where the bonding surfaces were laser treated.

Cohesive failure is an indication of better adhesion. The reason why the single lap shear strength values are higher than the reference specimen. The braided fibers were clearly visible on the fracture surface.

In order to reveal the laser effect on the joint surface, the fracture surfaces were also examined by SEM analysis after the Charpy impact test.

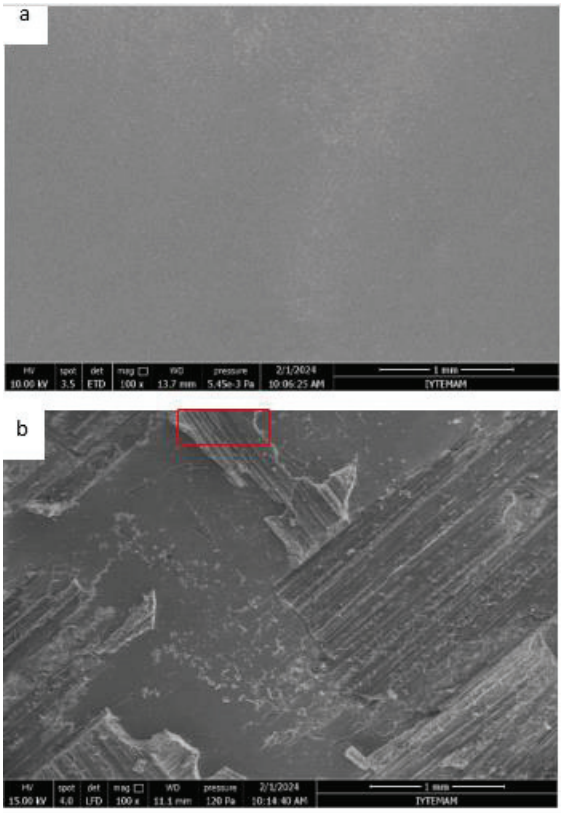

Figure 4.28. SEM images of a) reference, b) laser treated specimen fracture surfaces after single lap shear testing.

Images of the analysis are shown in Figure 4.29(a) and Figure 4.29(b) for the reference and laser surface treated specimens, respectively.

As shown in Figure 4.29(a), it is clear that there was no good adhesion at the adhesive and CF/PEEK bond interface. In the area shown in red in the SEM micrograph, the adhesive appears to have separated from the surface in the adhesive failure mode, as in the single lap shear test specimens.

In the area shown in red in Figure 4.29(b), it is clear that the adhesive has penetrated well in the specimens whose bonding surfaces were laser treated. There is no visible gap between the adhesive and the surface. In the laser treated specimens, the carbon fibers and adhesive are in contact at the joint interfaces.

As can be seen in Figure 4.29, it was observed that the samples whose surfaces were treated with the laser had better penetration with the adhesive. In other words, it can be seen from this image that mechanical interlocking occurs on the surface. This allows the mechanical performance of the bonding area to be increased.

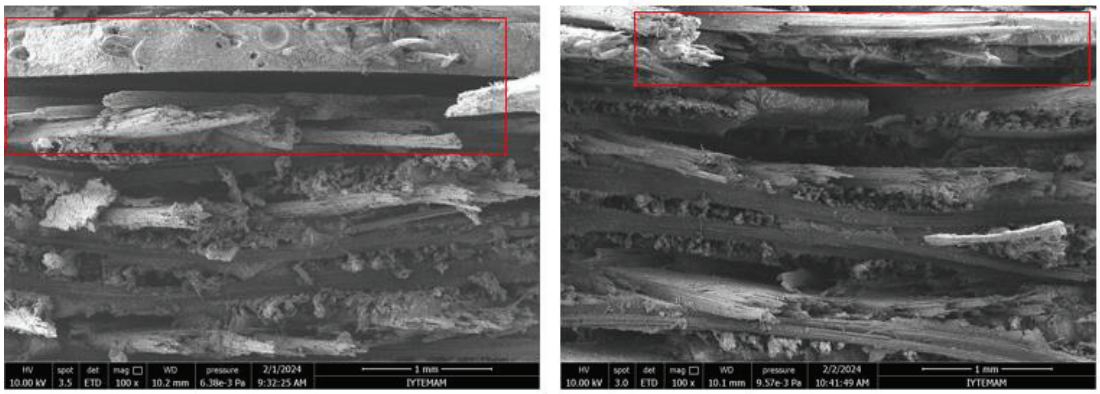

(a) (b)

Figure 4.29. SEM micrographs of fracture surfaces of Charpy impact test specimens after testing a) reference, b) laser treated specimen.

4.6.2. Surface Roughness Analysis (Profilometer)

The surface topography and roughness values of the laser-treated and reference specimens were obtained using profilometer that are shown in Figure 4.30(a) and Figure 4.30(b), respectively.

3D surface topographies show different surface structures. As shown in Figure 4.30, the laser-treated sample has more irregular peaks than the reference sample. The reference sample has a smoother surface.

In Figure 4.30, the maximum peak height of the laser sample is 133.137 μm, while the reference sample is 15.65 μm. It is believed that by increasing the surface roughness value targeted by the laser process, the adhesive can better penetrate the surface.

Various surface roughness parameters can be used to describe and measure the surface in terms of roughness.

Areal surface topography parameters are used for three-dimensional analysis the most common being the arithmetic mean height Sa.[155] This parameter can be calculated using Eqn. 4.1.

$$S_a = \int_a \int |Z(x,y)|(dx)dy \tag{4.1}$$

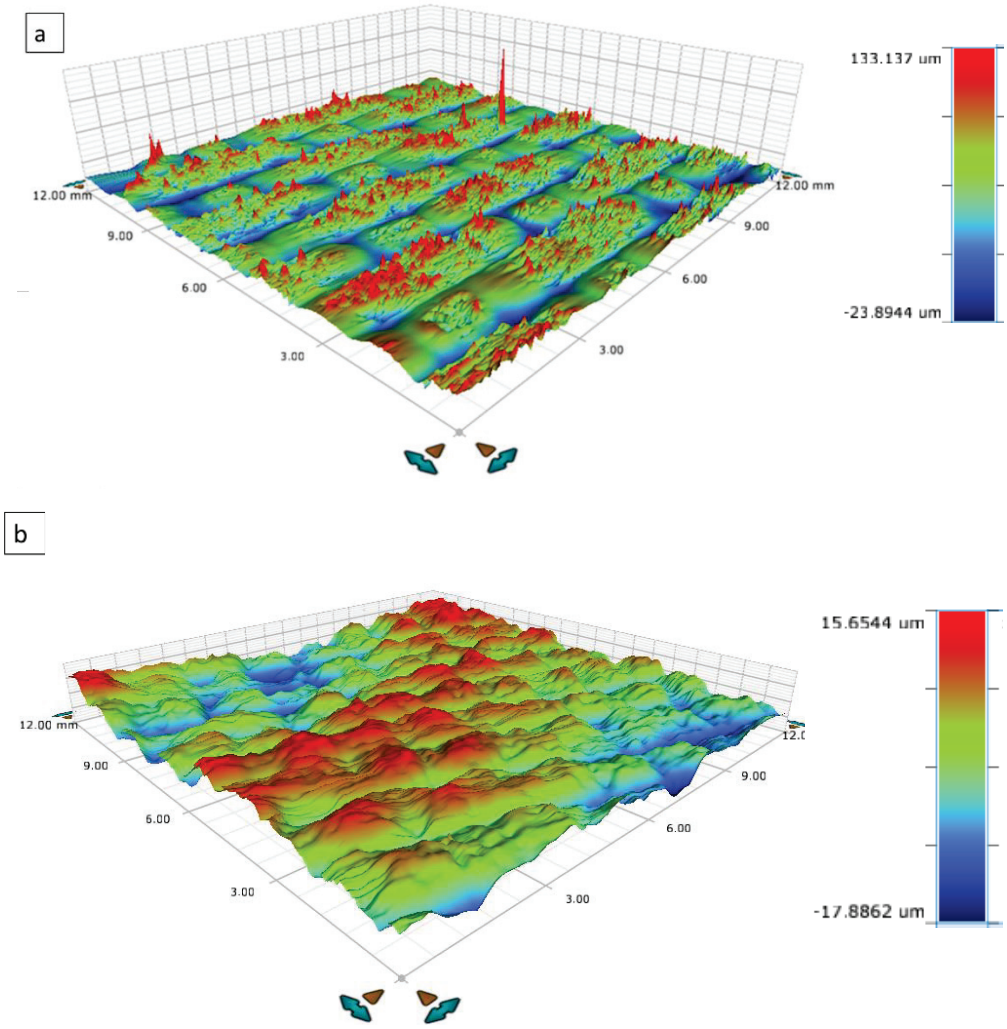

Figure 4.30. Surface 3D profiles of the specimens: a) laser treated specimen, b) reference specimen.

Since studies have shown that different surface profiles can have the same or similar Sa measurements, this parameter alone is not sufficient to evaluate surface topography. Considering the varying heights along a rough surface profile as a distribution, another parameter to measure (Eqn. 4.2) whether a profile is skewed toward broad peaks and jagged valleys, or broad valleys and jagged peaks is skewness (S_{sk}).[155]

$$S_{sk} = \frac{1}{S_q^3} \int_a \int (Z(x,y))^3 (dx) dy \tag{4.2}$$

where Sq is the root mean square of the roughness value. Skewness is a measure of the degree of asymmetry of the surface around the mean plane.

The third roughness parameter, S_{dr}, is the additional percentage of scanned area added by the surface texture, also known as the relative surface increase, can be calculated using Eqn. 4.3. [155]

$$S_{dr} = \frac{1}{A} \left[\iint_A \left(\sqrt{\left[1 + \left(\frac{\partial z(x,y)}{\partial x} \right)^2 + \left(\frac{\partial z(x,y)}{\partial y} \right)^2 \right]} - 1 \right) dxdy \right] \tag{4.3}$$

Some studies in the literature have shown that samples with higher S_{dr} parameters have higher adhesive bonding capabilities.[155–157] Zielecki et al.[157] investigated that the shear strength of steel adhesive bonded structurues had a linear relationship with the S_{dr} parameter. By increasing the S_{dr} parameter from 0.2% to 9%, the shear strength improved from 10 MPa to 20 MPa. Van Dam[155] reported higher average ultimate shear strength of a steel-epoxy adhesive interface for higher values of the S_{dr} parameter. The lap-shear bond strength of adhesive-bonded magnesium AZ31B was found to be related to the actual surface area by Zheng et al.[156] Since the S_{dq} and S_{dr} parameters are related to each other, the correlation between them is very strong. The S_{dq} and S_{dr} parameters, which are hybrid surface analysis parameters, have proven useful in this regard to provide a proper adhesive bond performance.[158]

In this context, arithmetic surface roughness (S_a), interfacial area ratio (S_{dr}), skewness (S_{sk}) and surface gradient (S_{dq}) values of both reference and laser-treated specimens are presented in Table 4.6

Table 4.6. Arithmetic surface roughness (S_a), interfacial area ratio (S_{dr}), skewness (S_{sk}) and gradient (S_{dq}) for different specimens.

Specimen	**S_a (µm)**	**S_{dr} (%)**	**S_{sk}**	**S_{dq} (deg)**
Reference	3.5	0.028	-0.271	1.35
Laser treated	4.391	1.759	1.851	10.971

According to Table 4.6, the high skewness value (1.851) for the laser-treated samples verifies the existence of sharp surface peaks observed in the profilometer images. In addition, the presence of local peaks in these samples caused a significant increase in the relative surface area. While the relative surface area (S_{dr}) was found to be 0.028% for the reference, this value was found to be 1.759% for the laser treated samples. Although no significant change in the arithmetic height value (S_a) was observed after laser surface treatment, since the S_{dr} value represents the relative surface area, the results indicate that the goal of the laser surface treatment was to increase the contact area with the adhesive.

On the other hand, $S_{sk}<0$ indicates a height profile above the mean plane, i.e. a flat surface with holes, and $S_{sk} >0$ indicates a height profile below the mean plane, i.e. a flat surface with peaks, where $S_{sk} >|1|$may represent large holes or peaks on the surface. (Figure 4.31).[159] To promote mechanical interlocking, positively skewed roughness is desirable.[155]

Negative Skewness Surface Positive Skewness Surface

Figure 4.31. Schematic representation of possible interaction with negative and positive skewness value surfaces.[159]

To observe the effect of the laser on the surface, SEM images of the cross-sectional areas of the reference and laser-treated samples taken from the side views are shown in Figure 4.32.

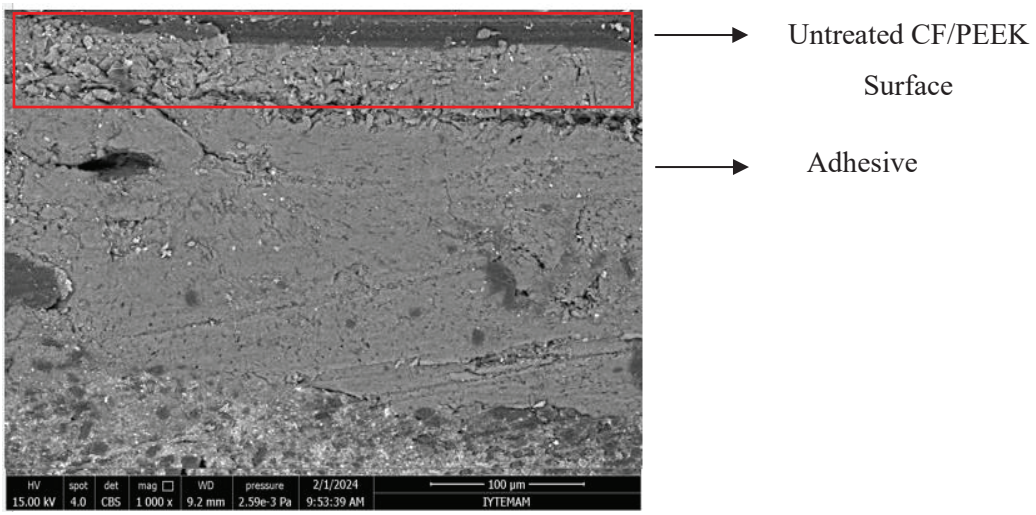

(a)

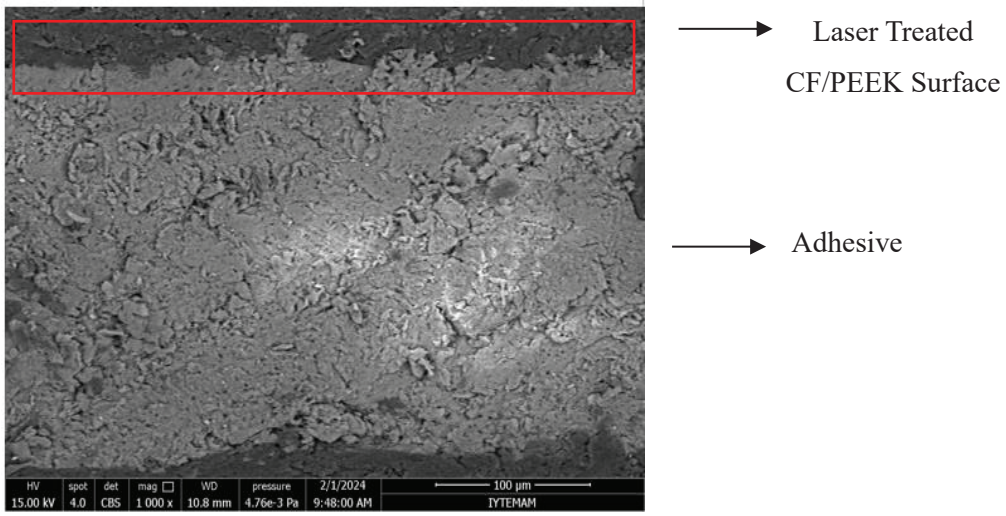

(b)

Figure 4.32. SEM images of (a) reference and (b) laser treated surfaces from the side view.

In Figure 4.32, as obtained from the surface roughness analysis, it is clearly seen that the adhesive-CF/PEEK interface of the reference sample is a very smooth surface, and the adhesive and the CF/PEEK surface can be sharply separated (Figure 4.32(a)), while the roughness of the surface in the laser sample (Figure 4.32(b)) is clearly seen in the areas highlighted in red.

Before bonding, the cavity structure at the interface created by the laser surface treatment is filled by the adhesive. It has been shown that the reason for the increase in mechanical properties of the laser sample compared to the reference sample is that this peak-valley interface structure allows the adhesive to better penetrate into the CF/PEEK surface, which is due to the mechanical locking mechanism at the adhesive-CF/PEEK interface.

According to Figure 4.31 and Figure 4.32, the surfaces of the reference samples are very close to the mean plane and have a flat surface with holes. Laser samples have larger pores and peaks on the surface. The porous morphologies of the laser-treated surfaces exhibited superior adhesion performance and appeared to be critical in triggering potential mechanical interlocking. This results in the penetration of the adhesive into the surface pores and provide mechanical resistance to the sample.

4.6.3. Contact Angle Results

Contact angle analysis was performed on the reference and laser samples to determine the wettability of the reference and laser samples as shown in Figure 4.33. Wettability properties calculated from sessile drop experiments. Pure water was used in the experiment and as seen in Figure 4.33, the contact angle values were determined by taking the point where the plate and the water drop meet as the baseline.

At the end of the 15 seconds, according to the values taken from both surfaces, the average contact angle value was found to be 84^0 for the reference sample, while this value was found to 65^0 for the laser sample. Along with the increase in surface roughness, the surface wettability also increased with laser surface treatment.

The surfaces of the control samples are more hydrophobic than the samples whose surfaces were laser treated. The laser treatment made the surface more hydrophilic. This means that the laser surface pre-treatment allows the adhesive to penetrate the surface better and increases the mechanical strength of the bonded CF/PEEK structure.

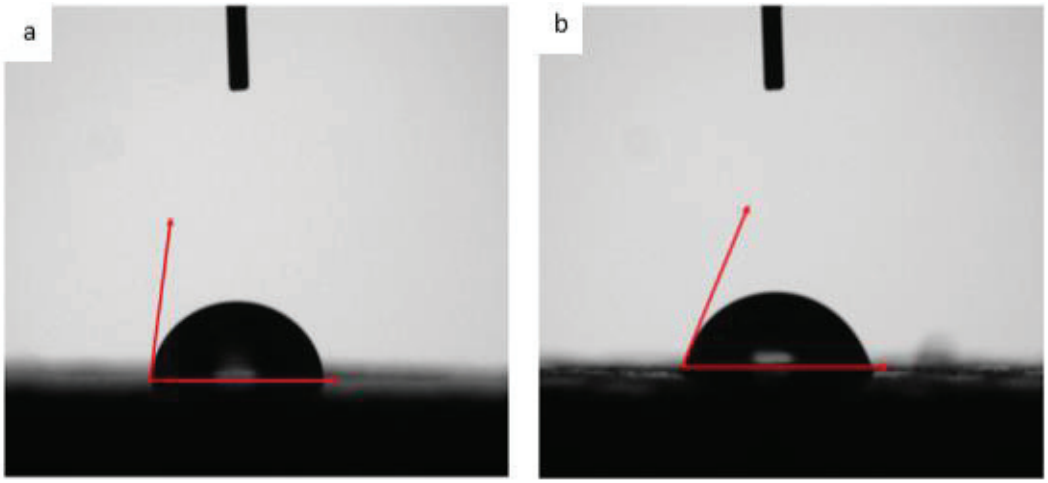

Figure 4.33. Contact angle measurement of a) reference and b) laser treated surfaces.

Many studies have shown that PEEK surfaces change the surface topography due to the craters and peaks created on the surface during laser surface treatment, and that this even contributes to the mechanical strength of the adhesive-substrate interface during the adhesive bonding process.[4]

CHAPTER 5

CONCLUDING REMARKS AND FUTURE WORKS

5.1. Conclusions

In recent years, fiber-reinforced composites have been used in major structural components, particularly in the automotive and aerospace industries, in renewable energy applications such as wind turbine blades, in pipes and tubes for infrastructure, in many industrial products, and in various engineering applications. There is a lot of interest in thermoplastics around the world because they are sustainable, have high mechanical performance and are recyclable. Until now, they could only be used in certain engineering applications. However, considering the developments in production processes with developing technology, the interest in thermoplastic matrix fiber-reinforced composites has increased day by day.

As the increasing interest in these materials leads to their use in various structures, it is expected that their mechanical properties will also be improved. It is very difficult to use fiber-reinforced composites, especially in joint areas, because of the extra stress areas created by traditional joining methods and the damage to the fiber structure. The newly developed bonding methods eliminate these disadvantages and achieve the desired performance in the parts joined with fiber-reinforced composites. Adhesive bonding is one of the most commonly used methods. In this method, the performance of the bonded part is achieved to the desired values by methods such as the selection of reinforcement and matrix materials and the improvement of the adhesive-matrix interface. Therefore, researchers are trying to find ways to improve the mechanical performance of the adhesive-matrix interface. To this end, surface pretreatment methods applied prior to bonding offer new solutions for improving the mechanical properties of these fiber-reinforced thermoplastic composites. The purpose of the applied surface treatments is to increase the roughness of the surfaces to be bonded, to change their chemical properties and to increase the wettability. The surface pretreatments to be applied should be selected according to the material to be bonded. In recent years, interest in laser surface treatment

has increased due to the advantages it offers. It has come to the forefront because it is more environmentally friendly, faster, and easier to apply, especially compared to chemical surface pretreatment processes. The most important step in the laser treatment process is to determine the optimum laser parameters according to the surface to be joined. These parameters vary depending on the type of laser used, the wavelength and the material to be processed. Especially for CF/PEEK thermoplastics, it has been observed that there are gaps in the literature regarding the effect of nanosecond IR-Yb fiber laser parameters on the bond area, microstructural studies of the surfaces formed on the CF/PEEK surface by changing these parameters, and then experimental studies of the mechanical properties of the structures bonded with adhesive film. Mode-I fracture toughness values, which are particularly important for the bonded area, have not been widely reported in the literature.

In this study, the CF/PEEK plates were successfully produced by hot pressing. Reasons for choosing PEEK as a raw material include its high strength even at high temperatures, high chemical resistance, thermal stability, and its widespread use in the aerospace industry. The thermal behavior of PEEK was determined using differential scanning calorimetry (DSC) analysis.

In the laser surface treatment process prior to bonding, it has been found that three parameters play an important role in the removal of selective matrix material from the surface without fiber damages. These parameters are laser power, scanning speed and frequency. Many experiments were conducted to optimize these three parameters. The effect of laser parameters on the bonded CF/PEEK surfaces was determined by optical microscopy and SEM.

According to the studies carried out to determine the optimum working range for laser parameters, it was observed that the laser could not affect the CF/PEEK surface even at the lowest speed with a power of 7W and below. In laser surface treatment, laser parameters can be controlled with released energy values (Espec) to achieve the desired surface finish. According to the analysis, if the Espec value is greater than 0.1 J/mm^2 at power levels of 10 W and above, unwanted fiber breakage and surface contamination are observed. This is the threshold at which fiber damage begins to occur. In this case, this energy level must be reduced as it will negatively affect the mechanical strength of the joint area. In addition, it was observed that with the parameters of 8 W laser power and 0.1 m/s scan speed, almost the entire matrix was removed from the surface by ablation, and the energy value was quite high. This shows that the matrix ablation observed in this

example occurs by a different mechanism compared to other laser-treated surfaces. Although no fiber fractures were observed on the examined surfaces, thermal degradation of the fibers was observed in some regions because the energy value was very high. For this reason, according to the mechanical test results, the highest mechanical strength results do not belong to these specimens.

According to the microstructural analysis, three different laser parameters were able to produce surfaces close to the desired finish surfaces. SLS test specimens were prepared using these three parameters and the one that provided the best results was selected. It was found that the optimum power of 20 W, scanning speed of 20 m/s, frequency value of 200 kHz gave the best results according to the results of these experiments.

The optimal laser parameters were determined, and their accuracy was verified by mechanical tests. Single-lap shear, Charpy impact, and DCB tests were performed on the specimens to determine if the bond was successful.

According to the results of the single lap shear test, an increase in strength of approximately 142% was observed for the laser-treated samples compared to the reference sample. In addition, an approximately 2 times increase in strain value was observed compared to the reference sample. This means that the sample is more resistant to the applied load due to the laser surface treatment. Also, the average Charpy impact strength of the laser-treated specimens was approximately 80% greater than the reference specimens. According to the DCB test results, the average Mode-I fracture toughness value of the laser-treated specimens is approximately 22 times higher than that of the reference specimens.

In order to demonstrate the relationship between the observed increase in mechanical strength in the joint area of the bonded CF/PEEK structures and the change in surface topography due to the laser surface treatment, the surface topographies of the samples were obtained using a profilometer. In the surface profilometer analysis, the surface topography parameters, S_a, and the hybrid surface analysis parameters, S_{dq} and Sdr, that affect the adhesive bonding performance were determined for both the samples whose surface was laser treated and the reference samples. The relative surface area (S_{dr}) value for the reference sample was 0.028%, while the value for the laser treatment samples was 1.759%. Since the S_{dr} value is a measure of relative surface area, the results show that the goal of the laser surface treatment was to increase the contact area with the adhesive. On the other hand, according to the skewness results, the reference samples

have a negative skewness value (-0.271). This indicates that the reference samples are closer to the mean plane and have smaller gaps. For the laser samples, this value was found to be 1.851. This represents large holes or peaks on the laser treated surfaces. The porous structures of the laser-treated CF/PEEK surfaces had excellent adhesive performance and seemed to be essential for potential mechanical interlocking. This results in the adhesive penetrating the surface pores and providing mechanical resistance to the specimen.

When the contact angle results of the reference and laser-treated samples were examined, a shift in the wettability angle toward hydrophilicity was observed on the laser-treated surfaces. This means that the mechanical performance of the adhesive bonded CF/PEEK structure is increased because the laser surface treatment allows the adhesive to better penetrate the surface.

In accordance with the purpose of the study, the joint strength of the structures to be fabricated using CF/PEEK material and epoxy-based film adhesive was successfully increased by laser surface treatment. Thanks to this method, the range of applications of CF/PEEK composites can be extended. In addition, the effects of changing laser parameters on the CF/PEEK material surface for the nanosecond pulsed IR-Yb fiber laser have been clearly demonstrated and appropriate working ranges for laser surface treatment have been determined. Laser process parameters can be determined for the CF/PEEK material according to the desired purpose. Adhesive bonding performance of carbon fiber reinforced PEEK composites is highly correlated with substrate surface roughness, wettability, and morphology. Proper surface roughness, higher surface wettability, and uniform and dense surface morphology result in better shear strength.

As a result of this study, the laser surface treatment method, which is an innovative approach, the thermoplastics (CF/PEEK) and the FM300K film adhesive, which are very important for the aerospace industry, can be used in more aerospace applications as intended.

5.2. Future Works

In recent years, as the concept of sustainability has become more important, the interest in recyclable, more environmentally friendly thermoplastic materials has increased in various applications in many industries. In order to further expand the

application area of CF/PEEK composite, which is very important for the aerospace industry, this study has shown that this material can be used in film adhesive bonded parts by providing high strength and impact resistance values through laser surface treatment. Thanks to the optimum laser operating parameters found for the CF/PEEK material, the increase in mechanical strength at the coupon level can be improved for parts used in different applications in the industry.

Future studies and investigations to provide a wider range of applications for the CF/PEEK material, adhesive bonding mechanisms, and to fully understand the changes formed on the surface as a result of laser surface pre-treatment may include the following;

- This study, which was conducted using the optimal laser parameters determined at the CF/PEEK coupon level, can be manufactured and tested on an industrial scale for some parts used in the aerospace industry. It is expected that the center wing box, one of the aircraft wing parts, may be suitable for this application.
- Due to the peak-and-valley structure created on the surface by laser surface treatment, paste adhesive can be used instead of film adhesive. Since paste adhesive is more fluid than film adhesive, it can penetrate the created structure better.
- The performance of composites whose surfaces are laser surface treated prior to adhesive bonding under static single-lap shear and Mode-I loading is one of the topics studied in this field. However, the fatigue behavior of bonded composites and the effect of laser surface treatment on this behavior is still an open question in the literature. If it is planned to produce parts to be used in industry, the fatigue life of these parts according to their intended use is also very important.
- The effects of parameters such as plate thickness and adhesive thickness on laser surface pre-treatment and bond performance can be studied.
- In addition, for this study, finite element analysis of bonded joints of CF/PEEK material can be performed by applying laser surface pretreatment.

REFERENCES

1. Gay D., Composite Materials: Design and Applications, *CRC Press (4th ed.),* 2022. https://doi.org/10.1201/9781003195788.

2. Skeist, I., Ed, Handbook of Adhesives, *Springer US: Boston, MA,* 1990. https://doi.org/10.1007/978-1-4613-0671-9.

3. Li, X.; Ehrhardt, M.; Lorenz, P.; Han, B.; Lai, S.; Zimmer, K.; Xu, L.; Nan, P.; Ni, X. Influence of Surface Treatment with Infrared Nanosecond Laser on Adhesion Performance of Adhesion-Bonded Carbon Fiber/Epoxy Composite. *J Adhes Sci Technol* 2020, *34* (13), 1399–1425. https://doi.org/10.1080/01694243.2019.1710990.

4. Wilson, A.; Jones, I.; Salamat-Zadeh, F.; Watts, J. F. Laser Surface Modification of Poly(Etheretherketone) to Enhance Surface Free Energy, Wettability and Adhesion. *Int J Adhes Adhes* 2015, *62*, 69–77. https://doi.org/10.1016/j.ijadhadh.2015.06.005.

5. Messler, R. W. *Joining of Materials and Structures: From Pragmatic Process to Enabling Technology*; 2004. https://doi.org/10.1016/B978-0-7506-7757-8.X5000-3.

6. Hull, N. D.; Clyne, T. W., An Introduction to Composite Materials, *Cambridge Solid State Science Series*, 1996.

7. R.R. Naslain, Ceramic Matrix Composites: Matrices and Processing. *Encyclopedia of Materials: Science and Technology*, 2001, pp.1060-1066. https://doi.org/10.1016/B0-08-043152-6/00196-0.

8. Merter N.E., Effects of Processing Parameters on The Mechanical Behavior of Continuous Glass Fiber/Polypropylene Composites. MSc Dissertation, Izmir Institute of Technology, 2009. https://gcris.iyte.edu.tr/handle/11147/3016. (accessed 2024-04-11)

9. Tsai, S. W.; Hahn, H. Thomas, *Introduction to Composite Materials*; Technomic Pub, 1980.

10. Barbero, E. J., *Introduction to composite materials design*, CRC press, 2010. https://doi.org/10.1201/9781439894132.

11. Hale, D. K., The physical properties of composite materials, *Journal of materials science*, 1976, *11*: 2105-2141.

12. Jones, R. M., Mechanics of composite materials. *CRC press*, 2018. https://doi.org/10.1201/9781498711067.

13. Yan, D. X.; Ren, P. G.; Pang, H.; Fu, Q.; Yang, M. B.; Li, Z. M. Efficient Electromagnetic Interference Shielding of Lightweight Graphene/Polystyrene Composite. *J Mater Chem* 2012, 22 (36), 18772–18774. https://doi.org/10.1039/c2jm32692b.

14. Sahmaran, M.; Li, V. C.; Andrade, C. Corrosion Resistance Performance of Steel-Reinforced Engineered Cementitious Composite Beams. *ACI Mater J* 2008, *105* (3), 243–250. https://doi.org/10.14359/19820.

15. Rajak, D. K.; Pagar, D. D.; Kumar, R.; Pruncu, C. I. Recent Progress of Reinforcement Materials: A Comprehensive Overview of Composite Materials. *Journal of Materials Research and Technology* 2019, *8* (6), 6354–6374. https://doi.org/10.1016/j.jmrt.2019.09.068.

16. Priyanka, P.; Dixit, A.; Mali, H. S. High-Strength Hybrid Textile Composites with Carbon, Kevlar, and E-Glass Fibers for Impact-Resistant Structures. A Review. *Mechanics of Composite Materials* 2017, *53* (5), 685–704. https://doi.org/10.1007/s11029-017-9696-2.

17. Xu, Y., Chung, D. D. L., & Mroz, C., Thermally conducting aluminum nitride polymer-matrix composites. *Composites Part A: Applied science and manufacturing,* 2001, 32(12), 1749-1757.

18. Ray, B. C. Temperature Effect during Humid Ageing on Interfaces of Glass and Carbon Fibers Reinforced Epoxy Composites. *J Colloid Interface Sci* 2006, *298* (1), 111–117. https://doi.org/10.1016/j.jcis.2005.12.023.

19. Davim, J. P., & Reis, P, Study of delamination in drilling carbon fiber reinforced plastics (CFRP) using design experiments. *Composite structures,* 2003, 59(4), 481-487.

20. Mukherjee, M.; Das, C. K.; Kharitonov, A. P. Fluorinated and Oxyfluorinated Short Kevlar Fiber-Reinforced Ethylene Propylene Polymer. *Polymeric Composites* 2006, *27* (2), 205–212. https://doi.org/10.1002/pc.20195.

21. Chung, D. D, *Composite materials: functional materials for modern technologies*. Springer Science & Business Media, 2003.

22. Samal, P.; Vundavilli, P. R.; Meher, A.; Mahapatra, M. M. Recent Progress in Aluminum Metal Matrix Composites: A Review on Processing, Mechanical and Wear Properties. *Journal of Manufacturing Processes*. Elsevier Ltd November 1, 2020, pp 131–152. https://doi.org/10.1016/j.jmapro.2020.09.010.

23. Li L*., Durability of ceramic-matrix composites.* Woodhead Publishing*,* (2020).

24. Kwon, D. J.; Kim, N. S. R.; Jang, Y. J.; Choi, H. H.; Kim, K.; Kim, G. H.; Kong, J.; Nam, S. Y. Impacts of Thermoplastics Content on Mechanical Properties of Continuous Fiber-Reinforced Thermoplastic Composites. *Composite B Eng* 2021, *216*. https://doi.org/10.1016/j.compositesb.2021.108859.

25. Villegas, I. F.; Moser, L.; Yousefpour, A.; Mitschang, P.; Bersee, H. E. N. Process and Performance Evaluation of Ultrasonic, Induction and Resistance Welding of Advanced Thermoplastic Composites. *Journal of Thermoplastic Composite Materials* 2013, *26* (8), 1007–1024. https://doi.org/10.1177/0892705712456031.

26. Dornoff, J.; Mock, P.; Baldino, C.; Bieker, G.; Díaz, S.; Miller, J.; Sen, A.; Tietge, U.; Wappelhorst, S. *Fit for 55: A Review and Evaluation of the European Commission Proposal for Amending the CO 2 Targets for New Cars and Vans*; 2021. https://theicct.org/publications/eu-co2-.

27. European Commision. *Reducing Emissions from Aviation*. https://climate.ec.europa.eu/eu-action/transport/reducing-emissions-aviation_en (accessed 2024-03-30).

28. *Thermoplastic Composites Market Report*; 2023. https://www.precedenceresearch.com/thermoplastic-composites-market (accessed 2023-08-29).

29. Offringa, A. R. Thermoplastic composites—rapid processing applications. *Composites Part A: Applied Science and Manufacturing*,1996, 27(4), 329-336.

30. Gardiner G., PEEK vs. PEKK vs. PAEK and Continuous Compression Molding, 2023. https://www.compositesworld.com/articles/peek-vs-pekk-vs-paek-and-continuouscompression- molding (accessed 2024-03-30).

31. Sudhin, A. U.; Remanan, M.; Ajeesh, G.; Jayanarayanan, K. Comparison of Properties of Carbon Fiber Reinforced Thermoplastic and Thermosetting Composites for Aerospace Applications. *Mater Today Proc* 2020, *24*, 453–462. https://doi.org/10.1016/J.MATPR.2020.04.297.

32. Campbell Jr, F. C., *Manufacturing technology for aerospace structural materials*. Elsevier, 2011.

33. Milne, I., Ritchie, R. O., & Karihaloo, B. L. (Eds.). Comprehensive structural integrity: Cyclic loading and fatigue. *Elsevier*, 2003, (4).

34. Skirbutis, G.; Dzingutė, A.; Masiliūnaitė, V.; Šulcaitė, G.; Žilinskas, J., A review of PEEK polymer's properties and its use in prosthodontics. *Stomatologija*, 19(1), 19-23.

35. Wang, W.; Luo, C. J.; Huang, J.; Edirisinghe, M. PEEK Surface Modification by Fast Ambient-Temperature Sulfonation for Bone Implant Applications. *J R Soc Interface* 2019, *16* (152). https://doi.org/10.1098/rsif.2018.0955.

36. Choudhury, S. S.; Pandey, M.; Bhattacharya, S. Recent Developments in Surface Modification of PEEK Polymer for Industrial Applications: A Critical Review. *Reviews of Adhesion and Adhesives* 2021, *9* (3), 401–433. https://doi.org/10.47750/RAA/9.3.03.

37. Qin, Q. H., Introduction to the Composite and Its Toughening Mechanisms. *Toughening Mechanisms in Composite Materials* 2015, 1–32. https://doi.org/10.1016/B978-1-78242-279-2.00001-9.

38. Kumlutas, D.; Tavman, I. H.; Turhan, M. C. Thermal conductivity of particle filled polyethylene composite materials. *Composites science and technology*, 2003, 63(1), 113-117.

39. Zhang, B.; Jia, L.; Tian, M.; Ning, N.; Zhang, L.; Wang, W. Surface and Interface Modification of Aramid Fiber and Its Reinforcement for Polymer Composites: A Review. *European Polymer Journal*. Elsevier Ltd March 15, 2021. https://doi.org/10.1016/j.eurpolymj.2021.110352.

40. Campbell Jr, F. C. (Ed.), *Manufacturing processes for advanced composites*. Elsevier,2003.

41. Vara Prasad, V.; Talupula, S. A Review on Reinforcement of Basalt and Aramid (Kevlar 129) Fibers; *Materials Today: Proceedings*, 2018, *5*(2), 5993-5998.

42. Rezaei, F.; Yunus, R.; Ibrahim, N. A. Effect of Fiber Length on Thermomechanical Properties of Short Carbon Fiber Reinforced Polypropylene Composites. *Mater Des* 2009, *30* (2), 260–263. https://doi.org/10.1016/j.matdes.2008.05.005.

43. Das, S.; Warren, J.; West, D.; Schexnayder, S. M., Global Carbon Fiber Composites Supply Chain Competitiveness Analysis; *Oak Ridge National Lab.(ORNL), Oak Ridge, TN (United States); The University of Tennessee, Knoxville,* 2016.

44. Soutis, C., Fibre Reinforced Composites in Aircraft Construction. Progress in Aerospace Sciences. *Elsevier Ltd* 2005, pp 143–151. https://doi.org/10.1016/j.paerosci.2005.02.004.

45. Fu, S.-Y.; Lauke, B.; Mäder, E.; Yue, C.-Y.; Hu, X. Tensile properties of short-glass-fiber-and short-carbon-fiber-reinforced polypropylene composites. *Composites Part A: Applied Science and Manufacturing,* 31(10), 1117-1125.

46. Kuriger, R. J.; Khairul Alam, M.; Anderson, D. P.; Jacobsen, R. L., Processing and characterization of aligned vapor grown carbon fiber reinforced polypropylene. *Composites Part A: Applied Science and Manufacturing, 2002, 33(1), 53-62.*

47. Cevahir, A. Glass Fibers. *Fiber Technology for Fiber-Reinforced Composites* 2017, 99–121. https://doi.org/10.1016/B978-0-08-101871-2.00005-9.

48. Campbell Jr, F. C., *Manufacturing technology for aerospace structural materials*. Elsevier, 2011.

49. Sathishkumar, T. P.; Satheeshkumar, S.; Naveen, J. Glass Fiber-Reinforced Polymer Composites - A Review. *Journal of Reinforced Plastics and Composites*.2014, pp 1258–1275. https://doi.org/10.1177/0731684414530790.

50. Rajak, D. K.; Wagh, P. H.; Linul, E. Manufacturing Technologies of Carbon/Glass Fiber-Reinforced Polymer Composites and Their Properties: A Review. *Polymers*. MDPI, 2021. https://doi.org/10.3390/polym13213721.

51. Boparai, K.; Singh, R.; Singh, H. Comparison of Tribological Behaviour for Nylon6-Al-Al2O3 and ABS Parts Fabricated by Fused Deposition Modelling: This Paper Reports a Low Cost Composite Material That Is More Wear-Resistant than Conventional ABS. *Virtual Phys Prototyp* 2015, *10* (2), 59–66. https://doi.org/10.1080/17452759.2015.1037402.

52. Masood, S. H.; Song, W. Q. Development of New Metal/Polymer Materials for Rapid Tooling Using Fused Deposition Modelling. *Mater Des* 2004, *25* (7), 587–594. https://doi.org/10.1016/j.matdes.2004.02.009.

53. Hubert, P.; Fernlund, G.; Poursartip, A. Autoclave Processing for Composites. *Manufacturing Techniques for Polymer Matrix Composites (PMCs)* 2012, 414–434. https://doi.org/10.1533/9780857096258.3.414.

54. Ekuase, O. A.; Anjum, N.; Eze, V. O.; Okoli, O. I. A Review on the Out-of-Autoclave Process for Composite Manufacturing. *Journal of Composites Science*. MDPI June 1, 2022. https://doi.org/10.3390/jcs6060172.

55. Chohan, J. S.; Boparai, K. S.; Singh, R.; Hashmi, M. S. J. Manufacturing Techniques and Applications of Polymer Matrix Composites: A Brief Review. *Advances in Materials and Processing Technologies*. *Taylor and Francis,* 2022, pp884–894. https://doi.org/10.1080/2374068X.2020.1835012.

56. Da Cunha Saraiva F., Development of press forming techniques for thermoplastic composites: investigation of a multiple step forming approach, 2017, http://repository.tudelft.nl/.

57. Tatsuno, D.; Yoneyama, T.; Kawamoto, K.; Okamoto, M. Hot Press Forming of Thermoplastic CFRP Sheets. In Procedia Manufacturing; *Elsevier B.V*., 2018; Vol. 15, pp 1730–1737. https://doi.org/10.1016/j.promfg.2018.07.254.

58. Lee, M. G.; Kim, S. J.; Han, H. N.; Jeong, W. C. Application of Hot Press Forming Process to Manufacture an Automotive Part and Its Finite Element Analysis Considering Phase Transformation Plasticity. *Int J Mech Sci* 2009, *51* (11–12), 888–898. https://doi.org/10.1016/j.ijmecsci.2009.09.030.

59. Hu, J.; Zhu, S.; Wang, B.; Liu, A.; Ma, L.; Wu, L.; Zhou, Z. Fabrication and Compression Properties of Continuous Carbon Fiber Reinforced Polyether Ether Ketone Thermoplastic Composite Sandwich Structures with Lattice Cores. *Journal of Sandwich Structures and Materials* 2021, *23* (6), 2422–2442. https://doi.org/10.1177/1099636220909949.

60. Fahrenholz, H. Testing of Long Fiber-Reinforced Composites, *TestXpo,* 2018.

61. George Bullen Nick, B. N., *Assembly & Joining of Composite Materials Workshop*; 2017.

62. Agarwal, J.; Sahoo, S.; Mohanty, S.; Nayak, S. K. Progress of Novel Techniques for Lightweight Automobile Applications through Innovative Eco-Friendly Composite Materials: A Review. *Journal of Thermoplastic Composite Materials 2020* (7), 978–1013. https://doi.org/10.1177/0892705718815530.

63. Oztoprak, N.; Gunes, M. D.; Tanoglu, M.; Aktas, E.; Egilmez, O. O.; Senocak, C.; Kulac, G. Developing Polymer Composite-Based Leaf Spring Systems for Automotive Industry. *Science and Engineering of Composite Materials* 2018, *25* (6), 1167–1176. https://doi.org/10.1515/SECM-2016-0335/MACHINEREADABLECITATION/RIS.

64. Lan, P.; Nunez, E. E.; Polycarpou, A. A. Advanced Polymeric Coatings and Their Applications: Green Tribology. In *Encyclopedia of Renewable and Sustainable Materials: Volume 1-5*; Elsevier, 2020; Vol. 1–5, pp 345–358. https://doi.org/10.1016/B978-0-12-803581-8.11466-3.

65. Adams, R. D. (Ed.), Adhesive bonding: science, technology and applications. *Woodhead Publishing,* 2021. (accessed 2024-03-30).

66. Kupski, J.; Teixeira de Freitas, S. Design of Adhesively Bonded Lap Joints with Laminated CFRP Adherends: Review, Challenges and New Opportunities for Aerospace Structures. *Compos Struct* 2021, *268*. https://doi.org/10.1016/j.compstruct.2021.113923.

67. A&D Thermoplastic Composites Market | Strategic Assessment and Competitive Analysis. https://www.stratviewresearch.com/299/aerospace-&-defense-thermoplastic-composites-market.html (accessed 2024-03-30).

68. Abderrafai, Y.; Diouf-Lewis, A.; Sosa-Rey, F.; Farahani, R. D.; Piccirelli, N.; Lévesque, M.; Therriault, D. Additive Manufacturing and Characterization of High Temperature Thermoplastic Blends for Potential Aerospace Applications. *Compos Sci Technol* 2023, *231*. https://doi.org/10.1016/j.compscitech.2022.109839.

69. Mondal, M. K.; Bose, B. P.; Bansal, P. Recycling Waste Thermoplastic for Energy Efficient Construction Materials: An Experimental Investigation. *J Environ Manage* 2019, *240*, 119–125. https://doi.org/10.1016/j.jenvman.2019.03.016.

70. Potluri, P.; Kusak, E.; Reddy, T. Y. Novel Stitch-Bonded Sandwich Composite Structures. *Compos Struct* 2003, *59* (2), 251–259. https://doi.org/10.1016/S0263-8223(02)00087-9.

71. Boey, F. Y. C.; Lee, T. H.; Khor, K. A., Polymer crystallinity and its effect on the non-linear bending creep rate for a polyphenylene sulphide thermoplastic composite. *Polymer testing*, *14*(5), 425-438.

72. Cheldi, T.; Cavassi, P.; Serricchio, M.; Spinelli, C. M.; Vietina, G.; Ballabio, S. Use of Spoolable Reinforced Thermoplastic Pipes for Oil and Water Transportation. OnePetro March 27, 2019. https://dx.doi.org/ (accessed 2024-04-03).

73. Messler, R. W. Joining Composite Materials and Structures: Some Thought-Provoking Possibilities. *Journal of Thermoplastic Composite Materials* 2004, *17* (1), 51–75. https://doi.org/10.1177/0892705704033336.

74. Siddique, A.; Iqbal, Z.; Nawab, Y.; Shaker, K. A Review of Joining Techniques for Thermoplastic Composite Materials. *Journal of Thermoplastic Composite Materials*. SAGE Publications Ltd August 1, 2023, pp 3417–3454. https://doi.org/10.1177/08927057221096662.

75. Reis, J. P.; de Moura, M.; Samborski, S. Thermoplastic Composites and Their Promising Applications in Joining and Repair Composites Structures: A Review. *Materials*. MDPI AG December 2, 2020, pp 1–33. https://doi.org/10.3390/ma13245832.

76. Howie, I.; Gillespie, J. W.; Smiley, A. J.; Smiley, A. J. Resistance Welding of Graphite-Polyarylsulfone/Polysulfone Dual-Polymer Composites. *Journal of Thermoplastic Composite Materials* 1993, *6* (3), 205–225. https://doi.org/10.1177/089270579300600303.

77. Hou, M.; Ye, L.; Mai, Y.-W. An Experimental Study of Resistance Welding of Carbon Fibre Fabric Reinforced Polyetherimide (CF Fabric/PEI) Composite Material. *Applied Composite Materials* 1999, *6*, 35–49.

78. Adams, R. D. *Adhesive Bonding: Science, Technology and Applications*; CRC Press, 2005.

79. Dorworth, L. C., & Dillingham, G., Fundamentals of adhesive bonding of composite materials. *In AeroDef Manufacturing Conference, Fort Worth, Texas, USA,* 2017.

80. Jiang, B.; Chen, Q.; Yang, J. Advances in Joining Technology of Carbon Fiber-Reinforced Thermoplastic Composite Materials and Aluminum Alloys. *The International Journal of Advanced Manufacturing Technology*, 2020, *110*(9), 2631-2649.
https://doi.org/10.1007/s00170-020-06021-2/Published.

81. George Bullen Nick, B. N., *Assembly & Joining of Composite Materials Workshop*; 2017.

82. Da Silva, L. F. M. Design Rules and Methods to Improve Joint Strength, *Handbook of adhesion technology*, 2011. https://doi.org/10.1007/978-3-319-55411-2_27.

83. Hart-Smith J., Aerospace Industry Applications of Adhesive Bonding. *Adhesive Bonding: Science, Technology and Applications* 2021, 763–800. https://doi.org/10.1016/B978-0-12-819954-1.00001-0.

84. Nwankwo, E.; Fallah, A. S.; Louca, L. A. An Investigation of Interfacial Stresses in Adhesively Bonded Single Lap Joints Subject to Transverse Pulse Loading. *Journal of Sound and Vibration*, 2012, 332(7), 1843-1858. https://doi.org/10.1016/j.jsv.2012.11.008.

85. Scarselli, G.; Corcione, C.; Nicassio, F.; Maffezzoli, A. Adhesive Joints with Improved Mechanical Properties for Aerospace Applications. *Int J Adhes Adhes* 2017, *75*, 174–180. https://doi.org/10.1016/j.ijadhadh.2017.03.012.

86. Banea, M. D.; Da Silva, L. F. M. Adhesively Bonded Joints in Composite Materials: An Overview. *Proceedings of the Institution of Mechanical Engineers, Part L: Journal of Materials: Design and Applications*. January 1, 2009, pp 1–18. https://doi.org/10.1243/14644207JMDA219.

87. Quan, D.; Alderliesten, R.; Dransfeld, C.; Tsakoniatis, I.; Teixeira De Freitas, S.; Scarselli, G.; Murphy, N.; Ivanković, A.; Benedictus, R. Significantly Enhanced Structural Integrity of Adhesively Bonded PPS and PEEK Composite Joints by Rapidly UV-Irradiating the Substrates. *Compos Sci Technol* 2020, *199*. https://doi.org/10.1016/j.compscitech.2020.108358.

88. Valarinho, L.; Correia, J. R.; Branco, F. A. Experimental Study on the Flexural Behaviour of Multi-Span Transparent Glass–GFRP Composite Beams. *Constr Build Mater* 2013, *49*, 1041–1053. https://doi.org/10.1016/J.CONBUILDMAT.2012.11.024.

89. Genna, S.; Leone, C.; Ucciardello, N.; Giuliani, M. Increasing Adhesive Bonding of Carbon Fiber Reinforced Thermoplastic Matrix by Laser Surface Treatment. *Polym Eng Sci* 2017, *57* (7), 685–692. https://doi.org/10.1002/pen.24577.

90. Chaves, F. J. P.; Da Silva, L. F. M.; De Moura, M. F. S. F.; Dillard, D. A.; Esteves, V. H. C. Fracture Mechanics Tests in Adhesively Bonded Joints: A Literature Review. *Journal of Adhesion*. Taylor and Francis Inc. November 2, 2014, pp 955–992. https://doi.org/10.1080/00218464.2013.859075.

91. ASTM D5573 *Standard Practice for Classifying Failure Modes in Fiber-Reinforced-Plastic (FRP) Joints*. https://www.astm.org/d5573-99r19.html (accessed 2024-04-08).

92. Omairey, S.; Jayasree, N.; Kazilas, M. Defects and Uncertainties of Adhesively Bonded Composite Joints. *SN Applied Sciences*. September 1, 2021. https://doi.org/10.1007/s42452-021-04753-8.

93. Quini, J. G.; Marinucci, G. Polyurethane Structural Adhesives Applied in Automotive Composite Joints. *Materials Research* 2012, *15* (3), 434–439. https://doi.org/10.1590/S1516-14392012005000042.

94. Da Silva, L. F. M.; Carbas, R. J. C.; Critchlow, G. W.; Figueiredo, M. A. V; Brown, K. Effect of Material, Geometry, Surface Treatment and Environment on the Shear Strength of Single Lap Joints. International *Journal of Adhesion and Adhesives*, 2009, 29(6), 621-632. https://doi.org/10.1016/j.ijadhadh.2009.02.012.

95. Kanerva, M.; Saarela, O. The Peel Ply Surface Treatment for Adhesive Bonding of Composites: A Review. *International Journal of Adhesion and Adhesives,* 2013, *43*, 60-69. https://doi.org/10.1016/j.ijadhadh.2013.01.014.

96. Islam, M. S.; Tong, L.; Falzon, P. J. Influence of Metal Surface Preparation on Its Surface Profile, Contact Angle, Surface Energy and Adhesion with Glass Fibre Prepreg. *International Journal of Adhesion and Adhesives*, 2014, 51: 32-41. https://doi.org/10.1016/j.ijadhadh.2014.02.006.

97. Iqbal, H. M. S.; Bhowmik, S.; Benedictus, R. Surface Modification of High Performance Polymers by Atmospheric Pressure Plasma and Failure Mechanism of Adhesive Bonded Joints. *Int J Adhes Adhes* 2010, *30*, 418–424. https://doi.org/10.1016/j.ijadhadh.2010.02.007.

98. Encinas, N.; Oakley, B. R.; Belcher, M. A.; Blohowiak, K. Y.; Dillingham, R. G.; Abenojar, J.; Martínez, M. A. Surface Modification of Aircraft Used Composites for Adhesive Bonding. *International Journal of Adhesion and Adhesives,* 2014, 50: 157-163. https://doi.org/10.1016/j.ijadhadh.2014.01.004.

99. Sinmazçelik, T.; Avcu, E.; Bora, M. Ö.; Çoban, O. A Review: Fibre Metal Laminates, Background, Bonding Types and Applied Test Methods. *Materials & Design*, 2011, 32.7: 3671-3685. https://doi.org/10.1016/j.matdes.2011.03.011.

100. Nattapat, M.; Marimuthu, S.; Kamara, A. M.; Esfahani, M. R. N. Laser Surface Modification of Carbon Fiber Reinforced Composites. *Materials and Manufacturing Processes* 2015, *30* (12), 1450–1456. https://doi.org/10.1080/10426914.2015.1019097.

101. Liu, J.; Xue, Y.; Dong, X.; Fan, Y.; Hao, H.; Wang, X. Review of the Surface Treatment Process for the Adhesive Matrix of Composite Materials. *Int J Adhes Adhes* 2023, *126*. https://doi.org/10.1016/j.ijadhadh.2023.103446.

102. See, T. L.; Liu, Z.; Cheetham, S.; Dilworth, S.; Li, L. Laser Abrading of Carbon Fibre Reinforced Composite for Improving Paint Adhesion. *Appl Phys A Mater Sci Process* 2014, *117* (3), 1045–1054. https://doi.org/10.1007/s00339-014-8527-8.

103. Awaja, F.; Pigram, P. J. Surface Molecular Characterisation of Different Epoxy Resin Composites Subjected to UV Accelerated Degradation Using XPS and ToF-SIMS. *Polym Degrad Stab* 2009, *94*, 651–658. https://doi.org/10.1016/j.polymdegradstab.2009.01.001.

104. Kanerva, M.; Sarlin, E.; Hoikkanen, M.; Rämö, K.; Saarela, O.; Vuorinen, J. Interface Modification of Glass Fibre-Polyester Composite-Composite Joints Using Peel Plies. *International Journal of Adhesion and Adhesives*, 2015, 59: 40-52. https://doi.org/10.1016/j.ijadhadh.2015.01.016.

105. Prolongo, S. G.; Gude, M. R.; Del Rosario, G.; Ureña, A. Surface Pretreatments for Composite Joints: Study of Surface Profile by SEM Image Analysis. In *Journal of Adhesion Science and Technology*; 2010; Vol. 24, pp 1855–1867. https://doi.org/10.1163/016942410X507623.

106. Barthel, A. J.; Luo, J.; Hwang, K. S.; Lee, J. Y.; Kim, S. H. Boundary Lubrication Effect of Organic Residue Left on Surface after Evaporation of Organic Cleaning Solvent. *Wear* 2016, *350–351*, 21–26. https://doi.org/10.1016/j.wear.2015.12.010.

107. Hu, Y.; Yuan, B.; Cheng, F.; Hu, X. NaOH Etching and Resin Pre-Coating Treatments for Stronger Adhesive Bonding between CFRP and Aluminium Alloy. *Composites Part B: Engineering*, 2019, 178: 107478. https://doi.org/10.1016/j.compositesb.2019.107478.

108. Zhou, L.; Qian, Y.; Zhu, Y.; Liu, H.; Gan, K.; Guo, J. The Effect of Different Surface Treatments on the Bond Strength of PEEK Composite Materials. *Dental Materials* 2014, *30* (8). https://doi.org/10.1016/j.dental.2014.03.011.

109. Fischer, F.; Kreling, S.; Jäschke, P.; Frauenhofer, M.; Kracht, D.; Dilger, K. Laser Surface Pre-Treatment of CFRP for Adhesive Bonding in Consideration of the Absorption Behaviour. In *Journal of Adhesion*; 2012; Vol. 88, pp 350–363. https://doi.org/10.1080/00218464.2012.660042.

110. Wang, Z.; Ma, Y.; Yuan, B.; Wu, C.; Li, C.; Sun, S. Development of Laser Processing Carbon-Fiber-Reinforced Plastic. *Sensors*. MDPI April 1, 2023. https://doi.org/10.3390/s23073659.

111. Oliveira, V.; Sharma, S. P.; de Moura, M. F. S. F.; Moreira, R. D. F.; Vilar, R. Surface Treatment of CFRP Composites Using Femtosecond Laser Radiation. *Opt Lasers Eng* 2017, *94*, 37–43. https://doi.org/10.1016/j.optlaseng.2017.02.011.

112. Akman, E.; Erdoğan, Y.; Bora, M. Ö.; Çoban, O.; Oztoprak, B. G.; Demir, A. Investigation of the Differences between Photochemical and Photothermal Laser Ablation on the Shear Strength of CFRP/CFRP Adhesive Joints. *Int J Adhes Adhes* 2020, *98*. https://doi.org/10.1016/j.ijadhadh.2020.102548.

113. Gebauer, J.; Burkhardt, M.; Franke, V.; Lasagni, A. F. On the Ablation Behavior of Carbon Fiber-Reinforced Plastics during Laser Surface Treatment Using Pulsed Lasers. *Materials* 2020, *13* (24), 1–17. https://doi.org/10.3390/ma13245682.

114. Delaporte, P.; Karnakis, D.; Zergioti, I. Laser Processing of Flexible Organic Electronic Materials. In *Handbook of Flexible Organic Electronics: Materials, Manufacturing and Applications*; Elsevier Inc., 2015; pp 285–313. https://doi.org/10.1016/B978-1-78242-035-4.00012-9.

115. Sobri, S. A.; Heinemann, R.; Whitehead, D.; Amini, M. H. M.; Mohamed, M. Damage to Carbon Fiber Reinforced Polymer Composites (CFRP) by Laser Machining: An Overview; *Machining and Machinability of Fiber Reinforced Polymer Composites,* 2021, 281-297. https://doi.org/10.1007/978-981-33-4153-1_10.

116. Herzog, D.; Jaeschke, P.; Meier, O.; Haferkamp, H. Investigations on the Thermal Effect Caused by Laser Cutting with Respect to Static Strength of CFRP. *Int J Mach Tools Manuf* 2008, *48* (12–13), 1464–1473. https://doi.org/10.1016/j.ijmachtools.2008.04.007.

117. Negarestani, R.; Li, L. Fibre Laser Cutting of Carbon Fibre-Reinforced Polymeric Composites. *Proc Inst Mech Eng B J Eng Manuf* 2013, *227* (12), 1755–1766. https://doi.org/10.1177/0954405413490513.

118. Wolynski, A.; Herrmann, T.; Mucha, P.; Haloui, H.; L'huillier, J. Laser Ablation of CFRP Using Picosecond Laser Pulses at Different Wavelengths from UV to IR. In *Physics Procedia*; Elsevier B.V., 2011; Vol. 12, pp 292–301. https://doi.org/10.1016/j.phpro.2011.03.136.

119. Palik, E. D., *Handbook of optical constants of solids*. Academic press, 1998.

120. Mathew, J.; Goswami, G. L.; Ramakrishnan, N.; Naik, N. K. Parametric Studies on Pulsed Nd:YAG Laser Cutting of Carbon Fibre Reinforced Plastic Composites. *J Mater Process Technol* 1999, *89*, 198–203.

121. Wang, X.; Li, R.; Leng, J.; Zhou, P.; Li, L.; Ma, P.; Huang, L.; Wu, H. 414W near Diffraction Limited All Fiberized Single Frequency Polarization Maintained Fiber Amplifier. *Optics Letters, Vol. 42, Issue 1, pp. 1-4* 2017, *42* (1), 1–4. https://doi.org/10.1364/OL.42.000001.

122. Su, X.; Hoang, T.; Long, P.; Zheng, Y.; Strickland, D. A Compact High-Average-Power Femtosecond Fiber-Coupled Two-Color CPA System. *IEEE Journal of Selected Topics in Quantum Electronics* 2018, *24* (5). https://doi.org/10.1109/JSTQE.2018.2808276.

123. Dixneuf, C.; Dixneuf, C.; Guiraud, G.; Bardin, Y.-V.; Rosa, Q.; Goeppner, M.; Hilico, A.; Pierre, C.; Boullet, J.; Traynor, N.; Santarelli, G. Ultra-Low Intensity Noise, All Fiber 365 W Linearly Polarized Single Frequency Laser at 1064 Nm. *Optics Express, Vol. 28, Issue 8, pp. 10960-10969* 2020, *28* (8), 10960–10969. https://doi.org/10.1364/OE.385095.

124. Lai, W.; Ma, P.; Ma, P.; Liu, W.; Huang, L.; Li, C.; Ma, Y.; Zhou, P.; Zhou, P. 550 W Single Frequency Fiber Amplifiers Emitting at 1030 Nm Based on a Tapered Yb-Doped Fiber. *Optics Express, Vol. 28, Issue 14, pp. 20908-20919* 2020, *28* (14), 20908–20919. https://doi.org/10.1364/OE.395619.

125. Ohkubo, T.; Tsukamoto, M.; Sato, Y. Numerical Simulation of Combustion Effects during Laser Processing of Carbon Fiber Reinforced Plastics. *Appl Phys A Mater Sci Process* 2016, *122* (3), 1–5. https://doi.org/10.1007/S00339-016-9735-1/FIGURES/4.

126. Köckritz, T.; Schiefer, T.; Jansen, I.; Beyer, E. Improving the Bond Strength at Hybrid-Yarn Textile Thermoplastic Composites for High-Technology Applications by Laser Radiation. *Int J Adhes Adhes* 2013, *46*, 85–94. https://doi.org/10.1016/j.ijadhadh.2013.06.004.

127. Zervas, M. N.; Codemard, C. A. High Power Fiber Lasers: A Review. *IEEE Journal on Selected Topics in Quantum Electronics* 2014, *20* (5). https://doi.org/10.1109/JSTQE.2014.2321279.

128. Yang, Z.; Tian, Y. L.; Yang, C. J.; Wang, F. J.; Liu, X. P. Modification of Wetting Property of Inconel 718 Surface by Nanosecond Laser Texturing. *Appl Surf Sci* 2017, *414*, 313–324. https://doi.org/10.1016/j.apsusc.2017.04.050.

129. Harder, S.; Schmutzler, H.; Hergoss, P.; Freese, J.; Holtmannspötter, J.; Fiedler, B. Effect of Infrared Laser Surface Treatment on the Morphology and Adhesive Properties of Scarfed CFRP Surfaces. *Compos Part A Appl Sci Manuf* 2019, *121*, 299–307. https://doi.org/10.1016/j.compositesa.2019.02.025.

130. İplikçi, H.; Barisik, M.; Türkdoğan, C.; Martin, S.; Yeke, M.; Nuhoğlu, K.; Esenoğlu, G.; Tanoğlu, M.; Aktaş, E.; Dehneliler, S.; İriş, M. E. Effects of Nanosecond Laser Ablation Parameters on Surface Modification of Carbon Fiber Reinforced Polymer Composites. *J Compos Mater* 2023, *57* (18), 2843–2855. https://doi.org/10.1177/00219983231178892.

131. Baldan, A. Adhesion Phenomena in Bonded Joints. *Int J Adhes Adhes* 2012, *38*, 95–116. https://doi.org/10.1016/J.IJADHADH.2012.04.007.

132. Yudhanto, A.; Alfano, M.; Lubineau, G. Surface Preparation Strategies in Secondary Bonded Thermoset-Based Composite Materials: A Review. *Compos Part A Appl Sci Manuf* 2021, *147*, 106443. https://doi.org/10.1016/J.COMPOSITESA.2021.106443.

133. Baburaj, E. G.; Starikov, D.; Evans, J.; Shafeev, G. A.; Bensaoula, A. Enhancement of Adhesive Joint Strength by Laser Surface Modification. *Int J Adhes Adhes* 2007, *27* (4), 268–276. https://doi.org/10.1016/J.IJADHADH.2006.05.004.

134. Coulon, J. F.; Tournerie, N.; Maillard, H. Adhesion Enhancement of Al Coatings on Carbon/Epoxy Composite Surfaces by Atmospheric Plasma. *Appl Surf Sci* 2013, *283*, 843–850. https://doi.org/10.1016/J.APSUSC.2013.07.028.

135. Lim, J. D.; Susan, Y. S. Y.; Daniel, R. M.; Leong, K. C.; Wong, C. C. Surface Roughness Effect on Copper–Alumina Adhesion. *Microelectronics Reliability* 2013, *53* (9–11), 1548–1552. https://doi.org/10.1016/J.MICROREL.2013.07.016.

136. Maia, B. S., Study on the effect of surface energy of polypropylene/Polyamide12 polymer hybrid matrix reinforced with virgin and recycled carbon fiber. *University of Toronto (Canada),* 2017. (accessed 2024-03-31).

137. Yang, S.; Gu, L.; Gibson, R. F. Nondestructive Detection of Weak Joints in Adhesively Bonded Composite Structures. *Compos Struct* 2001, *51* (1), 63–71. https://doi.org/10.1016/S0263-8223(00)00125-2.

138. Gude, M. R.; Prolongo, S. G.; Ureña, A. Adhesive Bonding of Carbon Fibre/Epoxy Laminates: Correlation between Surface and Mechanical Properties. *Surface and Coatings Technology*, 2012, 207: 602-607. https://doi.org/10.1016/j.surfcoat.2012.07.085.

139. Deng, S.; Djukic, L.; Paton, R.; Ye, L. Thermoplastic-Epoxy Interactions and Their Potential Applications in Joining Composite Structures-A Review. *Composites Part A: Applied Science and Manufacturing*, 2015, 68: 121-132. https://doi.org/10.1016/j.compositesa.2014.09.027.

140. Deng, S.; Djukic, L.; Paton, R.; Ye, L. Thermoplastic–Epoxy Interactions and Their Potential Applications in Joining Composite Structures – A Review. *Compos Part A Appl Sci Manuf* 2015, *68*, 121–132. https://doi.org/10.1016/J.COMPOSITESA.2014.09.027.

141.Toray Cetex ® *TC1200 PEEK PRODUCT DATA SHEET*.

142. *FM ® 300 Epoxy Film Adhesive*. www.cytec.com.

143. Sun, C.; Min, J.; Lin, J.; Wan, H.; Yang, S.; Wang, S. The Effect of Laser Ablation Treatment on the Chemistry, Morphology and Bonding Strength of CFRP Joints. *Int J Adhes Adhes* 2018, *84*, 325–334. https://doi.org/10.1016/j.ijadhadh.2018.04.014.

144. ASTM D5868 Test Method for Lap Shear Adhesion for Fiber Reinforced Plastic (FRP) Bonding, 2023. vol. 15.06. doi: 10.1520/D5868-01R23.

145. ISO 179-1 Plastics Determination of Charpy impact properties, *First Edition 2000-12-15*.

146. Shimamoto, K.; Sekiguchi, Y.; Sato, C. Effects of Surface Treatment on the Critical Energy Release Rates of Welded Joints between Glass Fiber Reinforced Polypropylene and a Metal. *Int J Adhes Adhes* 2016, *67*, 31–37. https://doi.org/10.1016/j.ijadhadh.2015.12.022.

147. ASTM D5528 Test Method for Mode I Interlaminar Fracture Toughness of Unidirectional Fiber-Reinforced Polymer Matrix Composites. https://doi.org/10.1520/D5528.

148. ASTM-American Society for Testing and Materials. ASTM Standard D5528: Test Method for Mode I Interlaminar Fracture Toughness of Unidirectional Fiber-Reinforced Polymer Matrix Composites 1. *Annual Book of ASTM Standards* 2001, *01* (Mode I), 1–12. https://doi.org/10.1520/D5528-13.2.

149. S. Dallmann S. PhD. Dissertation, Technical University of Dortmund, Dortmund, 2011. https://www.tu-dortmund.de/en/(accessed: 03-05-2024)

150. Karl, C. W.; Rahimi, W.; Lang, A.; Giese, U. Characterization of Modified Elastomer Surfaces by Wetting: A Review *Modifizierte Wilhelmy-Technik Chemische Heterogenität Rauheit Kontaktwinkelhysterese*; 2018. www.kgk-rubberpoint.de.

151. Wynn, M.; Zobeiry, N. Investigating the Effect of Temperature History on Crystal Morphology of Thermoplastic Composites Using In Situ Polarized Light Microscopy and Probabilistic Machine Learning. *Polymers 2023, Vol. 15, Page 18* 2022, *15* (1), 18. https://doi.org/10.3390/POLYM15010018.

152. Leone, C.; Papa, I.; Tagliaferri, F.; Lopresto, V. Investigation of CFRP Laser Milling Using a 30 W Q-Switched Yb:YAG Fiber Laser: Effect of Process Parameters on Removal Mechanisms and HAZ Formation. 2013. https://doi.org/10.1016/j.compositesa.2013.08.004.

153. Li, W.; Wang, J.; Sang, L.; Zu, Y.; Li, N.; Jian, X.; Wang, F. Effect of IR-Laser Treatment Parameters on Surface Structure, Roughness, Wettability and Bonding Properties of Fused Deposition Modeling-Printed PEEK/CF. *J Appl Polym Sci* 2021, *138* (40). https://doi.org/10.1002/app.51181.

154. Zimmermann, N.; Wang, P. H. A Review of Failure Modes and Fracture Analysis of Aircraft Composite Materials. *Eng Fail Anal* 2020, *115*, 104692. https://doi.org/10.1016/J.ENGFAILANAL.2020.104692.

155. van Dam, J. P. B.; Abrahami, S. T.; Yilmaz, A.; Gonzalez-Garcia, Y.; Terryn, H.; Mol, J. M. C. Effect of Surface Roughness and Chemistry on the Adhesion and Durability of a Steel-Epoxy Adhesive Interface. *Int J Adhes Adhes* 2020, *96*. https://doi.org/10.1016/j.ijadhadh.2019.102450.

156. Zheng, R.; Lin, J.; Wang, P. C.; Wu, Y. Correlation between Surface Characteristics and Static Strength of Adhesive-Bonded Magnesium AZ31B. *International Journal of Advanced Manufacturing Technology* 2016, *84* (5–8), 1661–1670. https://doi.org/10.1007/S00170-015-7788-5/METRICS.

157. Zielecki, W.; Pawlus, P.; PerŁowski, R.; Dzierwa, A. Surface Topography Effect on Strength of Lap Adhesive Joints after Mechanical Pre-Treatment. *Archives of Civil and Mechanical Engineering* 2013, *13* (2), 175–185. https://doi.org/10.1016/J.ACME.2013.02.005.

158. Pawlus, P.; Reizer, R.; Wieczorowski, M. Functional Importance of Surface Texture Parameters. *Materials 2021, Vol. 14, Page 5326* 2021, *14* (18), 5326. https://doi.org/10.3390/MA14185326.

159. Patel, K.; Doyle, C. S.; Yonekura, D.; James, B. J. Effect of Surface Roughness Parameters on Thermally Sprayed PEEK Coatings. *Surf Coat Technol* 2010, *204* (21–22), 3567–3572. https://doi.org/10.1016/j.surfcoat.2010.04.026.

VITA

Ceren TÜRKDOĞAN DAMAR

EDUCATION

- ***Ph.D.*** in English, 2024, Mechanical Engineering, İzmir Institute of Technology.

- ***M.Sc.*** in English, 2019, Mechanical Engineering, İzmir Institute of Technology.

- ***B.Sc.*** in 30% English, 2016, Metallurgical and Materials Engineering, Dokuz Eylül University.

SELECTED CONFERENCE PAPERS AND JOURNAL ARTICLES

İplikçi H., Barışık M., **Türkdoğan C**., Martin S., Yeke M., Nuhoğlu K., Esenoğlu G.,Tanoğlu M., Aktaş E., Dehneliler S., İriş M.E. 'Effects of nanosecond laser ablation parameters on surface modification of carbon fiber reinforced polymer composites' *Journal of Composite Materials, 2023, 57(18).*

Esenoğlu G., Barışık M., Tanoğlu M., Yeke M., **Türkdoğan C.** İplikçi H., Martin S., Nuhoğlu K., Aktaş E., Dehneliler S., İriş M.E, **'**Improving Adhesive Behavior of Fiber Reinforced Composites by Incorporating Electrospun Polyamide-6,6 Nanofibers in joining Region', *Journal of Composite Materials, 2022.*

Türkdoğan C., Tanoğlu M., 'Development of Adhesively Bonded Glass Fiber Reinforced Polypropylene / Aluminum Based Fiber Metal Laminates (FMLs)' *4th International Porous and Powder Materials Symposium and Exhibition (PPM 2019), 9-11 October 2019, Muğla, Turkey*

Türkdoğan C., et.al. **'**'Development of Composite Materials for the Textile Industry' *International Fiber and Polymer Research Symposium Proceedings Book,* (4:2018).